

University of Montana

ScholarWorks at University of Montana

Graduate Student Theses, Dissertations, &
Professional Papers

Graduate School

1992

Magmatic differentiation of Square Butte laccolith central Montana alkalic province

Cora Terrell Helm
The University of Montana

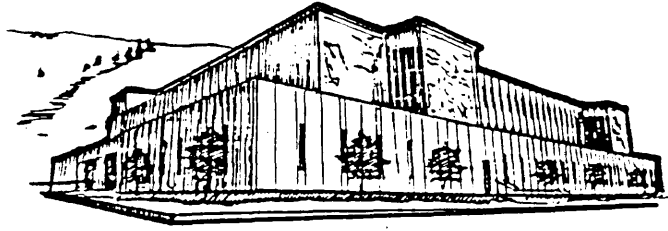
Follow this and additional works at: <https://scholarworks.umt.edu/etd>

Let us know how access to this document benefits you.

Recommended Citation

Helm, Cora Terrell, "Magmatic differentiation of Square Butte laccolith central Montana alkalic province" (1992). *Graduate Student Theses, Dissertations, & Professional Papers*. 5655.
<https://scholarworks.umt.edu/etd/5655>

This Thesis is brought to you for free and open access by the Graduate School at ScholarWorks at University of Montana. It has been accepted for inclusion in Graduate Student Theses, Dissertations, & Professional Papers by an authorized administrator of ScholarWorks at University of Montana. For more information, please contact scholarworks@mso.umt.edu.



Maureen and Mike
MANSFIELD LIBRARY

Copying allowed as provided under provisions
of the Fair Use Section of the U.S.

COPYRIGHT LAW, 1976.

Any copying for commercial purposes
or financial gain may be undertaken only
with the author's written consent.

University of
Montana

Magmatic Differentiation
of Square Butte Laccolith,
Central Montana Alkalic Province

by

Cora Terrell Helm

B.S., Sonoma State University, 1990

Presented in partial fulfillment of the requirements
for the degree of
Master of Science
University of Montana
1992

Approved by:

Donald W. Hyndman
Chairman, Board of Examiners

R. C. Murray
Dean, Graduate School

December 3, 1992
Date

UMI Number: EP41119

All rights reserved

INFORMATION TO ALL USERS

The quality of this reproduction is dependent upon the quality of the copy submitted.

In the unlikely event that the author did not send a complete manuscript and there are missing pages, these will be noted. Also, if material had to be removed, a note will indicate the deletion.



UMI EP41119

Published by ProQuest LLC (2014). Copyright in the Dissertation held by the Author.

Microform Edition © ProQuest LLC.

All rights reserved. This work is protected against unauthorized copying under Title 17, United States Code



ProQuest LLC.
789 East Eisenhower Parkway
P.O. Box 1346
Ann Arbor, MI 48106 - 1346

Helm, Cora Terrell, M.S., November, 1992

Geology

Magmatic Differentiation of Square Butte Laccolith, Central
Montana Alkalic Province

Chairman: Donald W. Hyndman *DWH*

Square Butte laccolith, the largest in the Central Montana alkalic province, has recently been cited as an example of silicate liquid immiscibility (Kendrick, 1980). Striking field relationships of syenite and shonkinite suggest coalescence and upward movement of large felsic blobs through a shonkinitic magma. Chemical data, although compatible with liquid immiscibility, are also compatible with crystal fractionation and the presence of volatiles. For example, specific gravity, lack of cumulus textures, and iron and magnesium content of pyroxene all support a model of liquid immiscibility but may also be indicative of migration of volatiles. Pseudoleucite in the syenite layer suggests crystal fractionation may have involved the floating of pseudoleucite, and chemistry of the cap syenite indicates the presence of volatiles. These and other data are used to propose an alternative model involving combined crystal fractionation and volatile movement.

Acknowledgements:

Warm and gracious thanks go to Don Hyndman, Mike Baxter, Janet Riddell, and Monte Smith. Thank you, also, to my husband Scott Helm for the photography, unending patience and support. Thank you to Dave Alt, for just being Dave. Thank you VERY MUCH to Blair Nack, Georgianna Rowland, Hugo and Judy Tureck, Jack and Shirley Smith, and the wonderful folks at Mike's Bar in Geraldine, Montana. And finally, thank you to Fred Youderian for an inspirational discussion at the base of the butte. And for people who don't always get recognized but should, thank you Judy Fitzner and Loreen Skeel.

I would also like to acknowledge sources of funding which are greatly appreciated: The Geological Society of America and NSF, Ms. Sara Foland and Amoco Corp., and Mr. and Mrs. P.D. Terrell, Jr.

Note:

ANY access to Square Butte MUST be cleared with local land-owners and ranch-managers.

TABLE OF CONTENTS

Introduction	1
Previous Studies	2
Previous Experimental Studies	
in Liquid Immiscibility	3
General Geology	7
Description of Rock Types	12
Field Relations/Descriptions	15
Sills	19
Shonkinite	20
Contact Zone	26
Syenite	30
Cap Syenite	38
Analytical Techniques	38
Petrography	40
Chill Zone	41
Shonkinite	43
Syenite	50
Cap Syenite	51
Differentiation Models	
1. Liquid Immiscibility	53
Evidence For and Against	54
Partitioning of Selected Elements	60
Phosphorus and Titanium	62
2. Crystal Fractionation	65
Major Element Oxides	66
Trace Element Variation	72
3a. Thermogravitational Diffusion	81
3b. Pneumatolitic Effects	82
Conclusions/Model for Differentiation	94
Model for Differentiation	99
References Cited	103
Additional References	106

APPENDICES

Appendix A - Explanation of Samples	A1
Appendix B - Whole-rock Chemical Analyses ...	A6
Appendix C - Precision Data for Chemical Analyses	A7
Appendix D - Chemical Composition of Clinopyroxene through Shonkinite	A13

LIST OF FIGURES

1 Location Map	8
2 Photo, Square Butte from SE	9
3 Photos, Rock Types	11
4 Specific Gravity	13
5 Percentage of Px and Grain Size	14
6 Photo, Large Circular White Patches in Syenite	17
7 Photo, Cap Syenite Cliff	18
8 Sills and Their Relation to Laccolith	21
9 Syenitic Veins and Dikes in Shonkinite ...	22
10 Photos, Ocelli in Shonkinite	24
11 Photo, Less Mafic Shonkinite in Contact Zone	25
12 Syenitic Streaks in Shonkinite	27
13 Photo, Horizon of Syenite Blobs at top of Shonkinite	28
14 Bulbous Syenite Outcrop in Contact Zone ..	29
15 Photo, Syenite Blob and it's Shonkinite Coating, Contact Zone	31
16 Photos, Syenite Blobs and Shonkinite Coating	32, 33
17 Photos, Outcrops of Syenite and Mafic Rind	34
18 Syenite and Mafic Rind	36

LIST OF FIGURES CONTINUED...

19 Syenite and Slightly More Mafic Coating	37
20 Average Pyroxene Composition	42
21 Photomicrograph, Pseudoleucite Shonkinite	44
22 Photomicrograph, Shonkinite	49
23 Photomicrograph, Syenite	52
24 Variation of FeO and MgO in Shonkinite ...	56
25 FMA Diagram of Ocelli and Host from Philpotts, 1976	58
26 FMA Diagram of Square Butte Samples	59
27 Rare-Earth Element Diagram	61
28 P ₂ O ₅ vs CaO	63
29 TiO ₂ vs CaO	64
30a-e Major-Element Trends	67-71
31a-c Fractionation Trends	74-76
32a-c Trace Elements vs CaO	77, 79-80
33a-c, 34a-c, 35a-d Trace Elements vs Elevation	83-85, 86-88, 90-93
36 Photo, Syenitic Dike and Patch in Lower Shonkinite	96
37 Pseudoleucite Sketches	97
38 Differentiation Model	100

LIST OF TABLES

Table 1 Petrography of Shonkinite	46
Table 2 Average and Normalized Percent Mafic Constituents of Shonkinite	73
Table 3 Summary of Differentiation Possibilities and Evidence for Each	95

INTRODUCTION

Square Butte laccolith has been studied intermittently over the past 100 years, but the precise mechanism of differentiation continues to elude researchers. Most recently, a process of liquid immiscibility was proposed (Kendrick, 1980; Hirsch and Hyndman, 1985). In spite of stunning field relationships which seemingly cannot be explained by crystal fractionation, Square Butte lacks enough convincing evidence to further advance a model of liquid immiscibility.

It is the purpose of this study, then, to examine the butte more closely by covering as much ground as was accessible, documenting field relationships, and collecting a vertical sequence of samples for geochemical analysis and detailed petrography. Originally, the thesis was expected to provide firm evidence for liquid immiscibility. On the contrary, data gathered provides no further evidence for liquid immiscibility, and also fails to provide a clear differentiation model to explain the odd globular structures. Working with the data and field relationships, I propose a hypothetical model involving crystal fractionation and movement of volatile constituents.

PREVIOUS STUDIES

Square Butte received attention in the late 1800's and early 1900's from several groups of geologists, who studied the butte because of its proximity to the Highwood Mountains and its alkaline affinity. The most notable of these papers was published by Weed and Pirsson, 1895, who discuss differentiation of the butte. Although they thought the butte was a syenite cone surrounded by shonkinite, Weed and Pirsson were convinced that differentiation occurred before crystallization, and that field evidence pointed "favorably" toward liquation (immiscibility) as the differentiation process. However, Pirsson later published a paper (1905) which is basically a repeat of the 1895 paper with some changes in theory and conclusions. In this, Pirsson determined that the syenite actually formed a cap resting on top of shonkinite. He also dismissed differentiation by liquation, replacing it with differentiation through fractional crystallization involving convection currents along the sides of the magma chamber.

Prior to 1895, Lindgren (1893) described a sample of sodalite syenite which was collected by C.A. White, presumably from the top of the butte. Since Lindgren did not go to the butte himself but was relying on White's notes, there is not much discussion or description of field relationships.

Square Butte did not receive attention again until the 1930's when a number of geologists began studying the Highwood Mountains and surrounding areas in greater detail. Hurlbut and Griggs (1939) closely examined Shonkin Sag laccolith and used it as a basis for comparison with other local laccoliths, including Square Butte. Influenced by Bowen's recent work (1928, and earlier papers), they suggested crystal fractionation as the differentiation process for all the laccoliths of the area. Later work by Larsen (1941) discusses mineralogy and textures of igneous rocks at Square Butte and the Highwood Mountains.

After the 1940's, no significant work was done at Square Butte until 1980. Master's theses by Kendrick (1980) and Edmond (1980) on Square Butte and Shonkin Sag laccolith, respectively, promote liquid immiscibility as the primary differentiation process for each laccolith. Marvin (1980) included a sample of shonkinite from Square Butte for radiometric dating of igneous rocks of north-central Montana.

PREVIOUS EXPERIMENTAL STUDIES IN LIQUID IMMISCIBILITY

Since liquid immiscibility has been proposed recently as the differentiation mechanism at Square Butte, this study focusses on the potential that it may have been the primary

differentiation process. Roedder (1951) discovered an immiscibility field in the leucite-fayalite-silica system and further found unequivocal evidence of immiscibility in lunar basalts (Roedder and Weiblen, 1970). Studies on the partitioning of minor and trace elements in the $K_2O-Al_2O_3-FeO-SiO_2$ system between immiscible mafic and felsic liquids revealed partitioning of elements through liquid immiscibility was often contrary to partitioning through crystal fractionation (Watson, 1976). In addition, phosphorus and titanium were found to increase the immiscibility field in the fayalite-leucite-silica field (Freestone, 1978).

In determining a differentiation process, partition coefficients for minor and trace elements are extremely useful. The preference of a particular element for a crystal over the melt is a function of the polymerization of the melt, as well as the structure of the crystals. The degree of polymerization depends on the composition of the melt. Partition coefficients for many elements vary considerably with composition of the host silicate melt. Francalanci et al., (1987) provide partition coefficients for selected trace elements in high-potassium alkaline rocks.

Field and petrographic studies have shown immiscibility to occur in several kinds of rocks; especially lamprophyres

(c.f. Foley, 1984; Eby, 1980; Strong and Harris, 1974). These instances are restricted to small rock bodies, and little work yet has shown liquid immiscibility to exist on a scale large enough to form mappable alkalic rock bodies. Most of the large laccoliths in the Montana alkalic province are bodies of shonkinite capped by an upper portion of syenite. Previous studies of Shonkin Sag and Square Butte laccoliths (Kendrick, 1980; Edmond, 1980; Hirsch and Hyndman, 1985;) suggest the bimodal rock sequence formed by the separation of immiscible magmas. Some of the evidence to support this includes: 1. The absence of rhythmic layering and cumulus textures; 2. A progressive upward increase in mafic mineral content in the shonkinite of Shonkin Sag laccolith; 3. The syenite and shonkinite fractions consist of the same mineral suites and show no sign of disequilibrium; 4. Globular masses and vertical pipes of syenite within the lower shonkinite of Shonkin Sag contradict the mechanism of crystal fractionation.

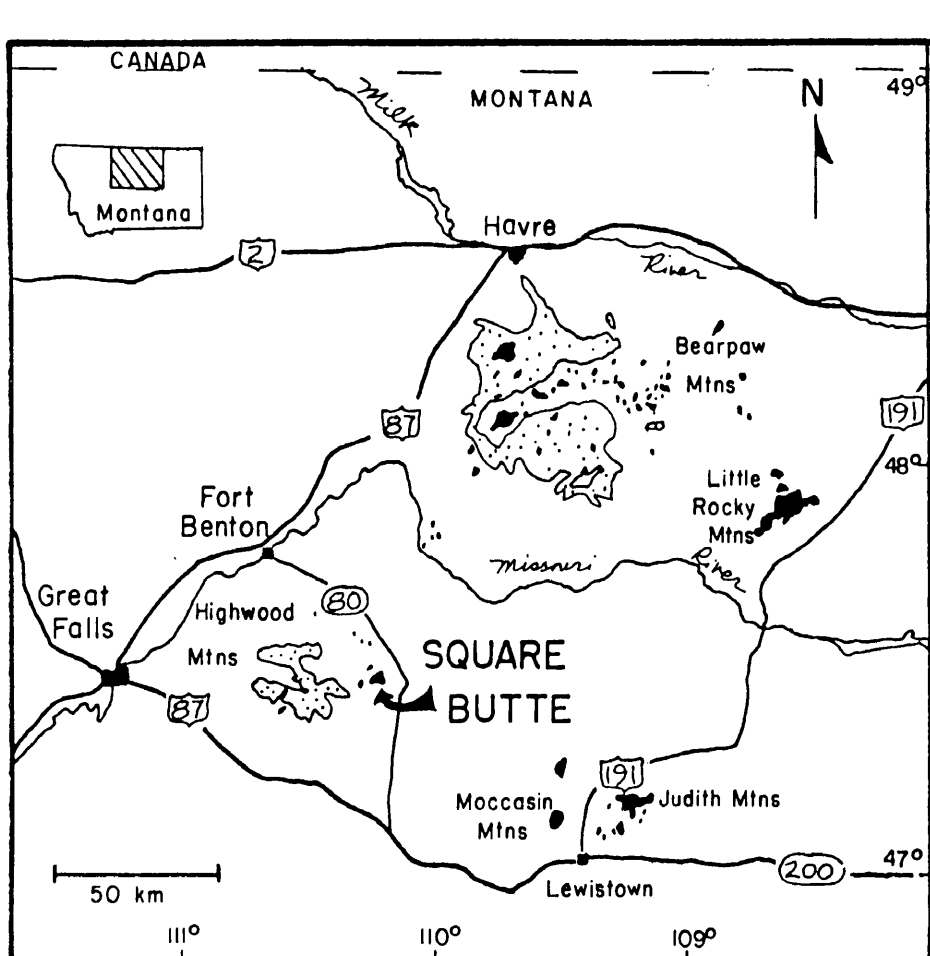
Many rocks used in liquid immiscibility studies, such as the lamprophyres noted above, contain small, spherical felsic structures termed ocelli. Ocellar and globular structures have been used as evidence for liquid immiscibility (Phillips, 1973; Philpotts, 1976; and Foley, 1984). The term ocellar structure as defined by Holmes (in Phillips, 1973) is "... the tangential arrangement of

minerals such as biotite, aegirine or hornblende around borders of spheroidal masses composed of nepheline, analcime and leucite." Any rounded masses in an igneous rock which cannot be described as ocelli, variolites, orbicules or amygdules are called globular structures. Globular structures maintain a similar texture and mineral composition as the host rock (Phillips, 1973). Philpotts (1976) demonstrated that liquid immiscibility is the primary mechanism in the formation of ocelli in dikes and sills in the Monteregian alkaline province of Quebec. Foley (1984) identified two different kinds of leucocratic globular structures in alkaline lamprophyres of the Aillik Bay alkaline dike swarm. The first, Type I, are believed to represent immiscible liquids, whereas Type II represent segregation of late stage melt. Small ocelli are observed at Square Butte as well, and previously were proposed as representing remnant immiscible globules (Kendrick, 1980). Leucocratic ocelli at Square Butte, however, have been determined, in the present study, to be pseudoleucite, and do not represent preserved immiscible droplets. This suggests the magma did not split into two immiscible liquids, but instead, crystallized pseudoleucite continuously throughout differentiation. For a complete discussion of the pseudoleucite, see Petrography section.

GENERAL GEOLOGY

Square Butte laccolith is located in the central Montana alkalic province, a geologic region of alkaline volcanism and intrusions spanning latest Cretaceous to nearly middle Eocene time (Figure 1, location map). The uncommon rock types are host to several economic deposits including precious metals and sapphires.

Square Butte, just south of Geraldine, towers over surrounding ranch and farmland. Approximately 20 km west of Square Butte are the Highwood Mountains which consist of alkaline and subalkaline domes, stocks, and flows. Numerous dikes radiate from the Highwoods and feed the surrounding laccoliths including among others, Shonkin Sag, Lost Lake, Round Butte, and Square Butte laccoliths. Square Butte is by far the largest of these laccoliths, rising to an elevation of 1737 m (5703 ft). The circumference of the base (lowermost exposed shonkinite) is approximately 12.5 km (7.5 mi), from which the terrain climbs steeply for 460 m (1500 feet). The top of the butte, which is nearly flat and covered by a dense young pine forest and grassland, is much smaller in area, with a circumference of approximately 5.3 km (3.2 mi). The butte is split into nearly equal vertical portions of shonkinite and syenite; the contact between the two appears sharp from a distance (Figure 2). The thickness



EXPLANATION



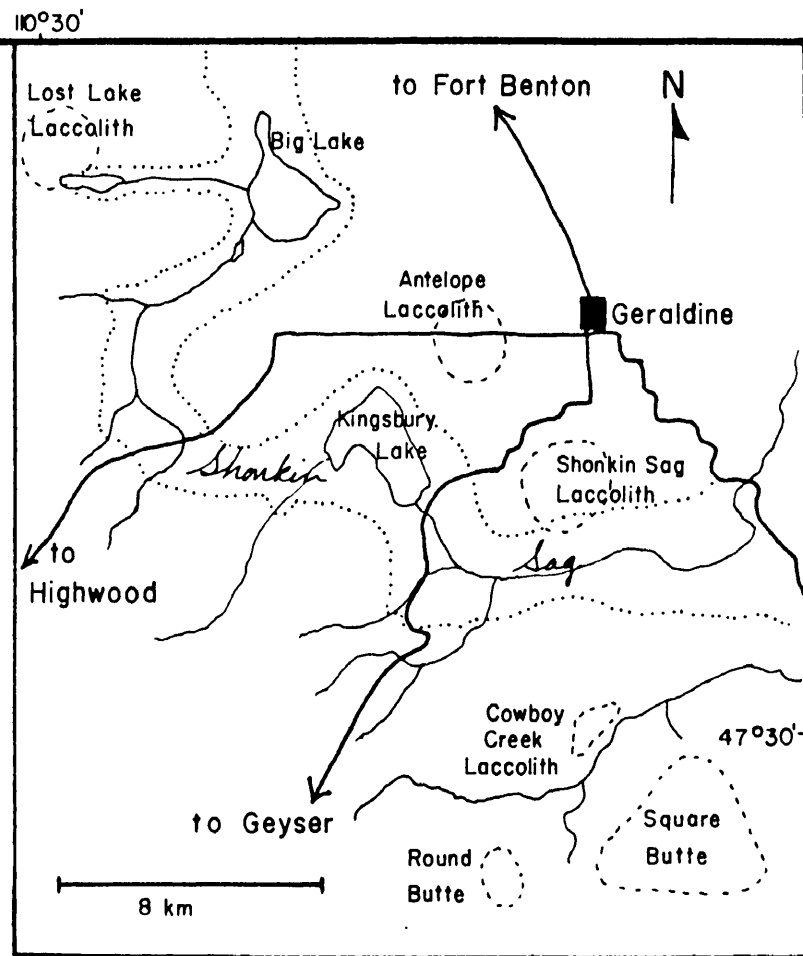
-  extrusive rocks
-  intrusive rocks

Figure 1a Index Map (modified from Hearn, 1989)




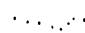
-  projected outline of laccoliths
-  glacial Missouri River

Figure 1b Map of Square Butte area and nearby laccoliths (modified from Hurlbut, 1939)

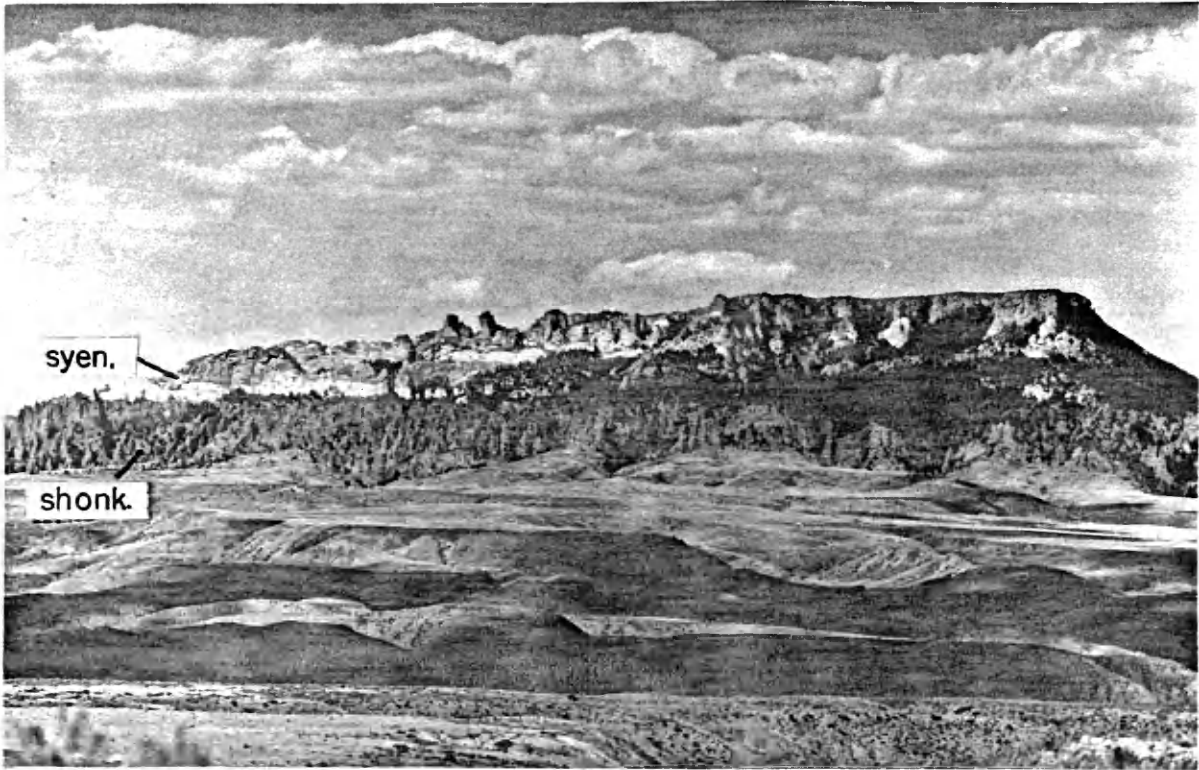


Figure 2 Square Butte from southwest.
Photo: Don Hyndman

of shonkinite is 150 m (500 ft) and thickness of overlying syenite is nearly 240 m (800 ft).

The laccolith intruded young, horizontal upper Cretaceous sediments in Eocene time. A potassium-argon date from biotite in the shonkinite is 50.4 ± 1.7 m.y. (Marvin, 1980). The sedimentary units are labeled by MacLachlan (1981) as the sandstones and shales of the lower part of the Montana Group. The most conspicuous sediments of this series are the grey-white bentonitic shales of the Telegraph Creek Formation, and the light-brown calcareous and porous Eagle Sandstone.

Igneous rocks of the Highwoods are dominated by shonkinite, syenite, mafic phonolite, latite, and monzonite. The bimodal sequence of silica-saturated and undersaturated rocks is typical of the province. The shonkinite may be considered as very mafic syenite containing nearly equal proportions of augite (salite) and sanidine, lesser amounts of biotite, pseudoleucite, zeolitized nepheline, olivine (forsterite), apatite, and magnetite (titanomagnetite?). The syenite has essentially the same mineral content, but with much less olivine and pyroxene. Furthermore, salite is often rimmed by hornblende, and accessory minerals include sphene and zoisite. The shonkinite and syenite can be divided into four rock types from the base of the butte to the top (Figure 3):

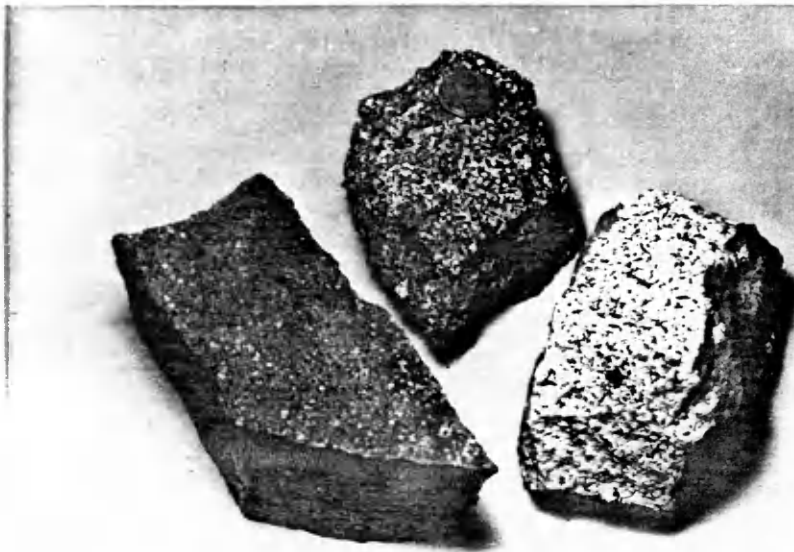


Figure 3a L-R: SB61, 1317 m, pseudoleucite shonkinite;
SB56, 1390 m, shonkinite; SB14, 1515 m, cap syenite.

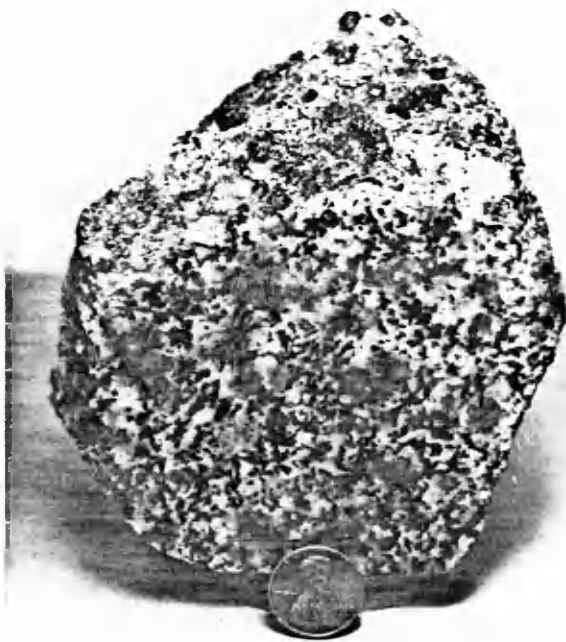


Figure 3b Syenite
with ocelli
(pseudoleucite).

SB23, 1545 m
(5070 ft)

Photos: Scott M. Helm

- 1 pseudoleucite shonkinite chill zone -- occurs as horizontal sills which surround the butte; as many as four sills can be seen in one vertical sequence alternating with sandstone. Rock is fine- to medium-grained porphyritic shonkinite with visible phenocrysts of salite and spherical pseudoleucite. Jointing in the sills is horizontal and vertical.
- 2 shonkinite -- dark-colored, friable, medium-grained intrusive rock containing approximately equal proportions of salite and sanidine + zeolite. Small (2-7mm) spherical and subspherical patches of leucocratic material, henceforth referred to as ocelli occur throughout, and are best seen in hand-sample. The shonkinite is not homogenous, as inferred by variation in specific gravity (see Figure 4) and grain size (Figure 5). A prominent joint pattern dips from 25 to 45 degrees outward from the butte.
- 3 syenite -- less-weathered intrusive rock that varies in color from blinding white to nearly as dark as shonkinite. The syenite also contains leucocratic ocelli which average 1 cm in diameter (Figure 3b). Jointing is nearly absent in the syenite.
- 4 cap syenite -- This is a light grey (yellowish from a distance) syenite which forms nearly 60 m (200 ft) of

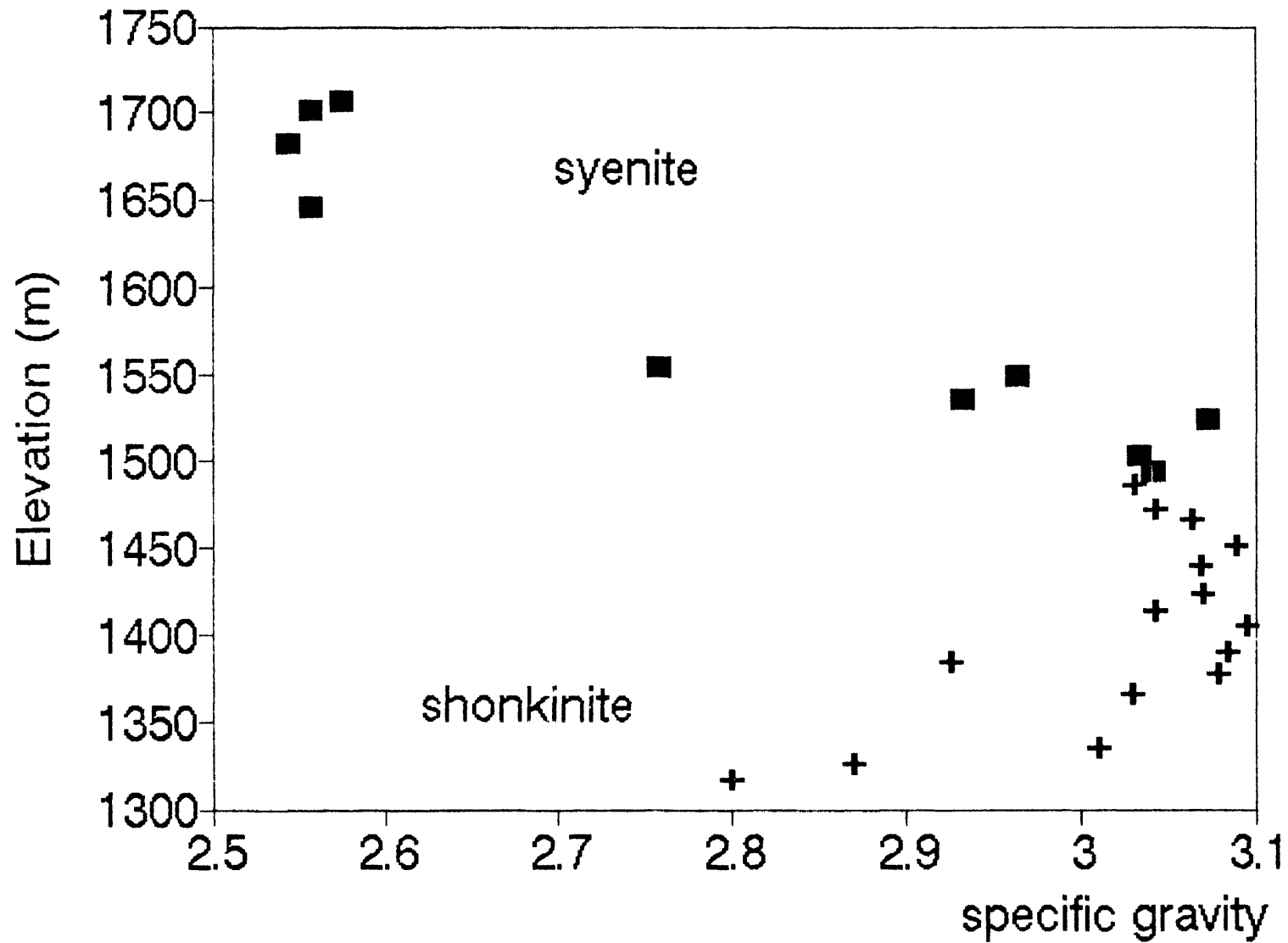


Figure 4 Plot of specific gravity versus elevation.
Solid squares: syenite.

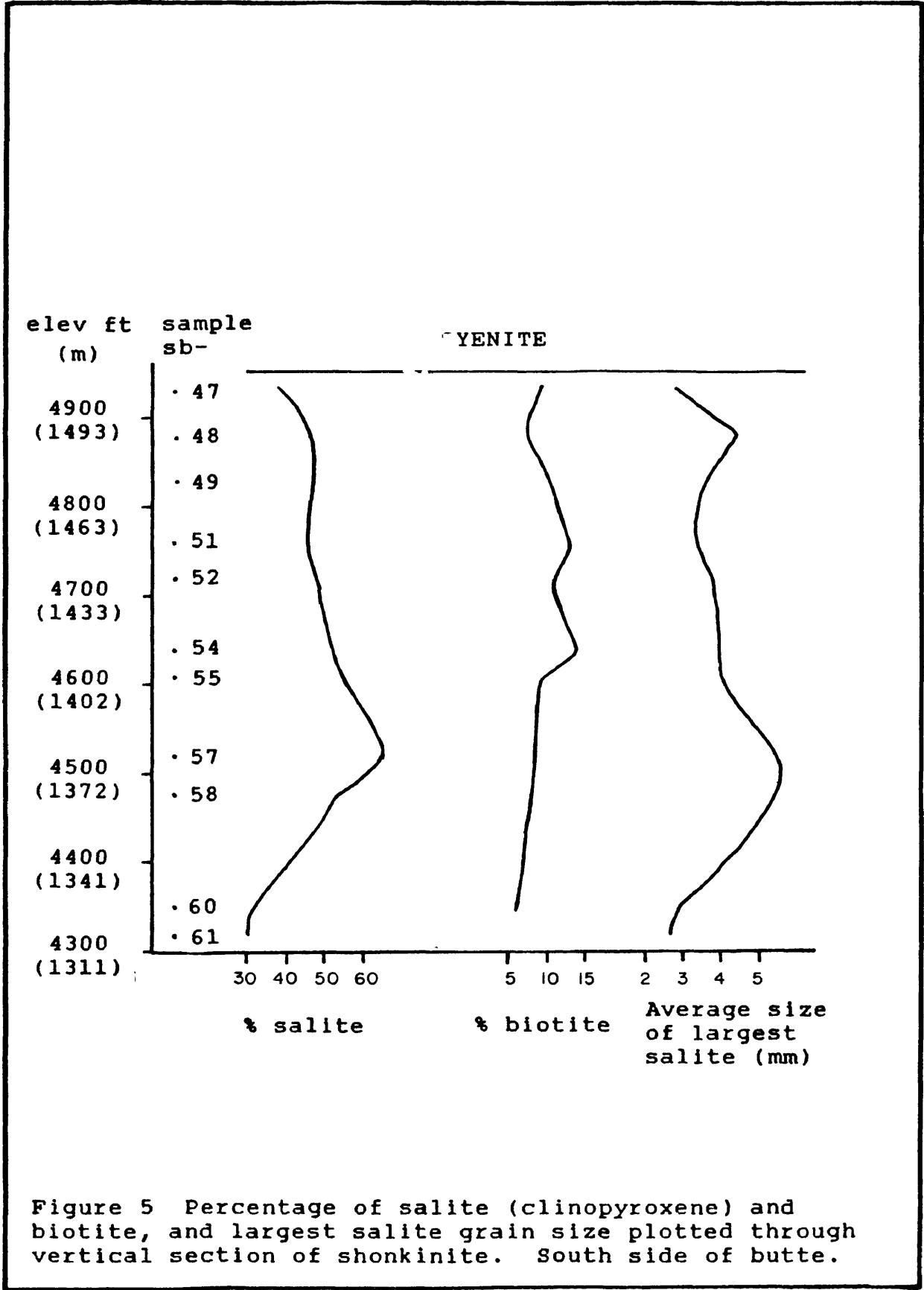


Figure 5 Percentage of salite (clinopyroxene) and biotite, and largest salite grain size plotted through vertical section of shonkinite. South side of butte.

vertical cliff, horizontally jointed, at the top of the butte. It is cut by pegmatitic veins and dikelets which contain feldspar phenocrysts up to 2 cm in length. The mafic constituent is dominantly amphibole, which appears as laths in a matrix of feldspar and sodalite.

FIELD RELATIONS/DESCRIPTIONS

The butte is a towering monster of rugged terrain, eroded spires of shonkinite and precipitous cliffs and walls of syenite. The shonkinite that makes up the lower half of the butte is more readily eroded than the overlying syenite. It erodes into towers and monoliths, often called hoodoos, which in places are separated by grassy slopes and open areas. On the southern side of the butte where erosion is more pronounced, these unique and eerie structures form a maze which is difficult to navigate.

The syenite has not eroded much and closely resembles the original shape of the upper half of the laccolith (Hirsch and Hyndman, 1985). It forms a level of smoother slopes in the contact zone, where it is possible to contour across much of the south and northwest sides of the butte. Above that contact zone, however, vertical cliffs, ridges, and smooth walls of syenite loom, virtually impossible to

scale for the squeamish. Tapering ridges or combs of syenite extend outward from the butte in three directions (Plate 1, topographic and geologic map). These ridges are nearly impassable and appear coated with a more mafic rind which splays off in an exfoliation pattern. Beneath this rind, which varies from 2 to 30 cm in thickness, is white syenite, usually appearing as large (up to 10 m) circular patches (Figure 6). The circular patches display a joint pattern that is thicker (25-35 cm) and oriented horizontally or at an angle dipping away from the butte. The rind appears all along the syenite ridges and combs and grades into the white syenite over a few centimeters. In a few areas, the sinuous, narrow ridges provide notches to pass through to the other side. These notches do not represent erosion because the more mafic rind is present on all sides. Interpretation of this rind a subject of debate. It appears to represent a chilled margin (or what is left of one), formed when the laccolith intruded into the young, probably moist, sediments (Hirsch and Hyndman, 1985). In addition to the joint pattern mentioned above, jointing in the shonkinite dips away from the butte. The cap syenite (top 150 m or so) is strictly horizontally jointed and forms a near-vertical cliff on all sides of the butte (see Figure 7). This combination of joint patterns mimics the structure of the overlying sediments after laccolith emplacement.

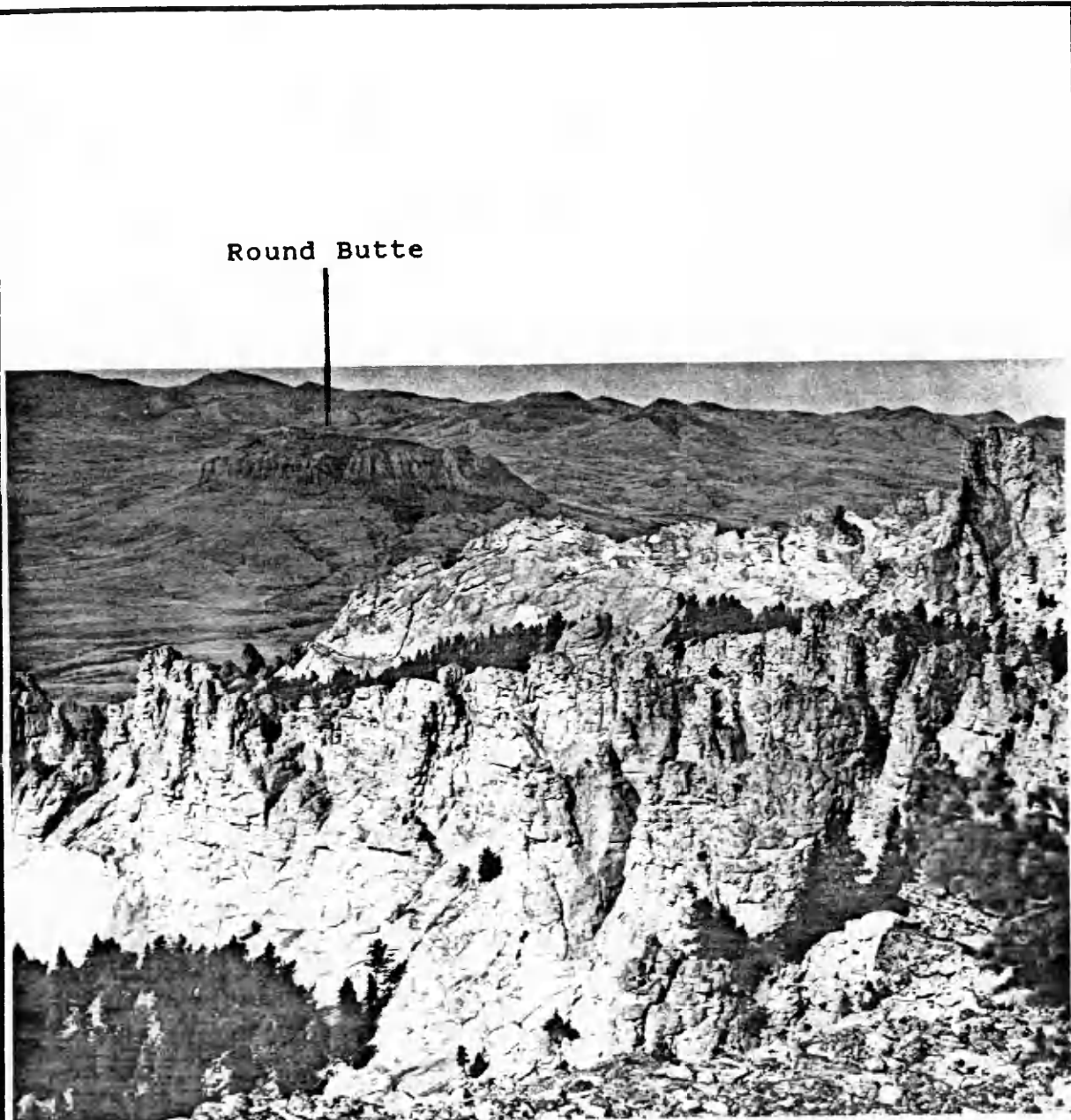


Figure 6 Large circular white patches in a syenite ridge.
Photo: Don Hyndman



Large tree is
approximately
8½ m high (28 ft).

Figure 7 Horizontally jointed cap syenite cliff.

Sills

Between two and four pseudoleucite shonkinite sills crop out around the butte nearly everywhere below the lowermost exposed shonkinite. These sills can be seen from Highway 80 in bluffs alternating with the light-colored sandstone and siltstone. The sills are approximately 1.5 to 12 meters thick and have knife-sharp contacts with the sandstone. At the contact with sediments, there is very little or no visible alteration or baking. Along the contacts, the shonkinite sill fingers into the sediments, and blocks of siltstone are caught up in the sill, but again, alteration is negligible. The sills display prominent vertical and moderate horizontal joint patterns.

The sills are generally very weathered and pseudoleucite is most visible on weathered surfaces. In samples which are very fresh, pseudoleucite is not discernible at all. Medium-grained, euhedral salite phenocrysts are visible and what was olivine is reduced to small anhedral spots of iron oxide. Salite lies in a preferred orientation parallel to the top of sills in some areas.

Previous authors believed the sills to underlie the butte (Weed and Pirsson, 1895). Other studies of similar laccoliths and surrounding sills (c.f., Gordon Butte, Emmart, 1981; Hyndman et al., 1989) document sills extending

from the laccolith into the surrounding sediments in a feather-like fashion. This type of sill injection is clearly visible in the Shonkin Sag laccolith where erosion exposes a complete cross-section of the laccolith and its contacts with surrounding sediments (Figure 8).

Furthermore, the pseudoleucite shonkinite sills surrounding Square Butte are identical in composition to the shonkinite of the butte itself. There is no reason to think that the butte and the sills were not contemporaneous and in contact.

Shonkinite

The massive shonkinite that comprises the lower 152 m of the butte (measured from top of highest sill) appears relatively homogeneous at first glance. Indeed, Hurlbut and Griggs in their 1939 study state that the specific gravity through the shonkinite is uniform (3.04-3.07). For the present study, specific gravity was found to range between 2.87 and 3.10 for a series of samples in a vertical sequence between the chill zone and the contact zone, inclusive (Figure 4). The shonkinite is highly variable with syenite dikes, veins, and subspherical blobs up to 70 cm in diameter occurring sporadically across the south side, well below the contact with the syenite (Figure 9). Such dikes and blobs in the lower shonkinite do not occur on the north side. The odd occurrence of these blobs may be evidence of liquid

Figure 8a Hypothetical sketch of sills emanating from Square Butte into sandstone (stippled).

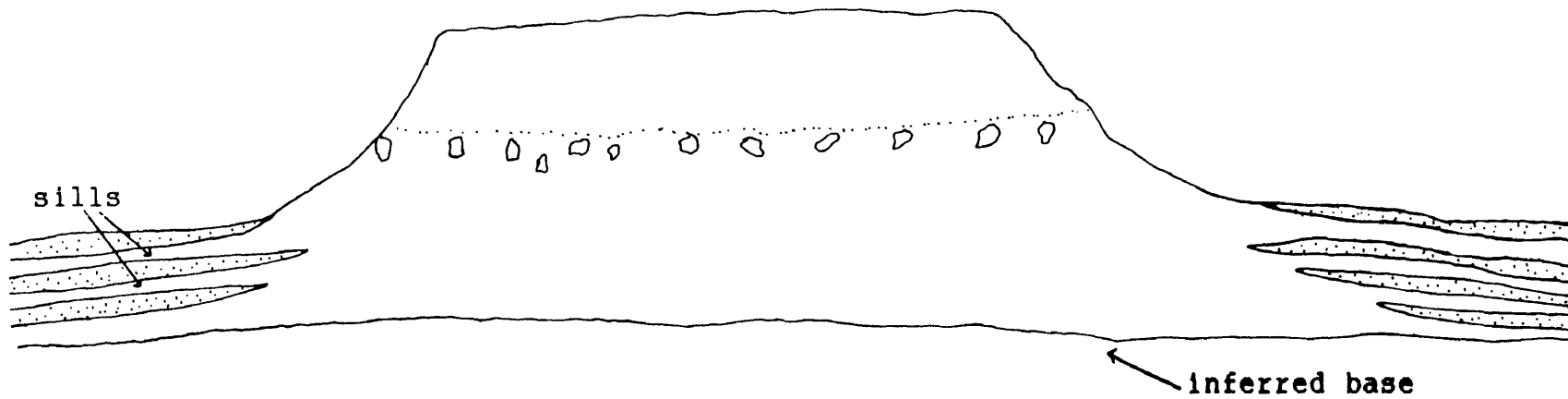
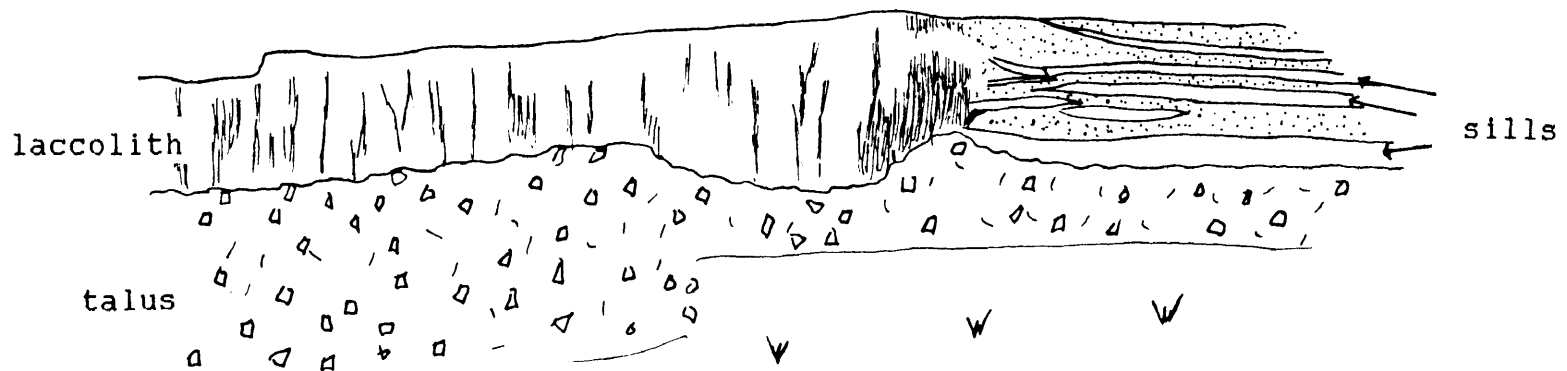
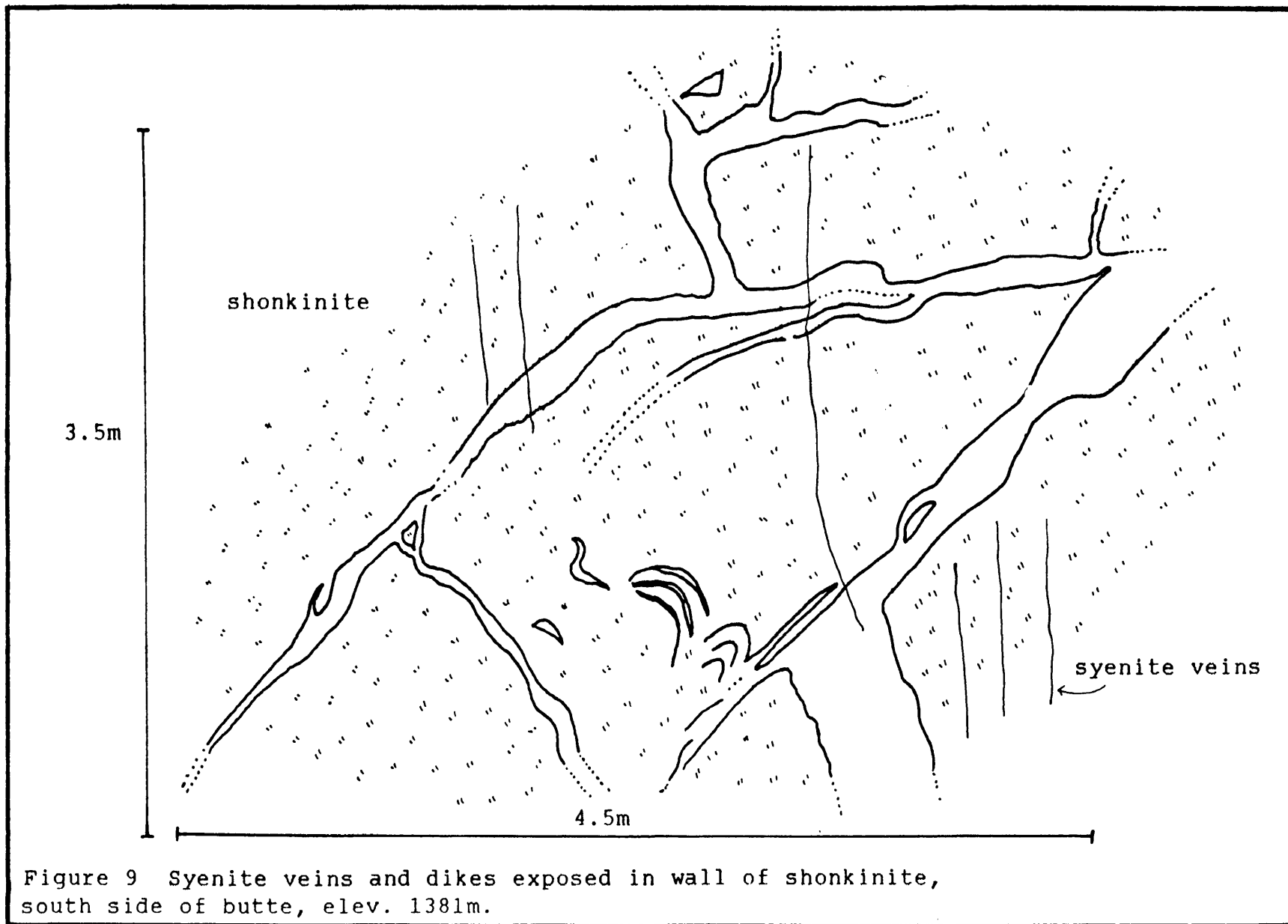


Figure 8b Photo-sketch of sills feathering into sediments (stippled) at Shonkin Sag laccolith.





immiscibility. The presence of zeolites and amphibole in the blobs and dikes, however, suggest migration of late stage fluids through the shonkinite.

Much of the shonkinite is characterized by small ocelli -- spherical aggregations of felsic minerals ranging in size from 2.5 to 10 mm. Euhedral prismatic augite (salite) crystals commonly provide a center for the ocelli, or form a radiating pattern within the spherical mass (Figure 10). In some areas of the shonkinite, the ocelli have coalesced into larger white patches. These white patches are bordered by clearly visible individual ocelli which emphasize their aggregation into a larger syenite patch. The ocelli become larger near the top of the shonkinite (elev. 1450 m), and the rock as a whole is more felsic and less dense than the lower shonkinite (Figure 11). This marks the gradation into the contact zone and a transition to syenite. Previous authors have used the presence of ocelli as evidence for liquid immiscibility in other alkaline rocks (Phillips, 1973; Philpotts, 1976; and Foley, 1984). For this study and contrary to other studies of Square Butte (c.f. Kendrick, 1980), the ocelli are interpreted as recrystallized pseudoleucite, not indicators of liquid immiscibility. For an explanation see section on Petrography.

In addition to varying amounts and sizes of ocelli and blobs throughout the syenite, there are syenite streaks 1.5

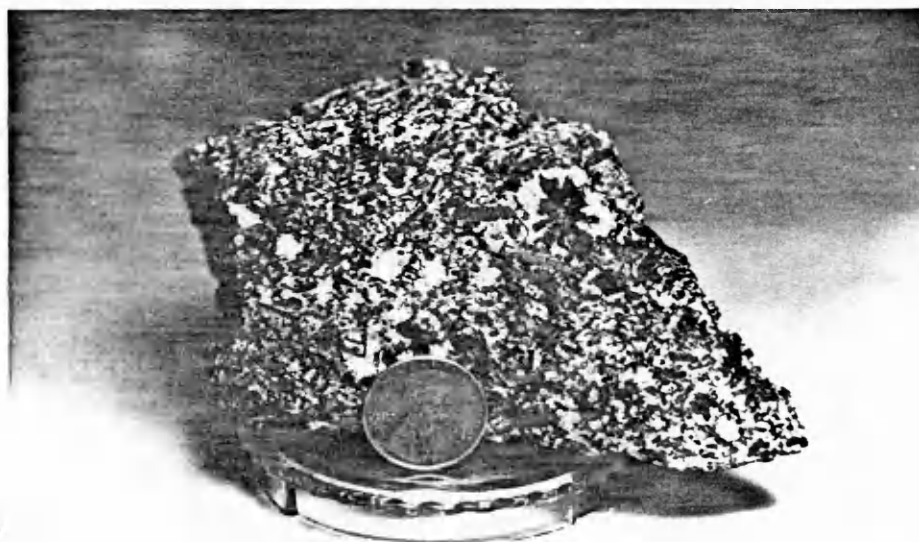
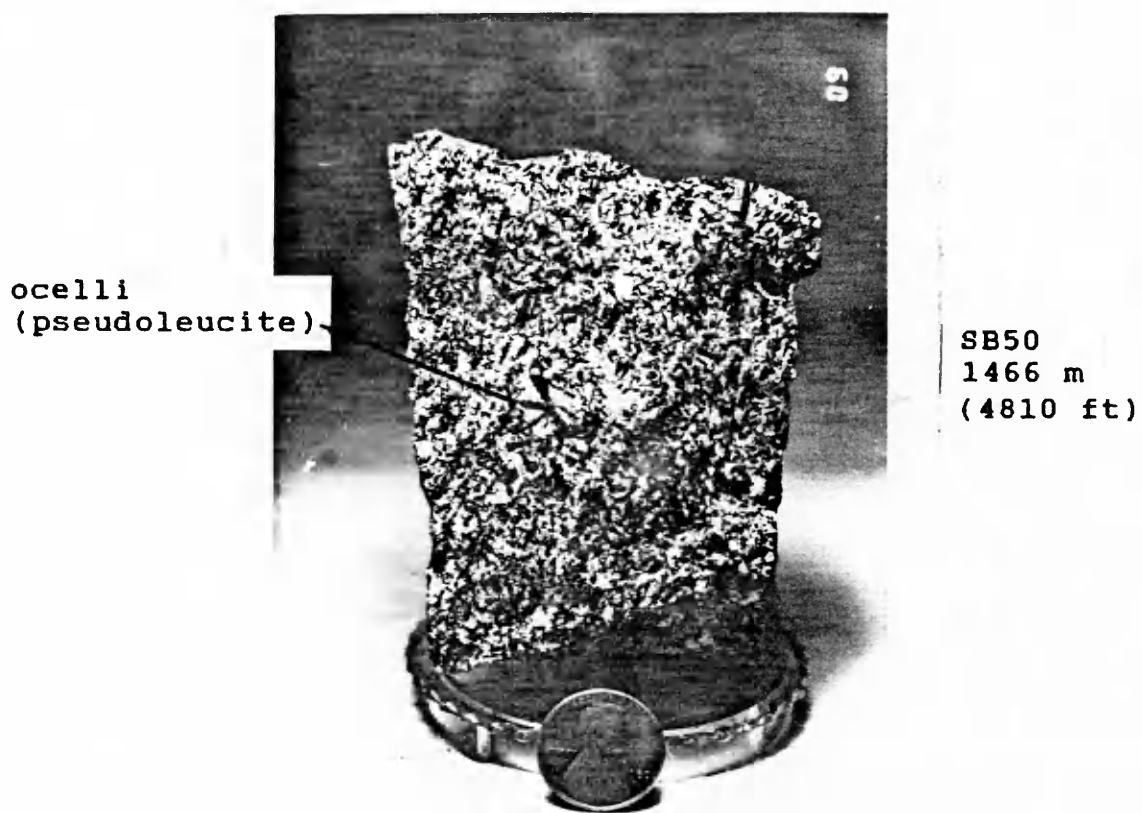
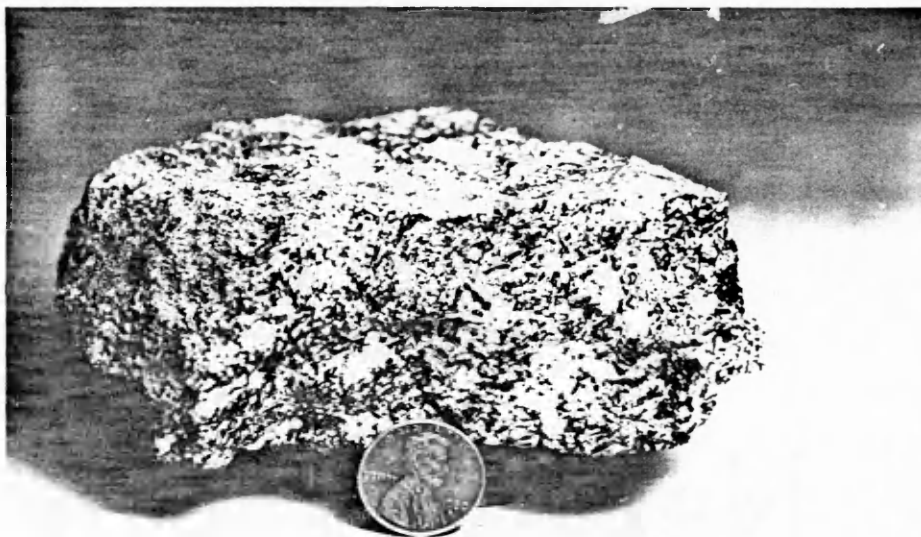


Figure 10 Pyroxene-centered ocelli (pseudoleucite) in shonkinite. SB57, 1378 m (4520 ft).
Photos: Scott M. Helm



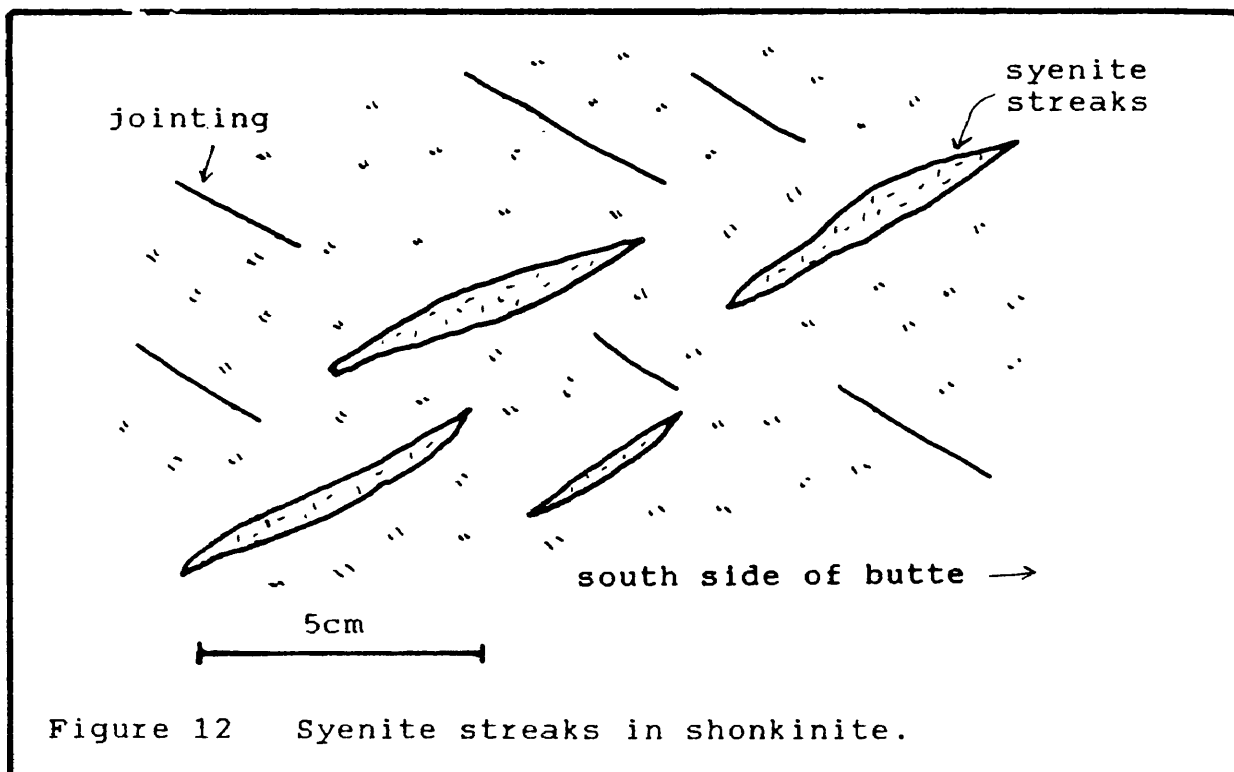
SB47 elev 1503 m (4930 ft)

Figure 11 Less mafic shonkinite from contact zone.
Photo: Scott M. Helm

cm wide and 6 cm long. These streaks are oriented about 70 degrees from jointing and formed in place, probably due to migration and diffusion of volatiles into areas of low pressure (Figure 12). Vertical white syenite veins 5 to 10 mm in width cut shonkinite towers near the base of the butte. These, along with the streaks were probably formed from extension as the laccolith settled and bulged into the sediments.

Contact Zone

The contact zone itself is variable, but is approximately 10 meters thick. From a distance, the contact between shonkinite and syenite looks quite sharp. Up close, however, it is not as distinct and sometimes hard to discern due to vegetation and erosion. At the top of the shonkinite is a horizon of large syenite blobs up to 10 m in diameter. They occur at the same elevation all around the butte -- approximately 1495 m (4900 ft), see Figure 13. The upward-protruding syenite blobs are coated with shonkinite; some are completely exposed as syenite knobs, others are syenite knobs covered by shonkinite (Figure 14). In some areas the contact between blobs and shonkinite appears diffuse; in other areas, the contact is very sharp -- less than one-half centimeter. The sharp contacts are marked by a physical boundary in which enclosing shonkinite overlaps



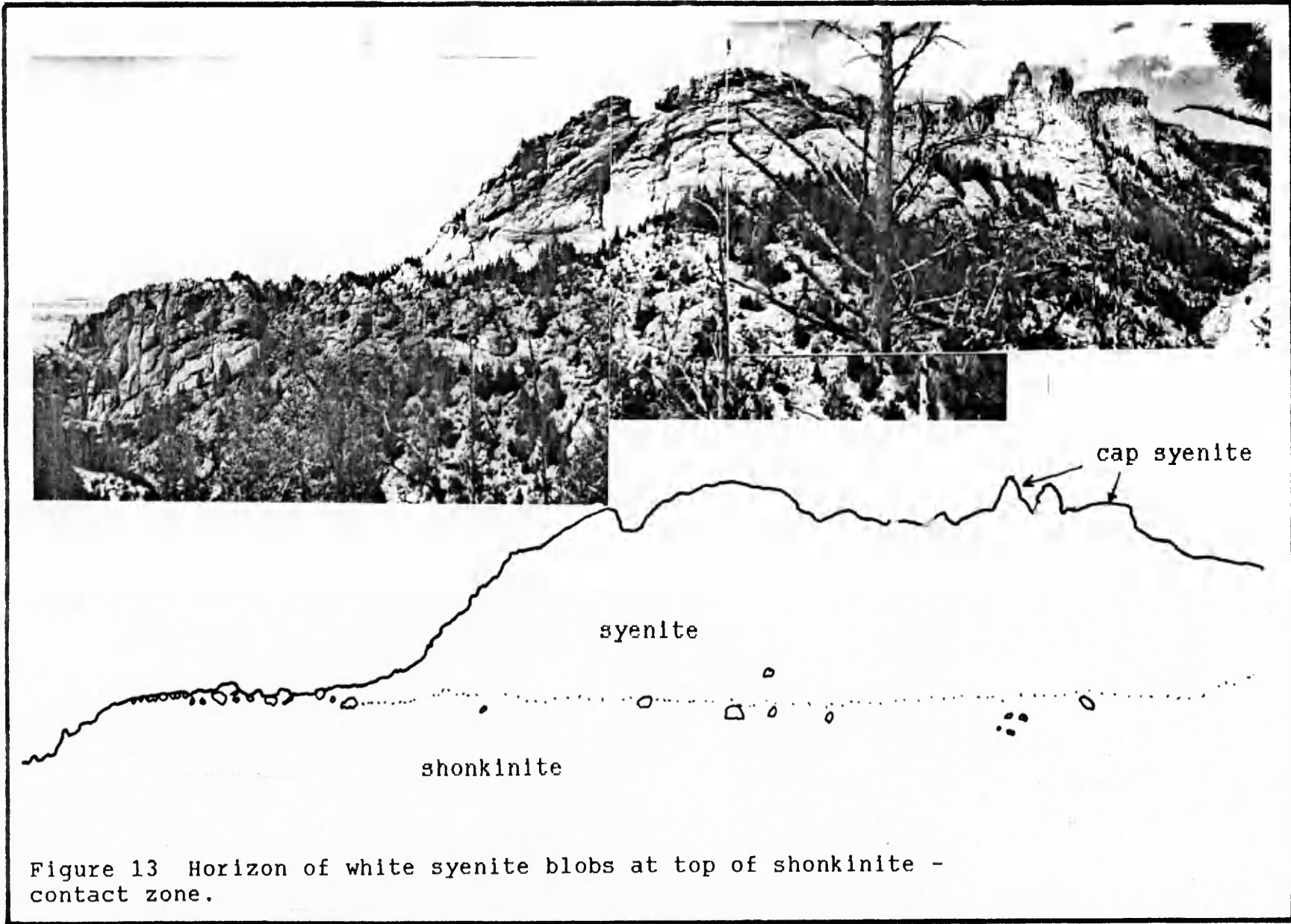
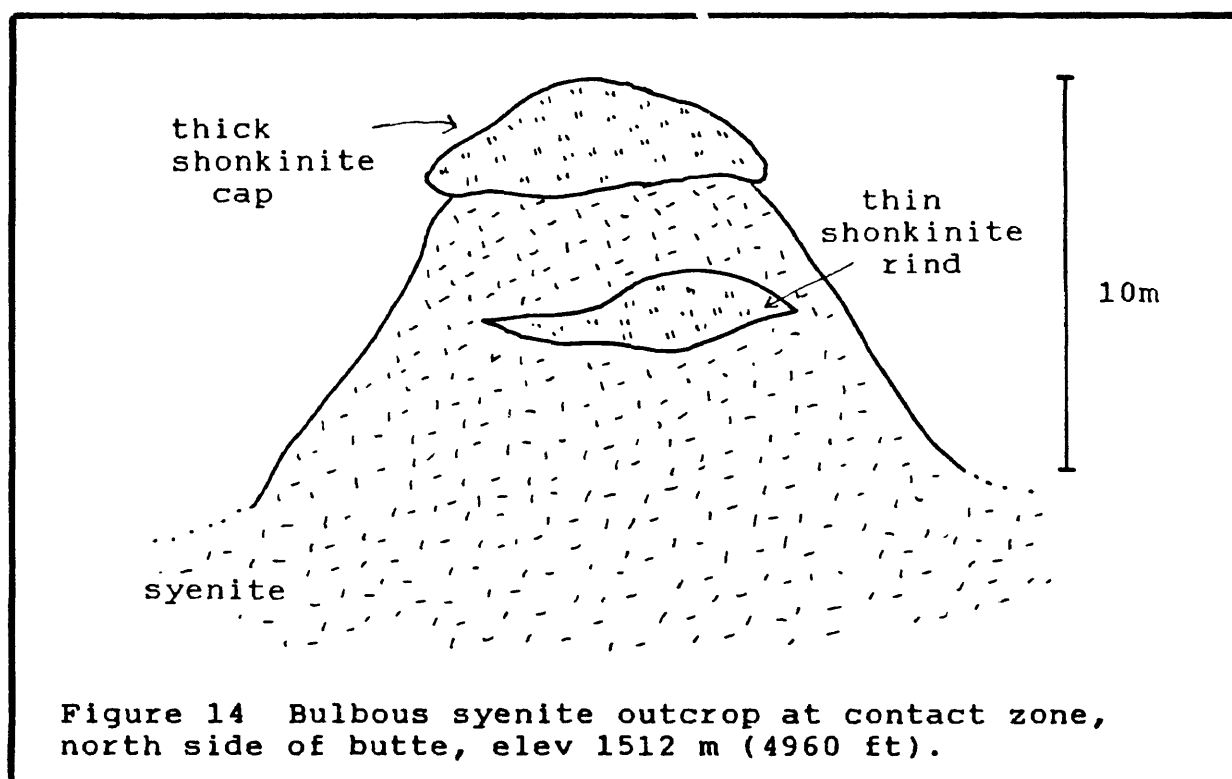


Figure 13 Horizon of white syenite blobs at top of shonkinite - contact zone.



the underlying syenite -- as if one could peel the mafic rind away from the syenite (Figure 15). The diffuse contact is marked by a change in mafic mineral content, but appears as a smooth transition from shonkinite to syenite, with no substantial boundary between (Figure 16a,b).

Syenite

Above the contact zone of blobs, the syenite erodes into a bit of a slope-former which allows traversing the contact zone across parts of the butte. In a short distance, however, the gentle slope gives way to steep, rugged hillsides of conifers and thick ground cover which break into the abrupt cliffs and precipitous walls of syenite. Here the syenite appears to be coated by the mafic rind of shonkinite (mentioned above). Exposed in the walls of syenite, the shonkinite coating resembles swirled streaks intermingled with syenite. Because these areas are on inaccessible cliffs, it is hard to examine them closely. In a few areas, the swirling is not convincing and is suggested here to be a shonkinite coating which has a swirled appearance due to irregular erosion and exfoliation. See Figure 17.

The large circular white patches, mentioned at the beginning of this section, are two-dimensional for the most part, and recessed into the cliff. In some areas, the

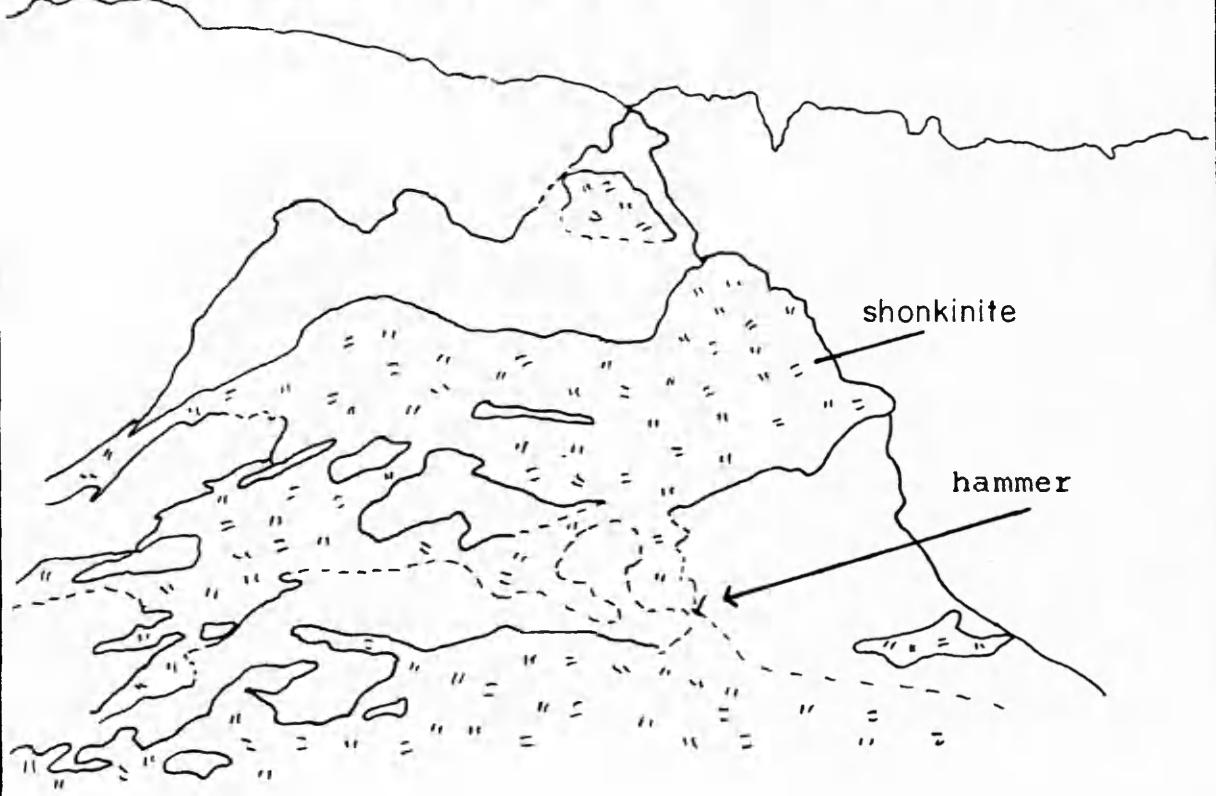


Figure 15 Syenite blob covered with shonkinite rind, contact zone, elev 1500 m (4920 ft). Base is 4 m.

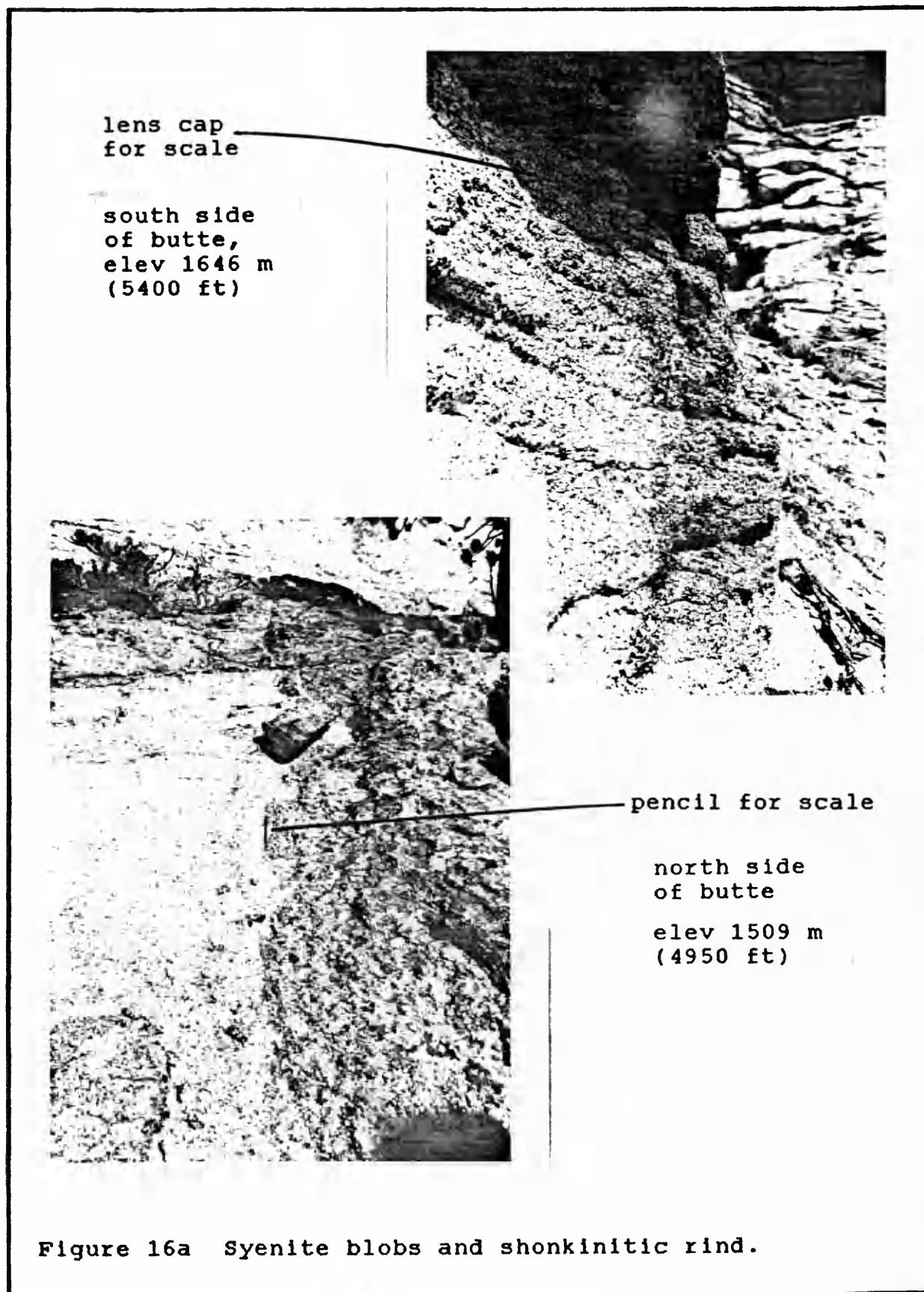
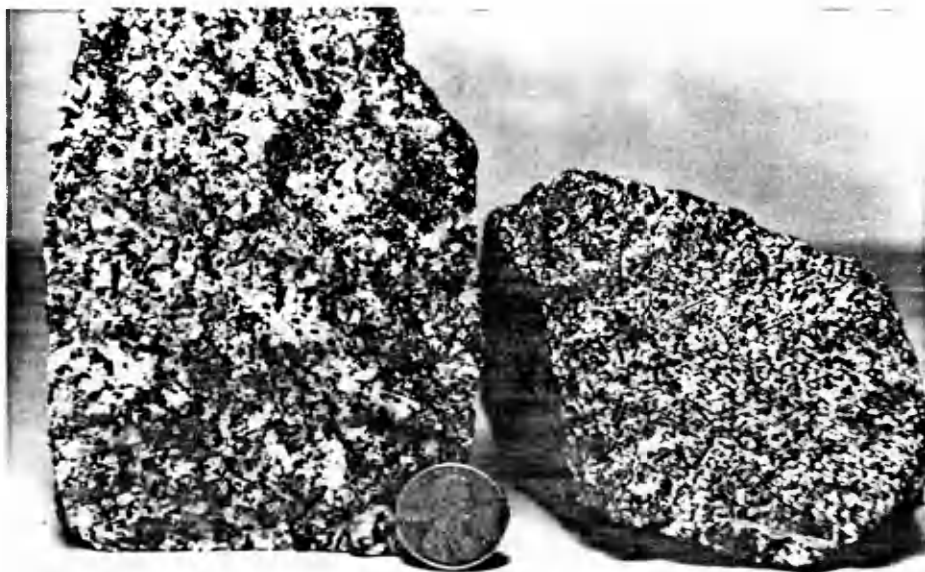


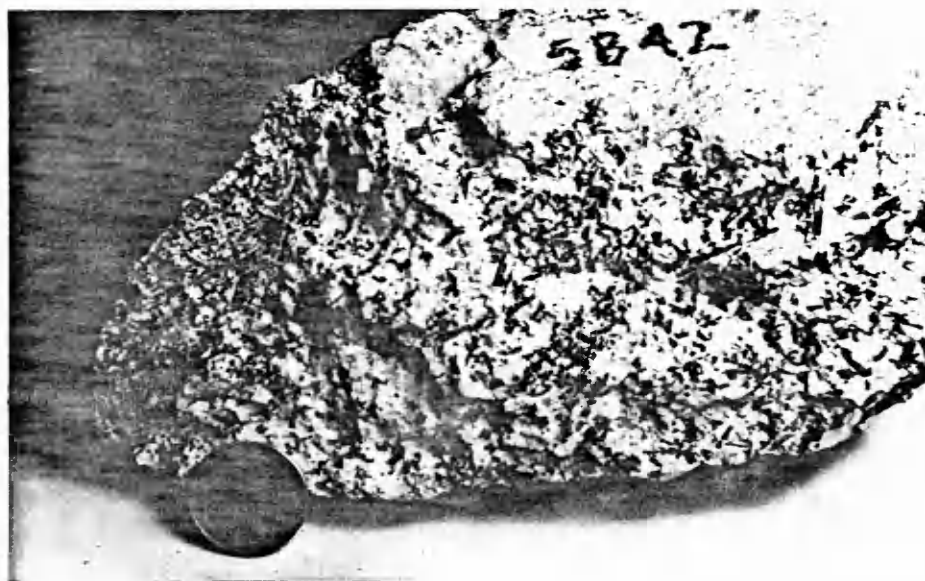
Figure 16a Syenite blobs and shonkinitic rind.



SB21b

SB21

elev 1500 m (4920 ft)



SB42 elev 1554 m (5100 ft)

Figure 16b Syenite and shonkinitic rind.
Photos: Scott M. Helm

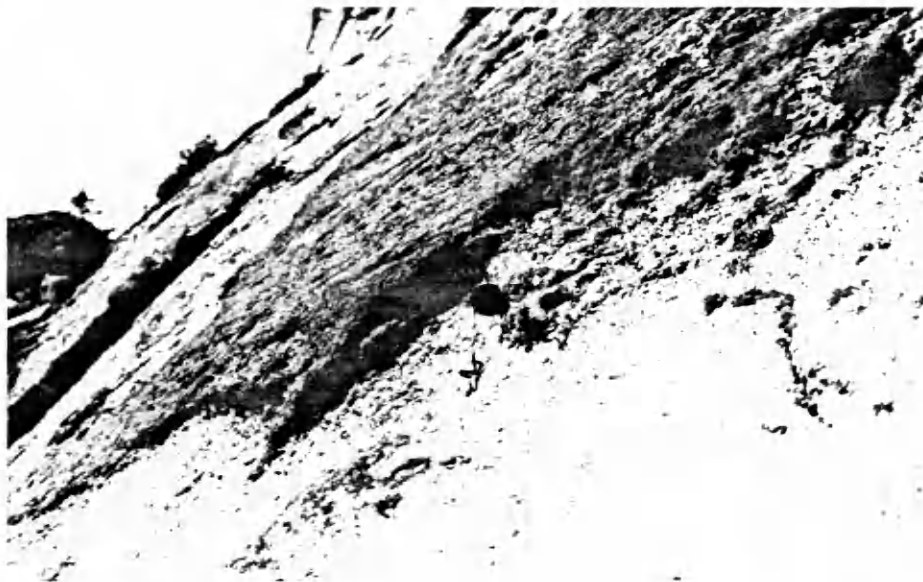


Figure 17a Smooth surface of syenite with shonkinite rind, South side of butte. Lens cap for scale.



Figure 17b Swirled streaks in syenite, and shonkinite rind, south side of butte. Field assistant is 1.8 m high (5'10")

syenite protrudes beyond the slope and is partly covered by a mafic rind (Figure 18). The origin of these features is unknown. If the mafic rind is the remains of a chill zone, then the protrusions may represent areas where the syenite bulged out into the surrounding sediments. The recessed patches may represent syenite bulges that splayed off.

The other unique features of the syenite, not mentioned previously, are large blobs, like those in the upper shonkinite, which are enclosed in syenite at the base of the cap syenite. Like the circular white patches, the white syenite blobs are coated by a slightly more mafic rind. The difference between these blobs and the white patches is their shape: these blobs are clearly three-dimensional and outcrop on the southeastern "corner" of the butte just below a cliff of cap syenite (Figure 19). From the base of the butte, these blobs are visible at the top of the main syenite and protruding up into the cap syenite. It is hard to determine exactly what the relationship of the blobs is to the surrounding syenite: whether they are completely isolated blobs, suspended in the surrounding material; or whether they are interconnected. These white blobs differ from the ones in the contact zone coated by shonkinite. Their coating is not very mafic and is much thicker than the rind that covers the two-dimensional circular white patches (compare Figures 16a and 19). Like the blobs at the top of

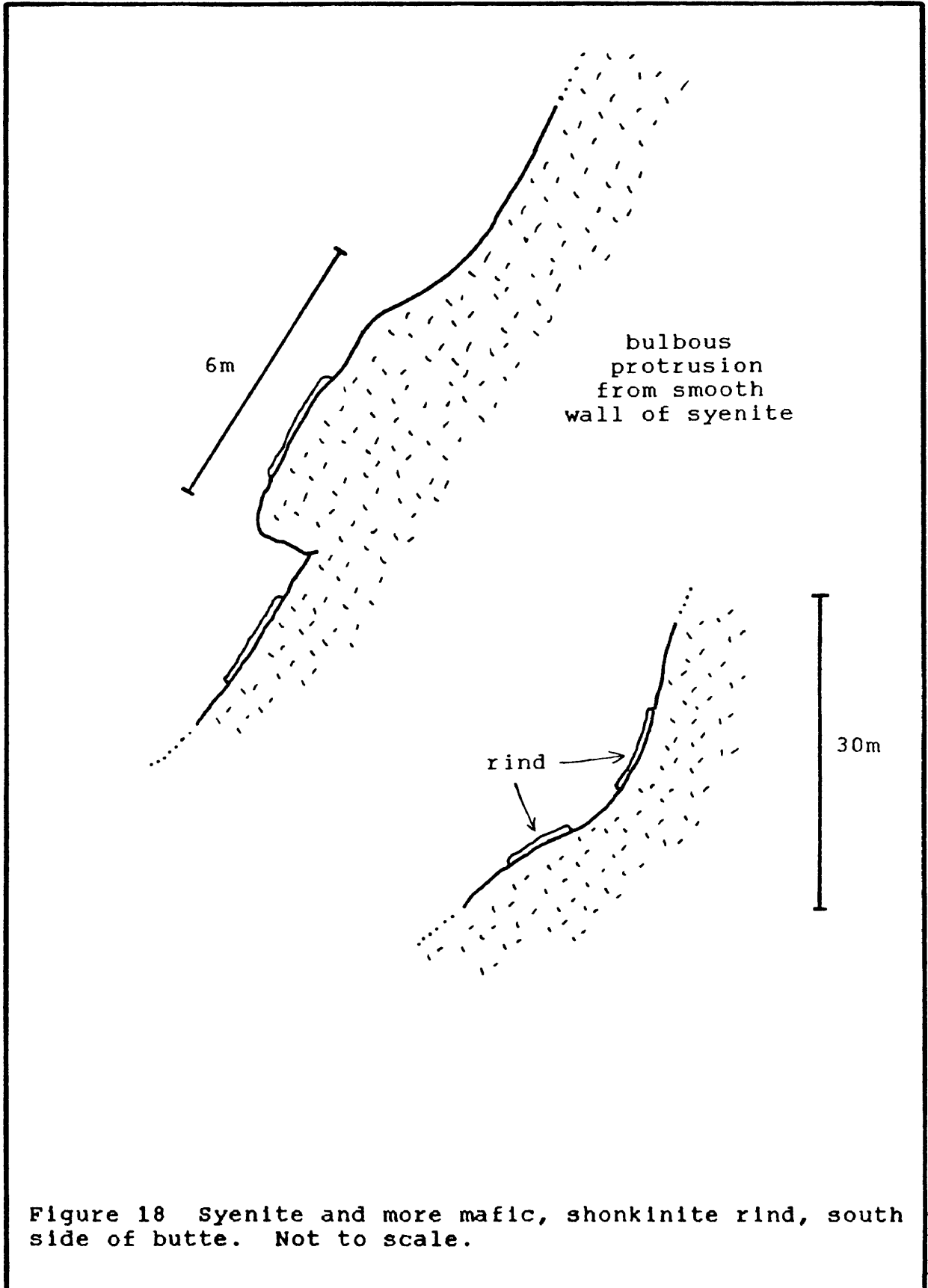


Figure 18 Syenite and more mafic, shonkinite rind, south side of butte. Not to scale.



Figure 19a
 Contact between
 white syenite blob
 and its slightly
 more mafic coating,
 southeast side of
 butte, elev 1646 m
 (5400 ft). Hammer
 is 28 cm (11 in).

Figure 19b
 Three-dimensional
 syenite blob with
 more mafic coating,
 same location as
 19a.

Small tree is
 approximately
 1 m high.



the shonkinite, these appear to have been trapped in their ascent through the magma chamber, and strongly suggest liquid immiscibility.

Cap Syenite

The cap syenite has been described as a sodalite syenite (Lindgren, 1893) with as much as ten percent sodalite. It is darker in color than the syenite below and horizontally jointed, which gives rise to the butte's flat top. It has a very small percentage of mafic minerals and no ocelli. The cap syenite is full of miarolitic cavities and cut by small pegmatitic veins with potassium feldspar crystals up to 3 cm.

ANALYTICAL TECHNIQUES

Whole-Rock Geochemical Analyses

The majority of the geochemical analyses used in this study were obtained from Donald Hyndman, University of Montana. This suite of 29 analyses includes one sample of a sill (chill zone), and 3 samples of cap syenite. The rest include shonkinite, syenite and mafic rind samples from various locations throughout the butte. I collected the remaining 5 samples for geochemical analysis; these include an extremely fresh sample of the chill zone (SB-7).

Appendix A is a complete list of samples, their elevations

and rock types. Plate 1 gives the locations of samples used Pullman for analysis on an automatic Rigaku 3370 X-Ray spectrometer. All other samples were analyzed by X-Ray Fluorescence and Neutron Activation at X-Ray Assay Laboratories, Inc, Don Mills, Ontario. See Appendix B for geochemical data, and Appendix C for information on precision and accuracy of results.

Election Microprobe

Seven polished thin sections were prepared by R.A. Petrographic, Los Angeles, California. Carbon-coating was done at University of Montana. Salite crystals from seven samples through a vertical sequence of shonkinite were analyzed at the University of Montana using an ARL EMX probe, operating at an accelerating voltage of 15 kV, a beam current of 0.04 μ amps, and a beam diameter of approximately 5-9 μ m. Probe samples include, from chill zone to uppermost shonkinite, SB-61 (sill), SB-60, SB-58, SB-55, SB-52, SB-49, and SB-47. Two or three euhedral, clear and unaltered bipyramidal grains from each sample were selected for analysis for silicon, aluminum, iron, magnesium, and calcium. Standards were run 2 or 3 times at intervals of about 1.5 hours between unknowns. Each run for standards consisted of 6-10 good analyses of two points on the grain. The unknowns were analyzed in a similar fashion, first 2

points in the core for at least 10 analyses, then 2 points on the rim. Due to problems obtaining consistently acceptable totals, analyses of cores and rims have been averaged to represent the composition of the entire grain. Microprobe data is tabulated in Appendix D.

Specific Gravity Measurements

Twenty-five samples from a vertical sequence of shonkinite and syenite were weighed for specific gravity. The samples were weighed in air, soaked overnight, then weighed in water on an OHAUS triple-beam balance. The procedure was repeated three times and the results averaged.

PETROGRAPHY

Approximately 28 samples of all rock types at Square Butte were studied petrographically for mineral composition and textures. Particular attention was paid to the chill zone and the vertical section of shonkinite samples.

Previous petrography on similar rocks in the Highwood Mountains and at Shonkin Sag laccolith refer to the opaque oxides as titanomagnetite (Nash and Wilkinson, 1970) or iron-titanium oxides (O'Brien et al., 1991). Although their composition was not determined here, all opaque oxides will be called magnetite for simplicity and because all the rocks with opaque oxides are magnetic.

In all samples the sanidine component of pseudoleucite is found intergrown with zeolites. That the zeolites are definitely an alteration product of nepheline was not determined; however, such is the inference of Nash and Wilkinson (1970) in their study of Shonkin Sag laccolith. Zeolites are not restricted to pseudoleucite. Fresh sanidine displays patchy alteration to zeolites, and zeolites fill interstices between minerals.

Microprobe analyses of pyroxene through a vertical section of shonkinite identify the mineral as salite (Figure 20). Analyses are compiled in Appendix D.

Chill Zone

This rock is referred to as a mafic phonolite by O'Brien et al., 1991, to be consistent with past literature. However, for this study it is called *porphyritic shonkinite* to stress that it is the same composition as the shonkinite, and differs only in texture. Approximately 30% euhedral salite and 1.5% subhedral-euhedral olivine phenocrysts are present in a fine-grained, chilled groundmass. Salite is strongly zoned, often twinned, pale green-yellow in plane light, and mainly occurs as individual stubby grains; occasionally it forms glomerophenocrysts. The largest salite phenocrysts are 3mm in length. A titanium content in the salite is inferred from anomalous grey-blue interference

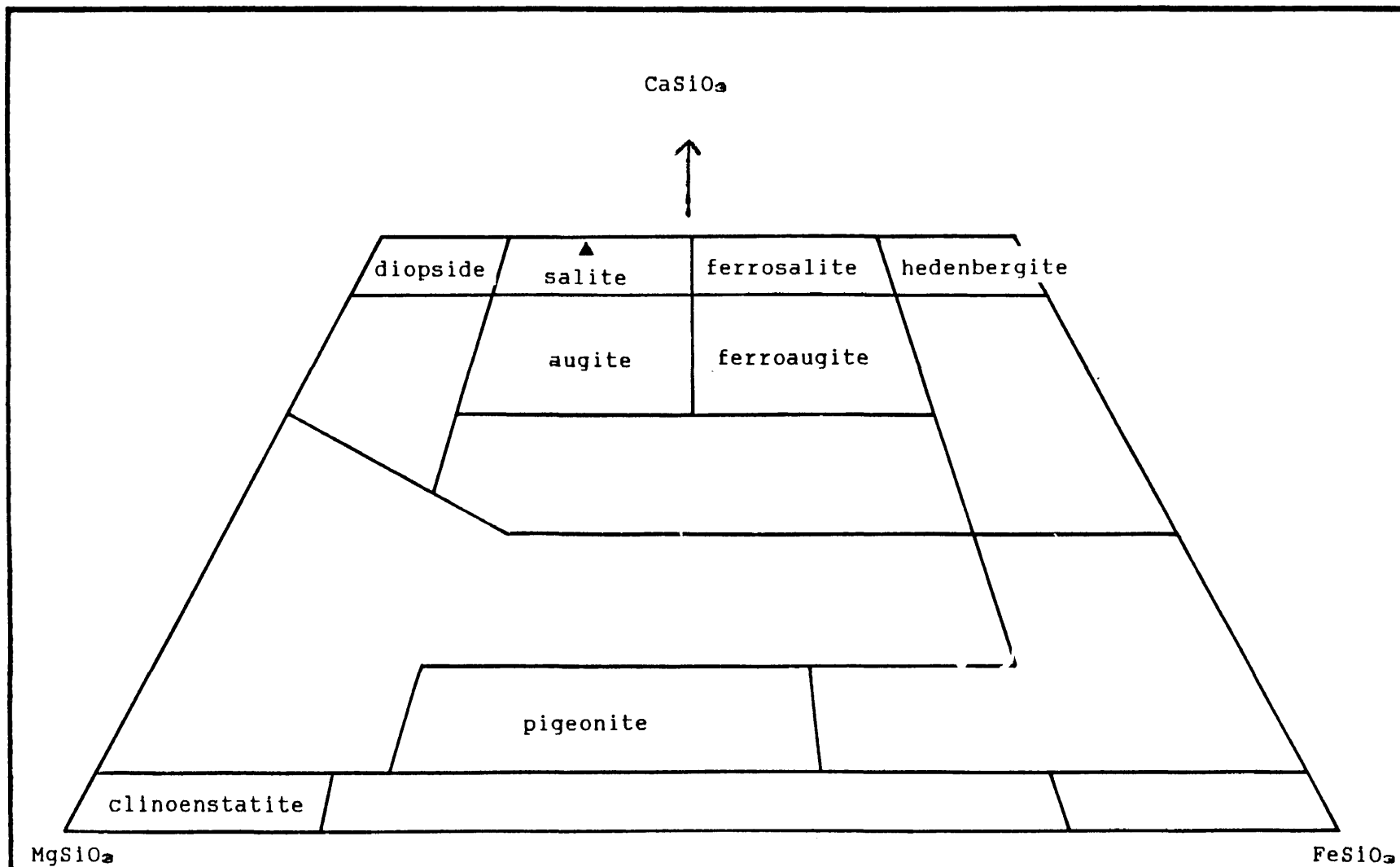


Figure 20 Average pyroxene composition plotted on pyroxene trapezoid. Fields after Tröger, 1979.

colors. Euhedral phenocrysts of pseudoleucite (sanidine + zeolite and analcime after nepheline?) cluster around clinopyroxene grains and are individually scattered throughout the rock (Figure 21, photos). Olivine is commonly altered to iddingsite. The groundmass exhibits a quench texture of acicular brown biotite, clinopyroxene, and feldspar. Magnetite and apatite are common.

Contained within chill zone sample SB-61 is a xenolith of the same mineralogy as the whole rock. The texture is different, however, setting it aside from the rest of the rock: The fine-grained holocrystalline groundmass of the xenolith surrounds resorbed phenocrysts of salite and olivine which contain numerous inclusions of magnetite and apatite. Fewer euhedral zoned salite crystals are present. The groundmass of the xenolith differs from the rest of the rock in that it is more felsic and that biotite is present, but not acicular. The xenolith is interpreted as having formed under slower cooling conditions (no quench texture), and brought up with the magma which crystallized under lower temperature/pressure conditions. There is no pseudoleucite in the xenolith.

Shonkinite

Samples SB-60 through SB-47 represent a vertical sequence through the shonkinite between elevations of 1326

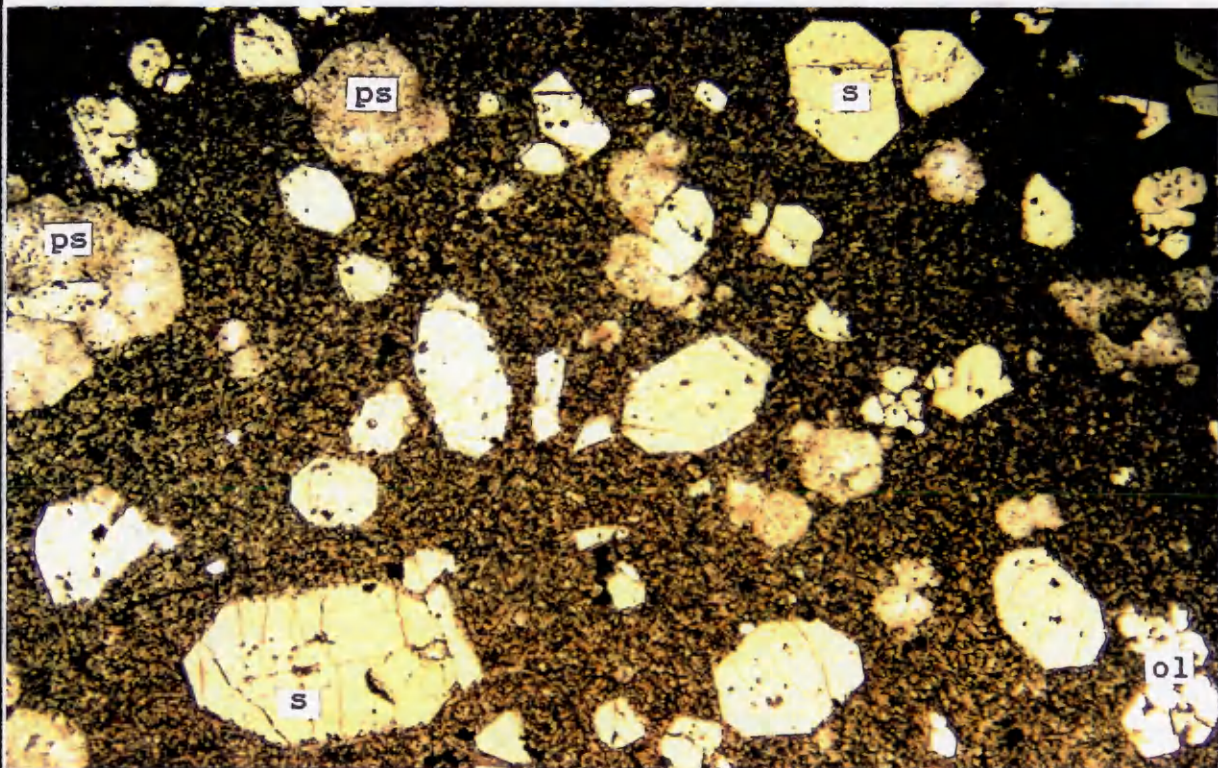
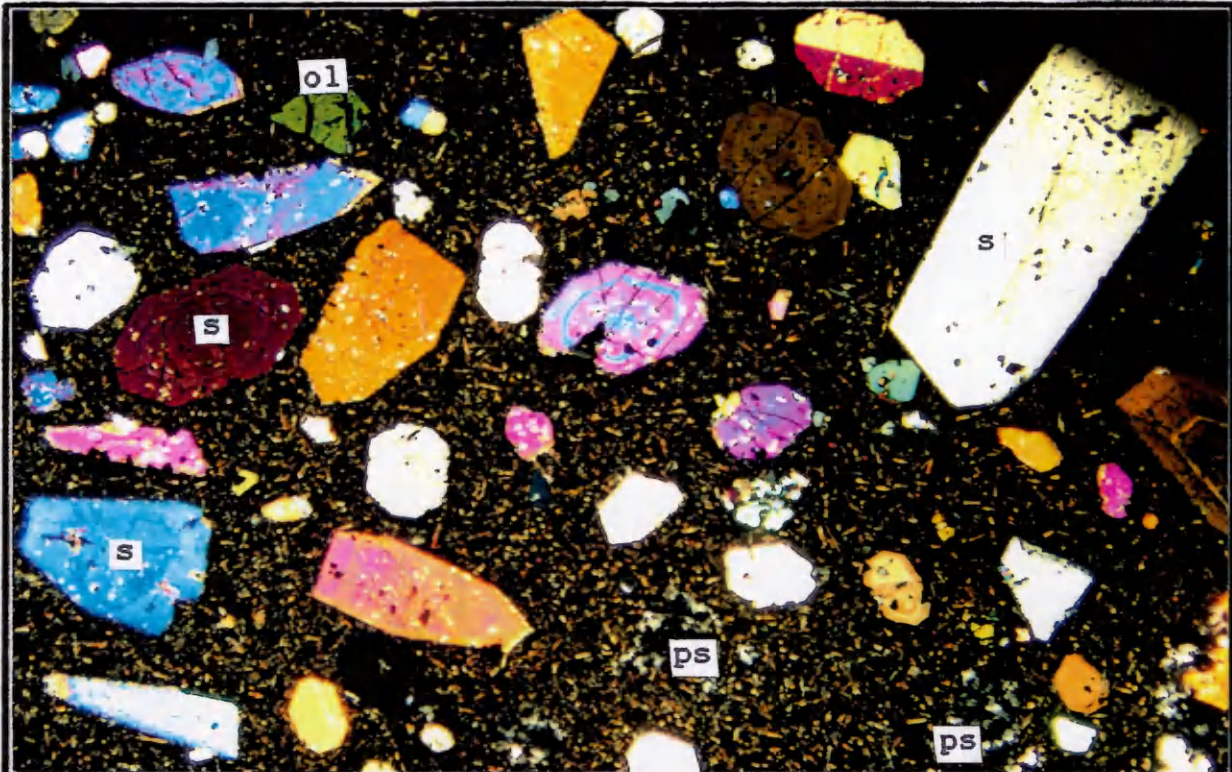


Figure 21 Photomicrographs of pseudoleucite shonkinite (chill zone). Top-crossed polars; bottom-plane light. ps=pseudoleucite, s=salite, o=olivine. View 8mm. Note: views are not the same.

and 1501 meters. Mineral composition is listed in Table 1. Texturally, there is a continuous gradation from chill zone through shonkinite in which aphanitic groundmass coarsens, pseudoleucite crystals lose their euhedral borders, and the rock becomes more equigranular. Generally, all shonkinite samples contain titaniferous subhedral to euhedral salite which is commonly twinned and exhibits hour-glass zonation and varying degrees of oscillatory zoning. The pyroxene is pale green in plane light. All samples have abundant apatite, varying amounts of opaques, and sanidine intergrown with zeolites analcime nepheline plagioclase. Anhedral to subhedral olivine varies in composition but is generally in the range of Fo85-88. Nearly all olivine is altered to iddingsite to some degree and much is rimmed by biotite. Magnetite increases in abundance upwards and biotite crystals become larger, redder (more ferric iron), and more poikilitic as well. Green biotite is a minor constituent. There are no cumulus textures. Order of crystallization started out as olivine + apatite + magnetite, followed by salite and (pseudo)leucite (?), followed by biotite, sanidine. With progressive cooling, pyroxene and feldspar crystallized together in a subophitic texture.

As mentioned previously, ocelli in the shonkinite and syenite have been determined to be pseudoleucite and not

Table 1 PETROGRAPHY OF SHONKINITE

Through a vertical section of shonkinite, south side of butte.

SB-61 is sill (chill zone) for comparison

sample	elev (m)	max salite size (mm)	avg of large salite (mm)	salite zoning	% sal, ol, bio, mgt (200-400 points counted per section)
SB-61	1317	3	2.7	very distinct	30, 1.2, gm
SB-60	1326	3.5	3	distinct	32, 2, 6, 3
SB-58	1365	10	5.5	faint to moderate	54, 2, 8, 2
SB-57	1378	8	5.5	moderate to distinct	65, 2.5, 8, 2.5
SB-55	1405	5.5	4	moderate to distinct	55, 3, 9, 2
SB-54	1414	6	4	faint to moderate	52, 2, 14.5, 2.5
SB-52	1439	4.25	3.8	very faint	48, 0.5, 11, 6
SB-51	1451	3.75	3.4	moderate	46, 5, 13, 5
SB-49	1472	6	3.7	very faint	47, 1, 11, 4
SB-48	1487	8	4.5	faint	47, 3, 5.5, 6.5
SB-47	1503	3.75	2.8	none	35, 0.5, 7, 10

sal=salite bio=biotite mgt=magnetite ol=olivine
gm= groundmass

immiscible blebs preserved in the rock. Indeed, blebs of immiscible felsic material would probably have the same composition and similar textures as the pseudoleucite in the shonkinite. Their presence would imply that a once-homogenous magma split into two immiscible ones. The immiscible blebs, then, would represent the immiscible liquid trapped in the host from which it was separating. In the chill zone, however, are clear, nearly euhedral crystals of pseudoleucite. If these were immiscible droplets, they would not have the characteristic leucite shape. In the lower shonkinite, and upwards through a vertical section of shonkinite, the pseudoleucite grains progressively lose their crystal borders. Also, felsic material making up the crystals becomes coarser-grained, and grows in a nearly radiating pattern. By observing this transition, I feel that the leucocratic blebs are pseudoleucite and did not form through liquid immiscibility.

Immiscible blebs in lamprophyres have been described by Foley (1984) as having "abundant centre-nucleated mafic minerals, principally clinopyroxene. The matrix minerals within the globular structure are nepheline and analcite, with minor K-feldspar. These globules may have smaller analcite-filled globules within them." Aside from the difference in matrix minerals, this could be a description of some of the ocelli at Square Butte. Foley's globules, or

ocelli, differ markedly in composition from their host. For example, silica is nearly 8% greater, alumina is over 6% greater and phosphate is double in the leucocratic globules. Similar analyses of leucocratic ocelli and host matrix in shonkinite at Square Butte may provide further evidence of their origin.

O'Brien et al. (1991) describe a similar occurrence of pseudoleucite in rocks from the Highwoods. In the coarser-grained shonkinites, the pseudoleucite "consists of rounded patches of coarse Ba-poor sanidine + nepheline symplectic intergrowths which merge with late crystallized sanidine laths to form the felsic component of the rock." Throughout the Square Butte shonkinite samples, two generations of feldspar are present. The first is altered sanidine in the pseudoleucite, and the second is large, tabular grains of sanidine which are often poikilitic and/or subophitic with other mineral constituents. See Figure 22 for photographs of typical shonkinite.

From these descriptions of immiscible felsic blebs in alkaline rocks and pseudoleucite from other shonkinites, it is easy to see how the felsic ocelli in the Square Butte samples could be thrown into either category.

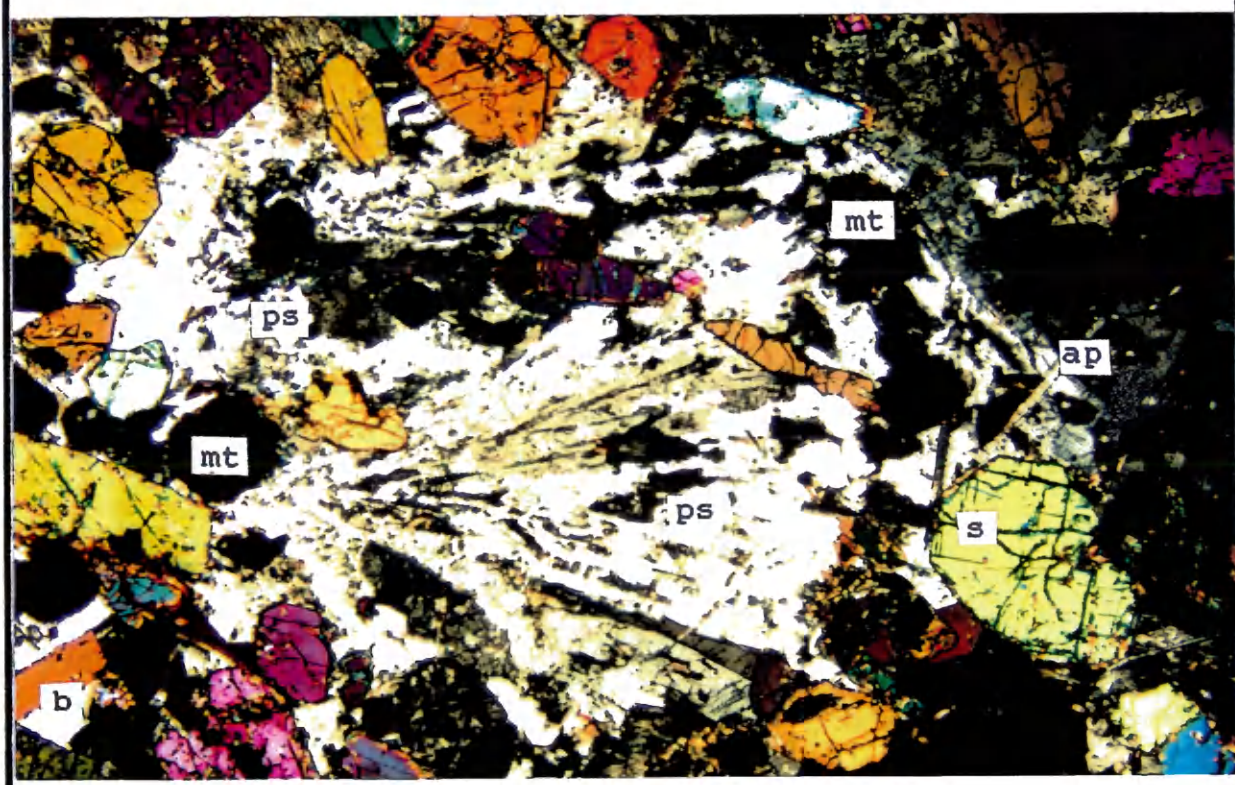
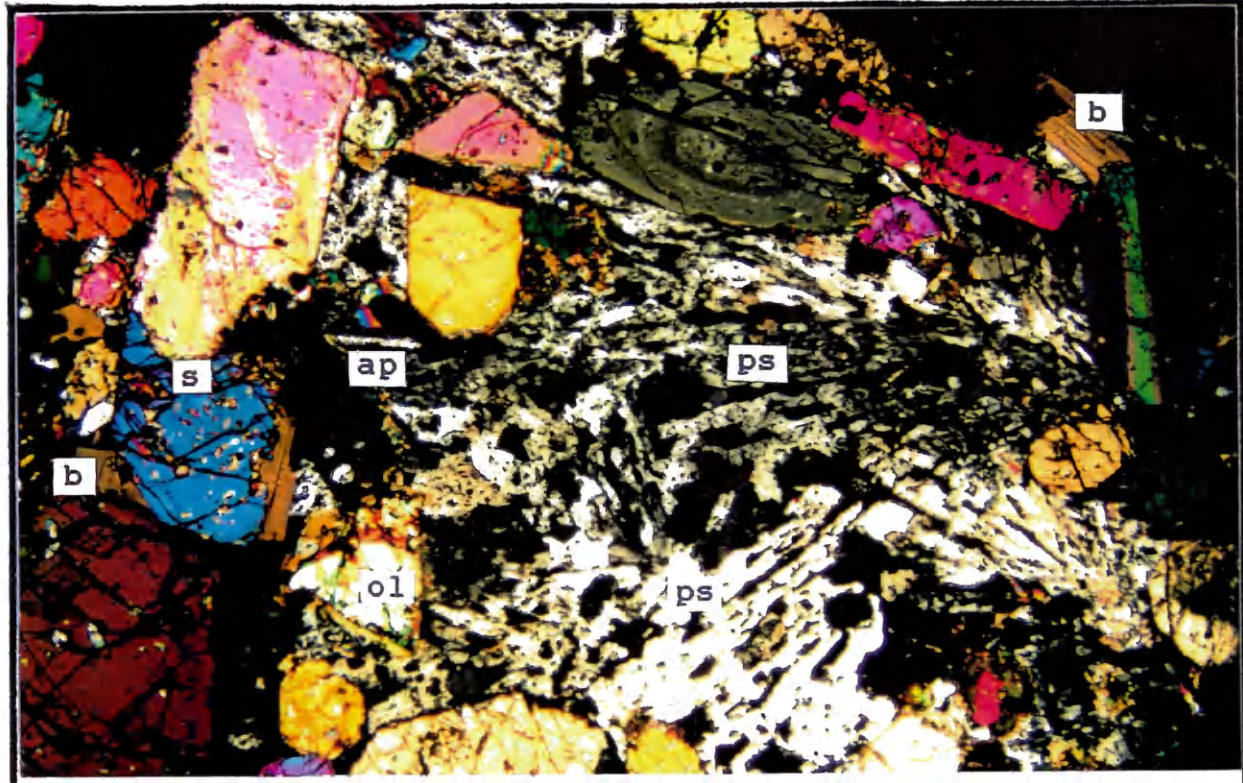


Figure 22 Photomicrographs of shonkinite, crossed polars. ps=pseudoleucite, s=salite, ol=olivine, b=biotite, ap=apatite, mt=magnetite. View 8mm.

Syenite

The mineralogy of the syenite is essentially the same as shonkinite with the major difference being the proportion of mafic minerals. Percentages of salite and hornblende are variable with elevation and range from 1-13% salite, and 3.3-10% hornblende. Biotite ranges from 1.3-8.7%, magnetite makes up approximately 2%, and olivine, where present, makes up less than 1%.

Two optically different compositions of potassium feldspar are present. Sanidine, with a 2V angle of 5 degrees or less, occurs within large (1 cm), spherical felsic patches (ocelli), graphically intergrown with zeolites. Orthoclase, some strongly zoned and with a 2V ranging from 35 to 90 degrees, commonly grows in long laths and as large grains optically intergrown with pyroxene and magnetite. Orthoclase occurs outside and between the ocelli. This clear identification of two different potassium feldspars, and their different occurrences and textures, confirms the ocelli as being pseudoleucite which crystallized earlier and floated towards the syenite. Much smaller, nearly euhedral pseudoleucite crystals also occur in large feldspar grains.

Salite is commonly rimmed by strongly colored green hornblende (ferrohastingsite?) and embayed. In some samples, the hornblende is deep brown (ferropargasitic

hornblende, formerly barkevikite). Olivine (Fo40-70) is present in small amounts in nearly all syenite samples, but is heavily embayed and occurs enclosed in large poikilitic brown biotite grains. Nepheline is scarce, but does occur as fresh anhedral grains in sanidine. Zeolites are ubiquitous, not only intergrown with feldspar, but also filling interstices between grains. Accessory minerals present in the syenite include plagioclase, muscovite, zoisite, sphene, opaques, apatite, and carbonate apatite. The composition of apatite is undetermined, but carbonate apatite is identified by higher birefringence and sector twinning in basal sections (Deer, Howie and Zussman, 1962); probably secondary. See Figure 23 for photographs of syenite.

Cap Syenite

The cap syenite is also referred to by previous authors as a sodalite syenite, for the presence of sodalite. The cap syenite contains brown ferropargasitic hornblende which is zoned and twinned. Sanidine occurs as long laths oriented such that the triangular interstices between crystals are filled with zeolites and sodalite. Opaque oxides are absent as is biotite; apatite is rare. Pegmatitic dikes have identical mineralogy and sport feldspar phenocrysts up to 3 cm. The feldspar is altered

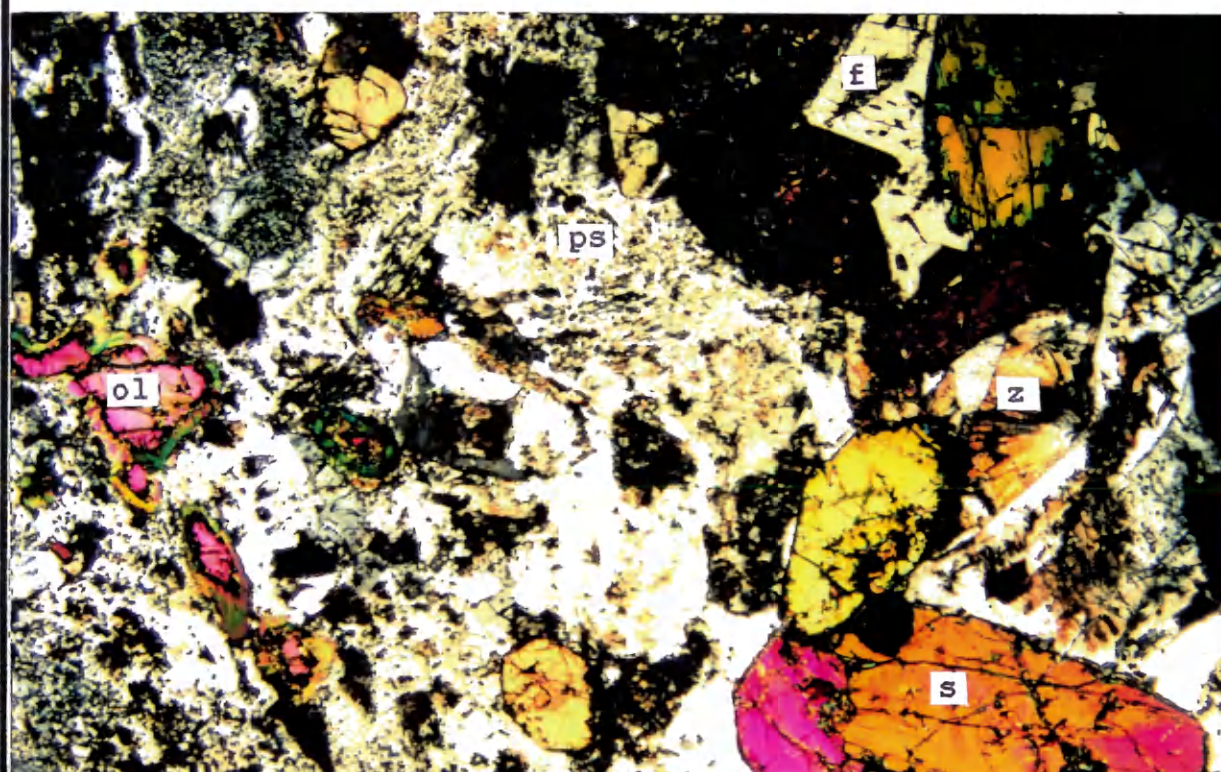
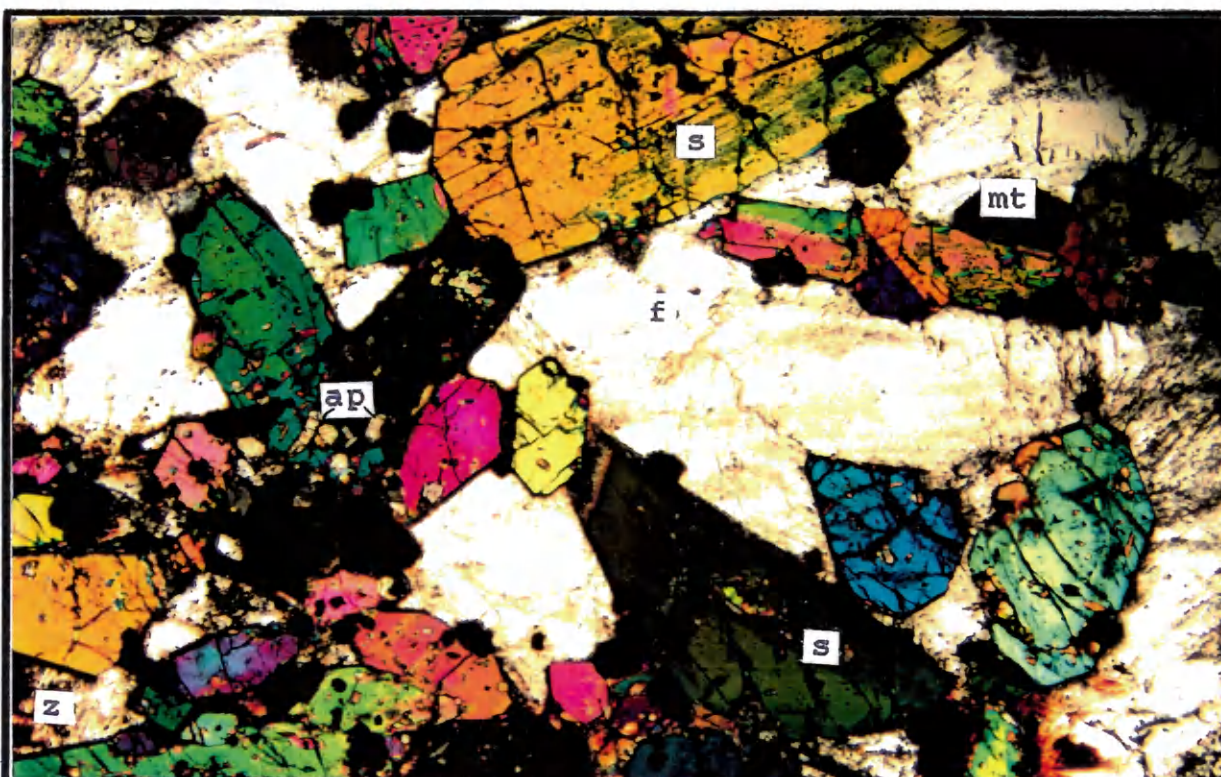


Figure 23 Photomicrographs of syenite, crossed polars. f=feldspar, s=salite, b=biotite, mt=magnetite, z=zeolite, ap=apatite, ol=olivine, ps=pseudoleucite (?). View 8mm.

and difficult to obtain optic figures from. It is identified as orthoclase with a 2V angle of about 30 degrees. Pseudoleucite is completely absent.

DIFFERENTIATION MODELS

1. LIQUID IMMISCIBILITY

A single magma may split into two immiscible magmas when a reduction in temperature and/or pressure causes a change in the free energy of the system. The magma may separate immiscibly into two liquids, one rich in metals and non-bridging oxygens and one rich in silica and a few metal cations (Ryerson and Hess, 1978).

While liquid immiscibility gives rise to a felsic portion with a gross composition of granite, such as can be derived by crystal fractionation, the partitioning of minor constituents in the two processes is quite different. Chemical work on immiscible felsic and mafic melts in the alumina, silica, potassium, and iron oxide system shows that rare-earth elements are depleted in a felsic melt, and incompatible elements are enriched in the mafic melt (Watson, 1976). This is a pattern opposite that for formation of magmas by fractional crystallization. Texturally, immiscible droplets of one liquid should be visible, trapped in the other liquid. And the two

immiscible phases should be in equilibrium with one another, at least at the time of formation.

Evidence for and against liquid immiscibility

Specific Gravity

Many field relations at Square Butte point toward liquid immiscibility as perhaps the primary differentiation mechanism, but no data exclusively support this process. Almost any line of evidence that suggests liquid immiscibility can be explained by other processes. For example, the specific gravity pattern through the shonkinite supports the model of liquid immiscibility (refer back to Figure 4). If a homogeneous magma split into two immiscible ones on cooling, relatively constant density patterns would be expected from both the felsic and mafic portions, although those two separate densities should be radically different. This is what is seen at Square Butte.

However, if crystal fractionation is solely responsible for the differentiation, then something was inhibiting crystal settling. For example, if the magma was degassing, the upward migration of volatiles may have inhibited crystal settling. Or, crystal fractionation involved the rise of pseudoleucite, rather than (explicitly) the settling of salite.

Iron and Magnesium Content of Salite

Microprobe analyses of salite crystals from a few representative samples of shonkinite are plotted in Figure 24 as iron and magnesium versus elevation (see Appendix D for microprobe data). The pattern agrees with the specific gravity measurements. Iron and magnesium behave antithetically and remain relatively constant throughout the shonkinite. There is a slight decrease in iron upward from the chill zone samples, and a slight increase in iron near the top of the shonkinite. Like the specific gravity measurements, the graph does not entirely support a model of crystal fractionation, but is compatible with liquid immiscibility and volatile migration.

Ocelli

Another feature at the butte which has been used previously to suggest liquid immiscibility is the ocelli. I believe, as stated above that the ocelli at Square Butte are believed to be pseudoleucite, but for the sake of discussion here, I will treat them as ocelli.

Philpotts (1976) studied dike and sill rocks in the Monteregean alkaline province of Quebec. In his study, oversaturated leucocratic ocelli were hand-picked from the undersaturated mafic host and each was analyzed separately. These analyses, when plotted on an FMA diagram, roughly

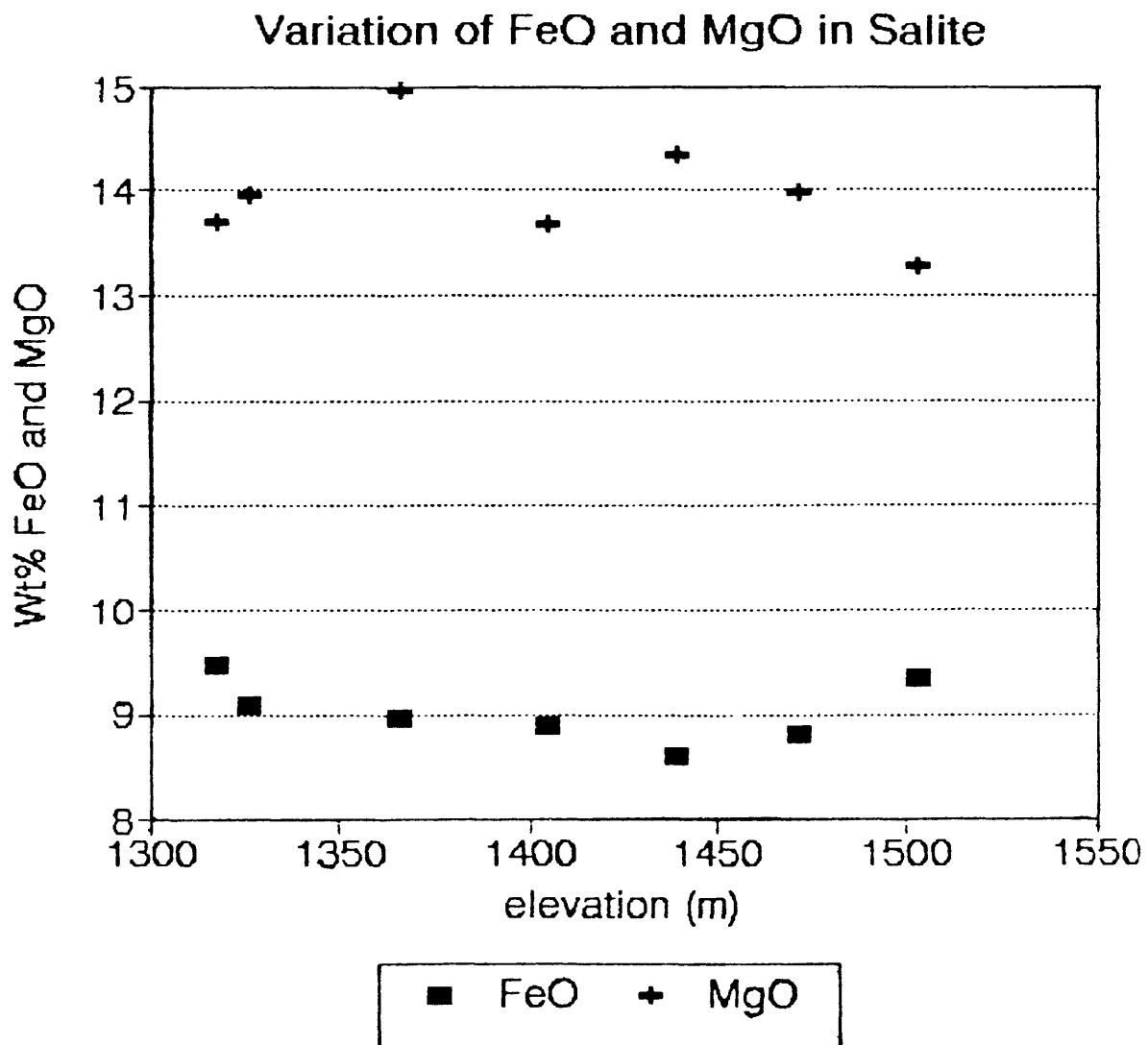
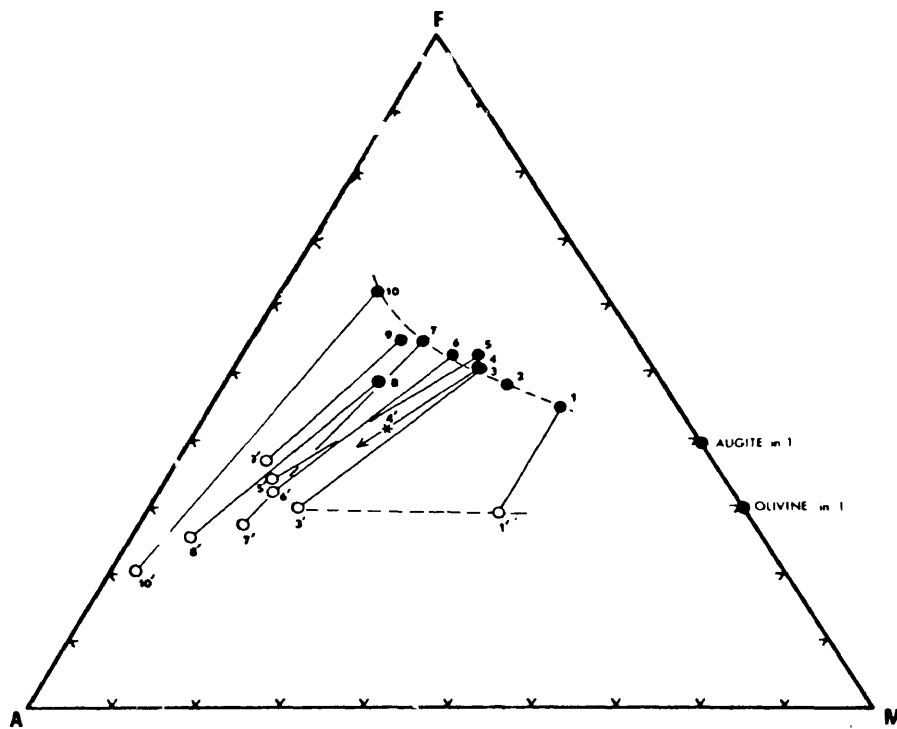


Figure 24 Variation of iron and magnesium content of salite crystals through shonkinite.

outline an interpreted immiscibility field (Figure 25).

I plotted syenite blobs and their more mafic syenite rinds on an AFM diagram as Philpott's did for his ocelli-matrix pairs (Figure 26). It should be noted that the experimental method here is crude compared to Philpott's, and perhaps a comparison cannot even be made. The large felsic blobs at Square Butte and more mafic rinds are all undersaturated with respect to silica and the analyses represent whole-rock composition, not individual ocelli-matrix pairs.

Additionally, Philpott's samples are significantly lower in potassium and calcium; higher in titanium. Ideally, I was hoping to see a slight separation of the syenite blobs from their mafic rinds, possibly outlining an immiscibility field. But the only separation is between the shonkinites and syenites. What is interesting, however, is the iron-rich character of the more mafic syenite relative to the magnesium-rich character of the shonkinite. This can be interpreted as an iron enrichment trend during crystallization, and does not provide any further insight into the possibilities of liquid immiscibility at Square Butte.



Modified from Philpotts, 1976

Figure 25 AFM plot of ocelli (open circles) and matrix (solid circles) from Montereyan dikes and sills. The dashed lines outline approximately the interpreted field of immiscibility.

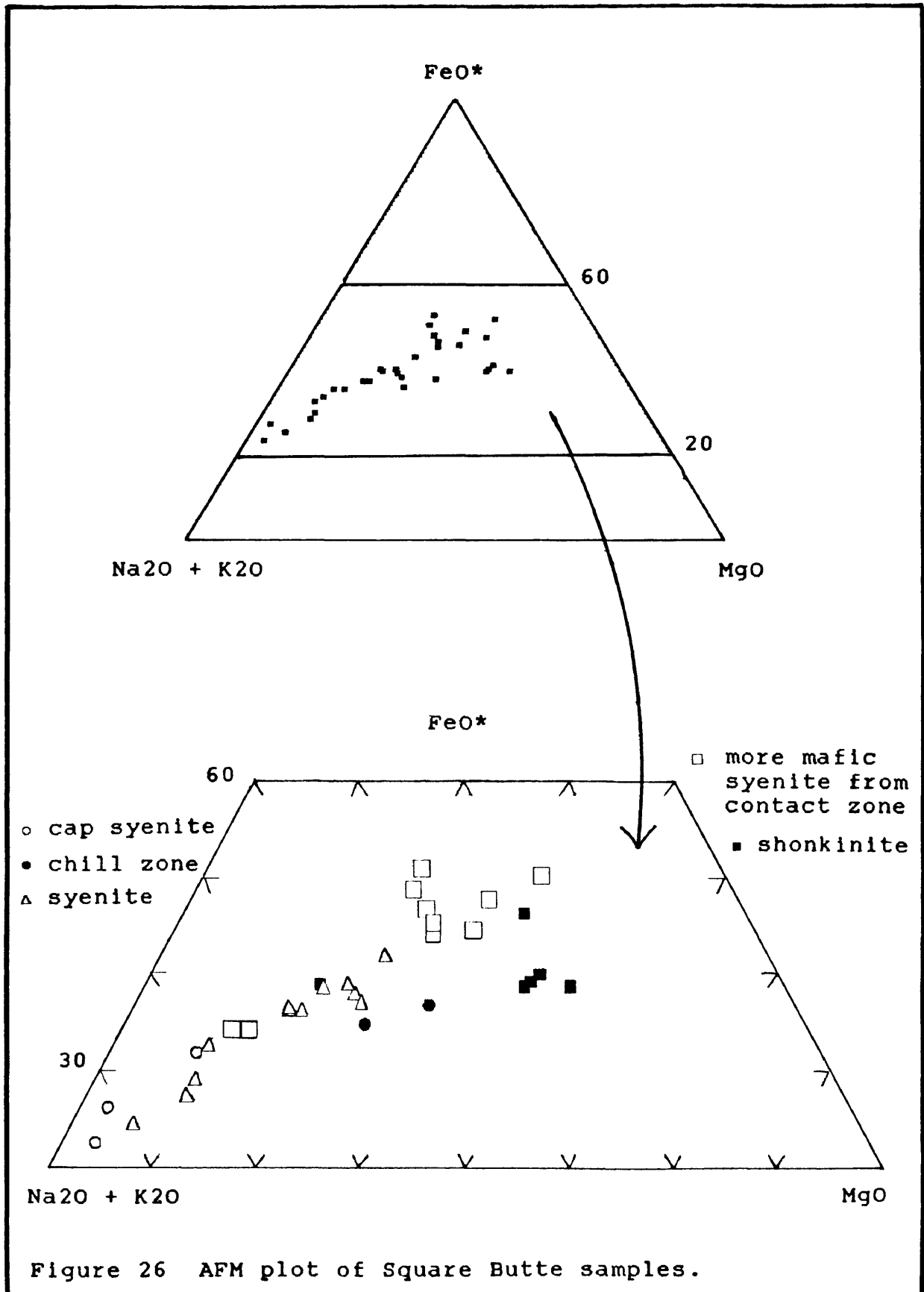


Figure 26 AFM plot of Square Butte samples.

Partitioning of Selected Elements

Rare-Earth Elements

The rare-earth elements, plotted against rock/chondrite values in Figure 27, show a constant pattern of light rare-earth element enrichment and heavy rare-earth element depletion. This same pattern is seen in rocks of the Highwoods as well (O'Brien, 1988). The cap syenite shows the greatest change in light/heavy rare-earth element ratio, being most strongly enriched in light rare-earth elements. A small negative europium anomaly in the cap syenite probably reflects the absence of significant salite, as, in the absence of plagioclase, this is the mineral most likely to host europium (Francalanci et al., 1987).

Notice also that the syenite sample has the lowest abundance of rare-earth elements. This is a pattern contrary to what is found through crystal fractionation in most rocks. In Watson's (1976) experimental studies, the rare-earth elements were found to be enriched in the immiscible mafic melt. However, other factors can explain this pattern. Partition coefficients calculated for rare-earth elements in high potassium rocks are consistently larger for clinopyroxene, biotite, and magnetite than for sanidine, leucite and haüyne (Francalanci, et al., 1987). The rare-earth elements, then, preferentially entered the

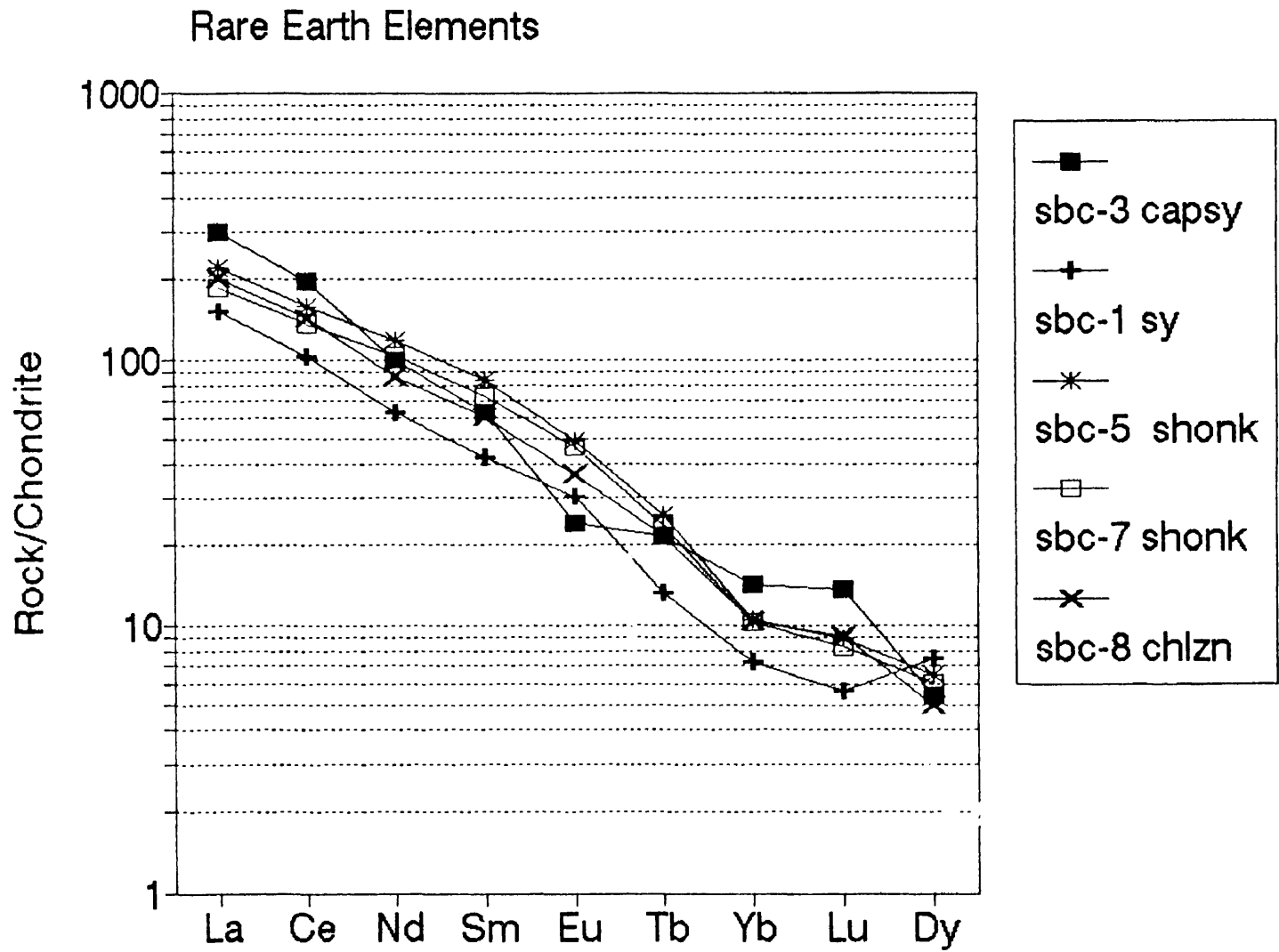


Figure 27 Rare-earth element diagram of selected, representative Square Butte samples.

early-formed salite crystals in shonkinite, leaving the syenite depleted in these elements.

Phosphorus and Titanium

Phosphorus and titanium have been shown to expand the immiscibility field (Freestone, 1978), and Watson (1976) found that phosphorus was strongly partitioned into an immiscible mafic melt, while titanium was less so. Square Butte samples are not highly enriched in phosphate or titanium (compared to alkaline lamprophyres which have been shown to be affected by liquid immiscibility). At Square Butte, phosphate is strongly partitioned into the shonkinite, as seen in Figure 28. This partitioning of phosphorus favors liquid immiscibility (Watson, 1976), assuming melt structures are equivalent in potassium-rich rocks to those in the experiments. The distribution of phosphate is represented by the greater abundance of apatite in the shonkinite, attributed to the early crystallization of apatite.

Titanium, Figure 29, shows a more disperse pattern. It is nearly equally distributed through syenite and shonkinite with a slight preference for the shonkinite and a strong dislike for the cap syenite. This distribution depicts decreasing crystallization of salite while simultaneously increasing crystallization of magnetite (titanomagnetite).

Variation of P₂O₅ vs Calcium

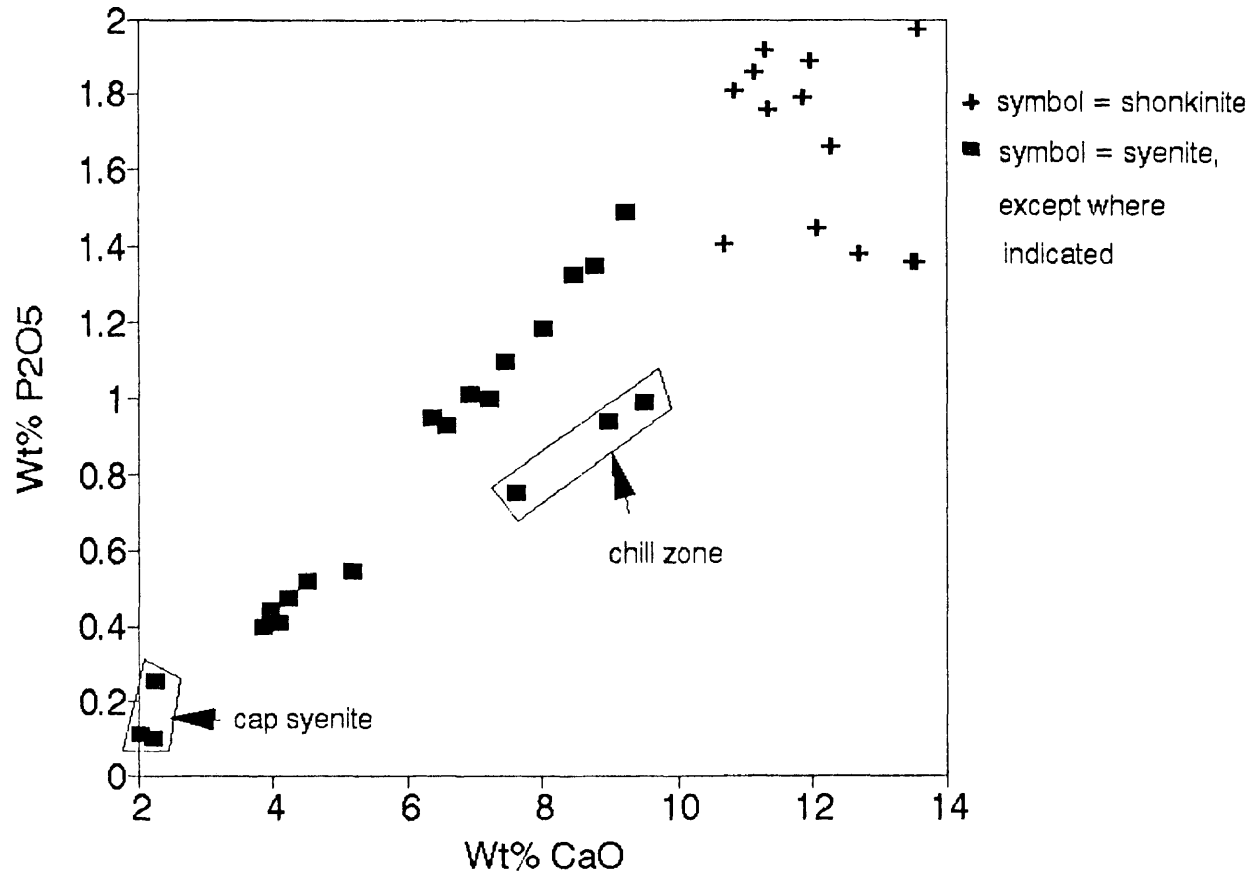


Figure 28 Variation of Phosphorus versus Calcium, all rock types.

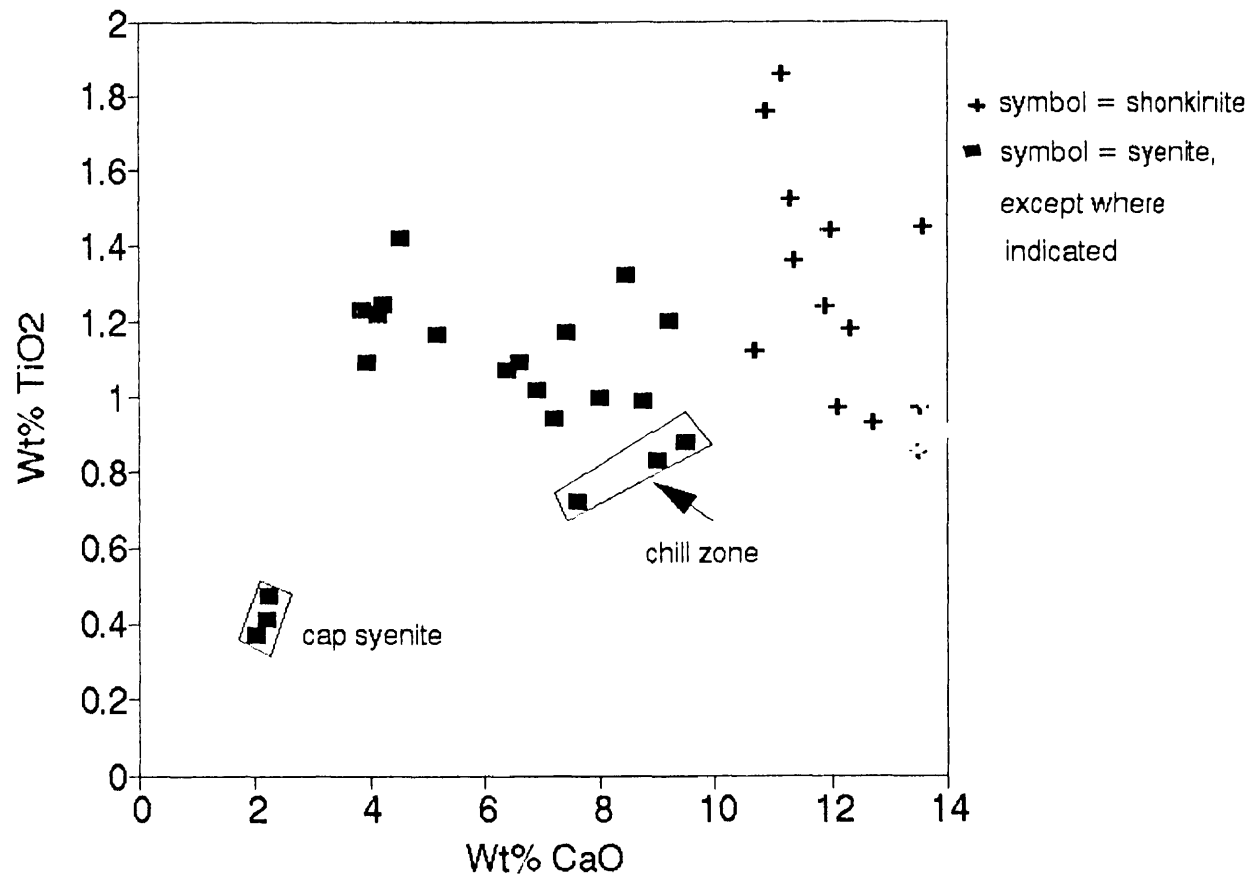


Figure 29 Variation of Titanium versus Calcium, all rock types.

2. CRYSTAL FRACTIONATION

Crystal fractionation, whereby early-formed crystals such as olivine and augite settle in a magma, continually changing the composition of the residual liquid, will produce an intrusion which is likely to be layered in respect to density and chemistry. This layering may be visible, as it is in layered intrusions such as the Bushveld or Stillwater intrusions, and/or the layering may be cryptic, and only seen in chemical analyses. Analyses of whole-rock or individual grains will show an increase in ferrous iron upward and a decrease in magnesium because magnesium is preferentially removed early. Consequently, alkalis will be enriched in the more felsic residuum. Cumulate textures should be visible if augite was settling out of the magma and collecting on the floor of the magma chamber.

In crystal fractionation, rare-earth elements will most likely be enriched in the more polymerized felsic portions and transition elements such as chromium, nickel, and cobalt will be concentrated in more mafic portions. The mafic melt, being less polymerized, permits coordination of cations by oxygen. Incompatible elements, such as rubidium, potassium, strontium, and barium, which do not readily enter the crystal lattice, will remain in the melt until the last of the felsic portion crystallizes.

One of the most significant problems with crystal fractionation at Square Butte is the lack of cumulus textures or any evidence of crystal settling. However, the presence of pseudoleucite, and the fact that these crystals get larger upwards through the laccolith, suggests that crystal fractionation involved, and perhaps was dominated by, pseudoleucite. Floating pseudoleucite, rather than sinking salite, may be responsible for the lack of cumulus textures at the butte.

Major-Element Oxides

It is not immediately apparent that crystal fractionation produced the rock types present at Square Butte. Absolutely no textures indicate crystal settling; neither iron/magnesium ratios nor specific gravity measurements are what would be expected from crystal fractionation. Regardless, variation diagrams of major-element oxides plotted against calcium oxide (Figure 30a-e) show linear trends that are compatible with simple fractionation. It must be noted, however, that the rocks are essentially bimodal and any spread of data must be attributed to the fact that sample collecting concentrated in the contact zone, at the top of the shonkinite, and it is these rocks that fall mid-way between the endpoints of

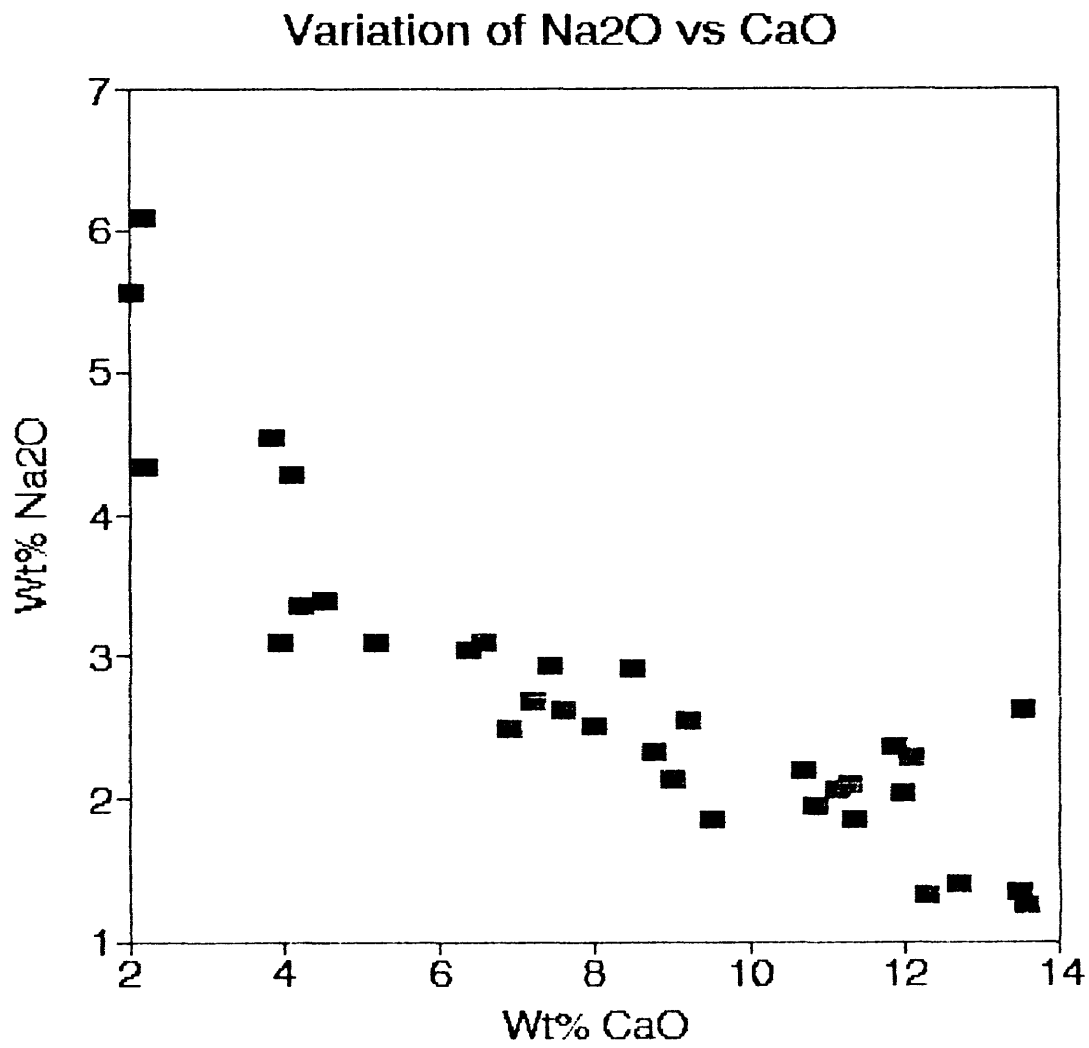


Figure 30a Variation of Sodium versus Calcium, all rock types.

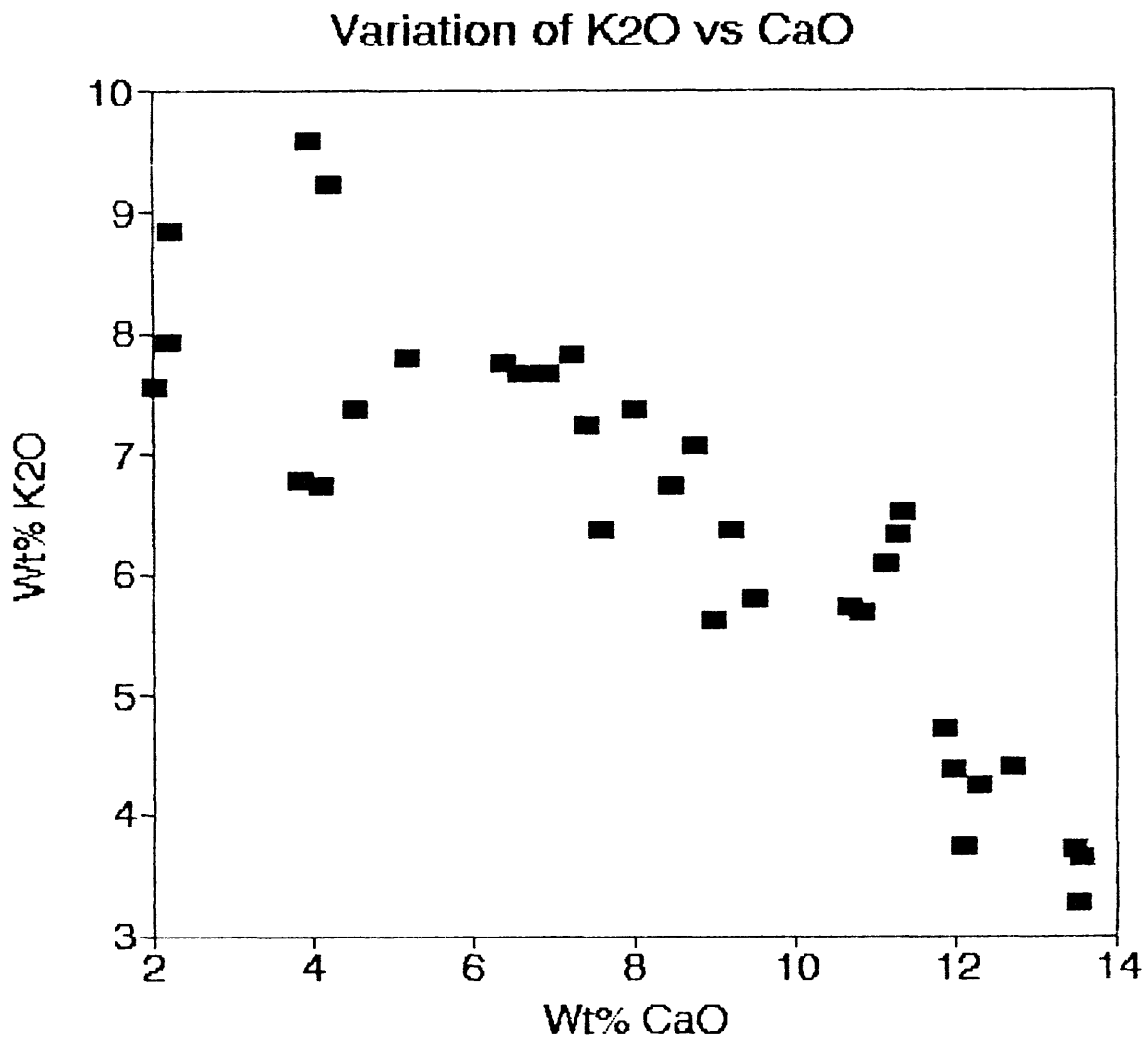


Figure 30b Variation of Potassium versus Calcium, all rock types.

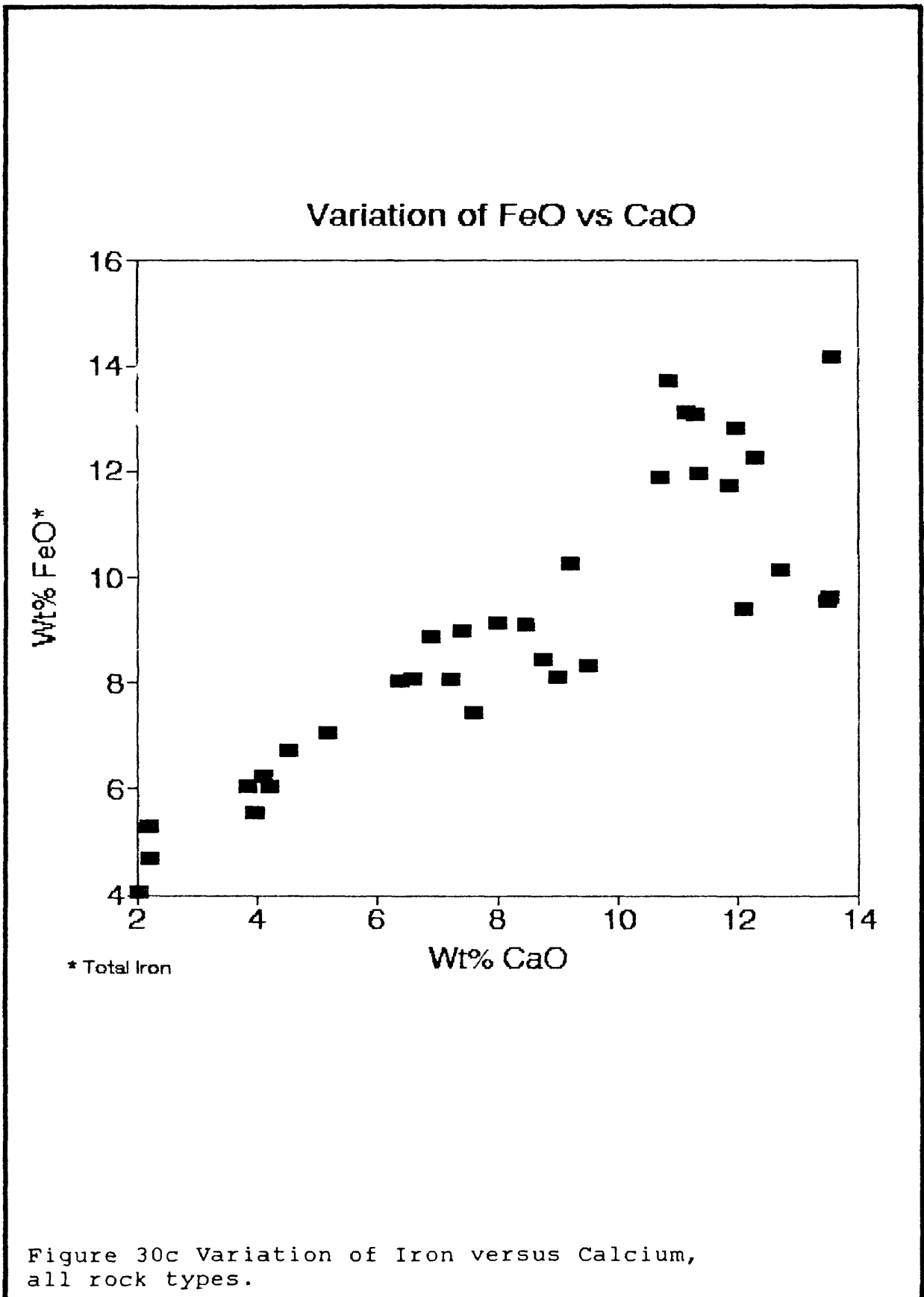
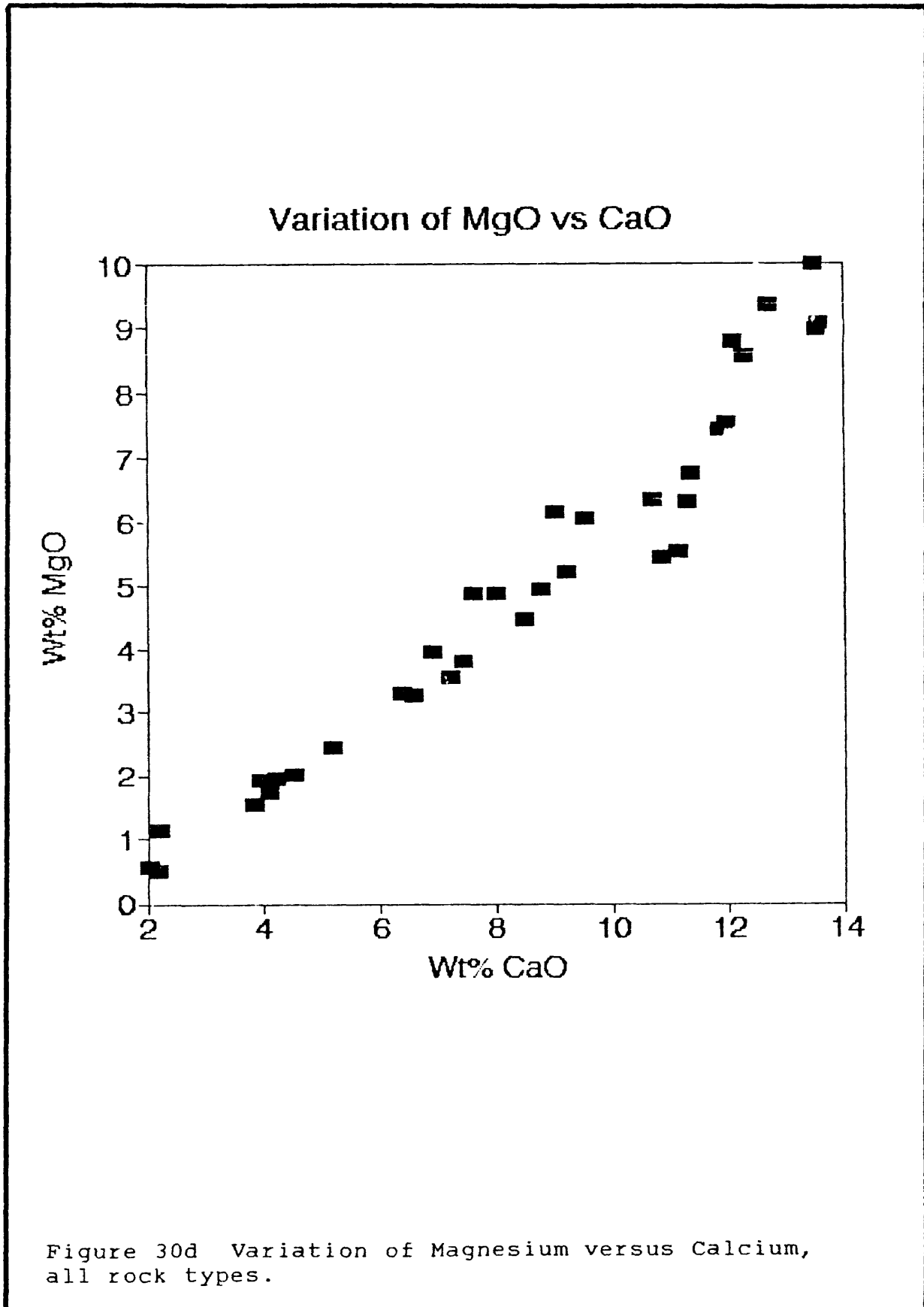


Figure 30c Variation of Iron versus Calcium, all rock types.



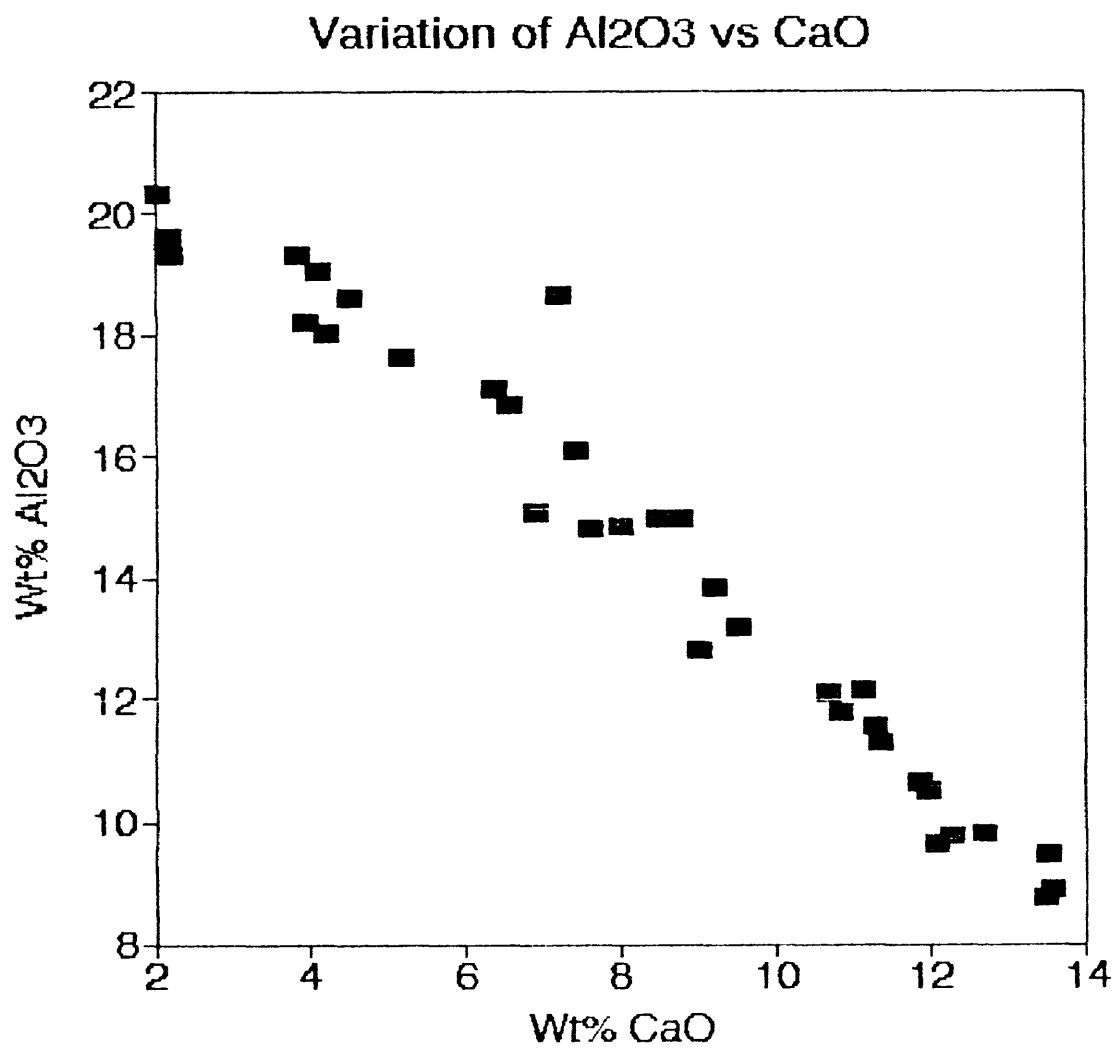


Figure 30e Variation of Aluminum versus Calcium, all rock types.

syenite and shonkinite. This bi-modal sequence, on the other hand, argues against crystal fractionation.

To further test crystal fractionation as a viable process, average compositions for salite, biotite, olivine and magnetite are plotted with the major element trends. Here, the best fit trends are those for the extraction of a rock with approximately 12.5% magnetite + olivine, 14% biotite and 73% salite (normalized). Mineral compositions and normalized percentages of mafic constituents are listed in Table 2. Pulling out a rock with the approximate mineral percentages noted above, produces rocks of the compositions at Square Butte (Figure 31a-c). The end point of the arrow which extends from the triangle represents the averaged mafic mineral percentages of shonkinite.

Trace-Element Variation

Plots of trace elements versus calcium show more scatter than the major oxide trends, due in part, to a much smaller number of analyses. Rare-earth elements (Figure 32a), however, do show a sort of linear trend, neglecting the cap syenite, but it is antithetic to the trend expected through crystal fractionation. As previously mentioned in the section on Liquid Immiscibility, this can be explained through partition coefficients in high potassium rocks. Rare-earth elements preferentially enter clinopyroxene over

**Table 2 AVERAGE AND NORMALIZED PERCENT
MAFIC CONSTITUENTS OF SHONKINITE**

AVERAGE MAFIC CONSTITUENTS

Sal = 46% Bio = 9% Mgt = 4.5% Ol = 3.5%

NORMALIZED MAFIC CONSTITUENTS

Sal = 73% Bio = 14% Mgt = 7% Ol = 5.5%

Mineral composition percent

	<u>Bio*</u>	<u>Sal</u>	<u>Mgt+</u>	<u>Ol*</u>
SiO ₂	34.6	50.4	0.02	39.2
Al ₂ O ₃	15.3	3.0	2.75	0.05
FeO	13.3	9.1	81.4	18.3
MgO	14.3	13.6	1.42	41.6
CaO	0.06	23.4	0.00	0.34

*data from O'Brien, 1988

+titanomagnetite, data from O'Brien, 1988

Sal= salite Bio= biotite Mgt= magnetite Ol= olivine

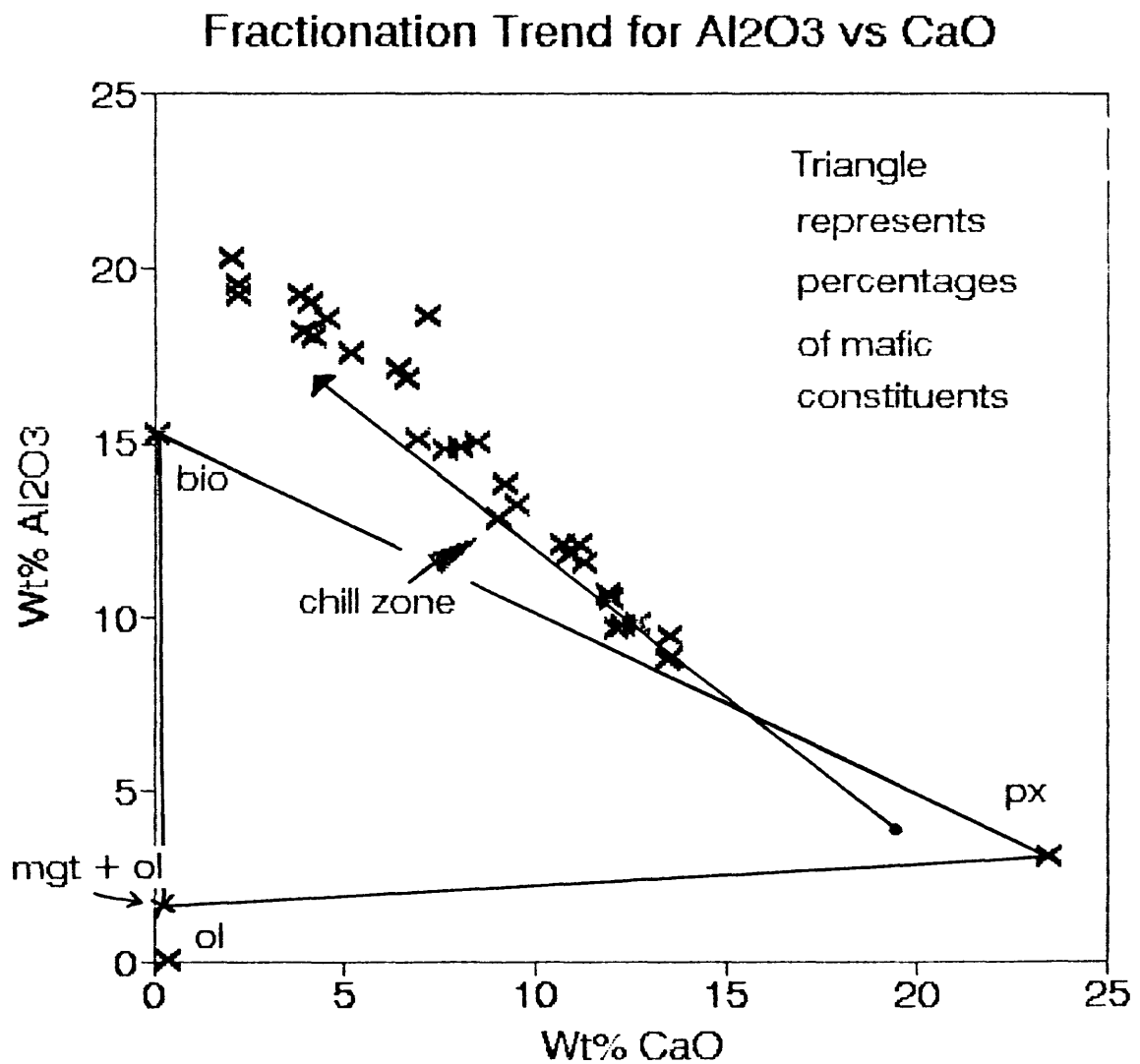
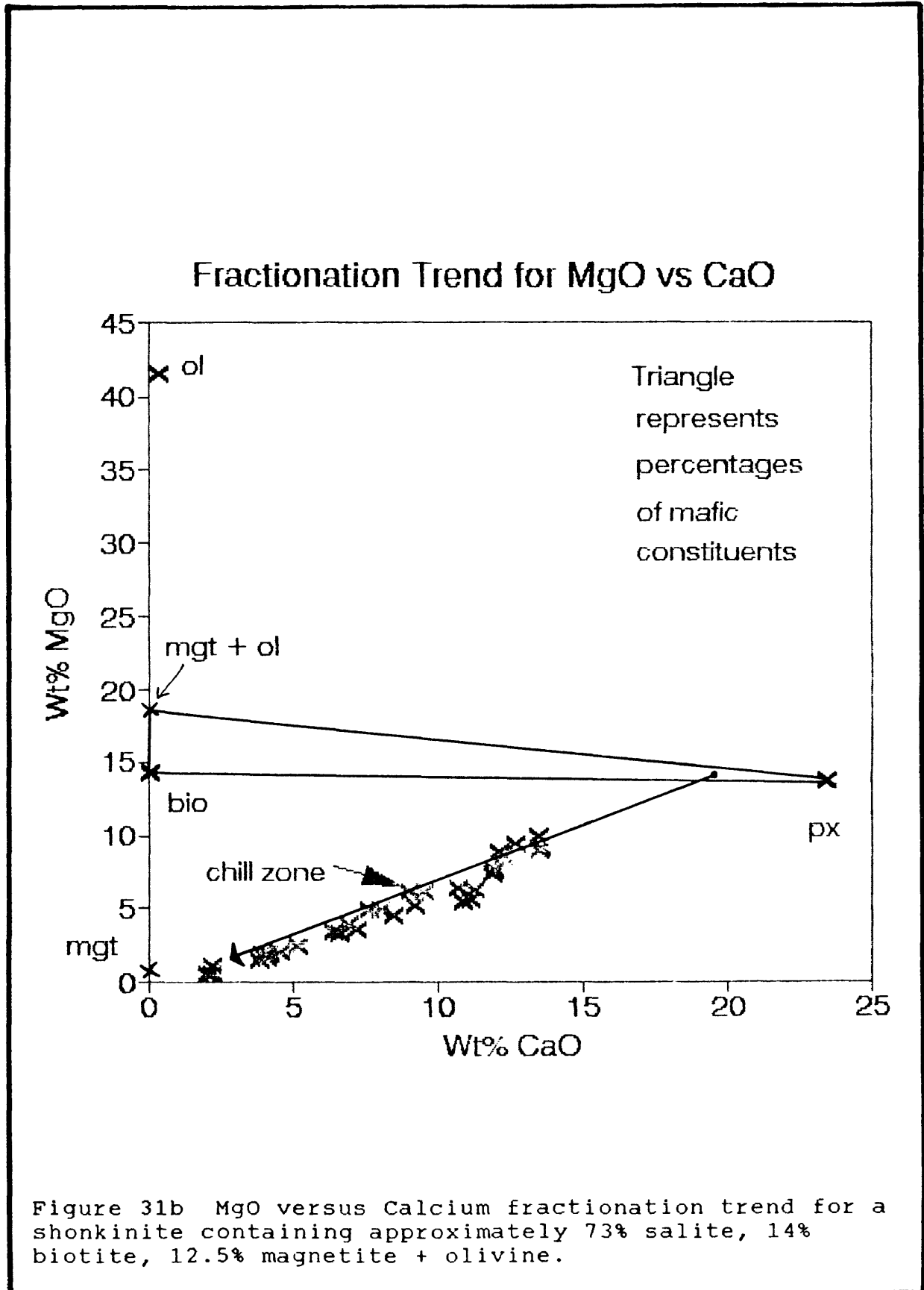
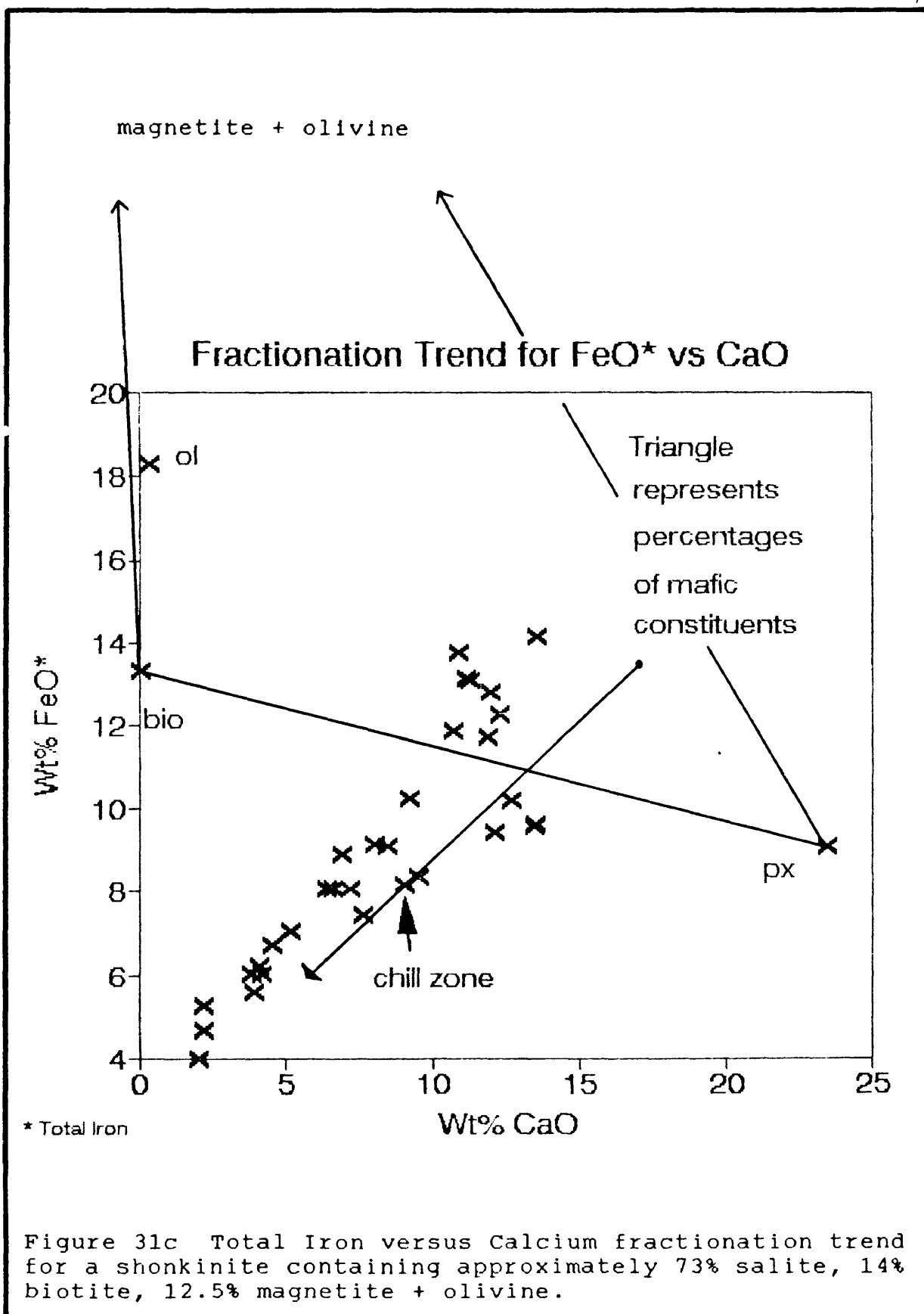


Figure 31a Aluminum versus Calcium fractionation trend for a shonkinite containing approximately 73% salite, 14% biotite, 12.5% magnetite + olivine.





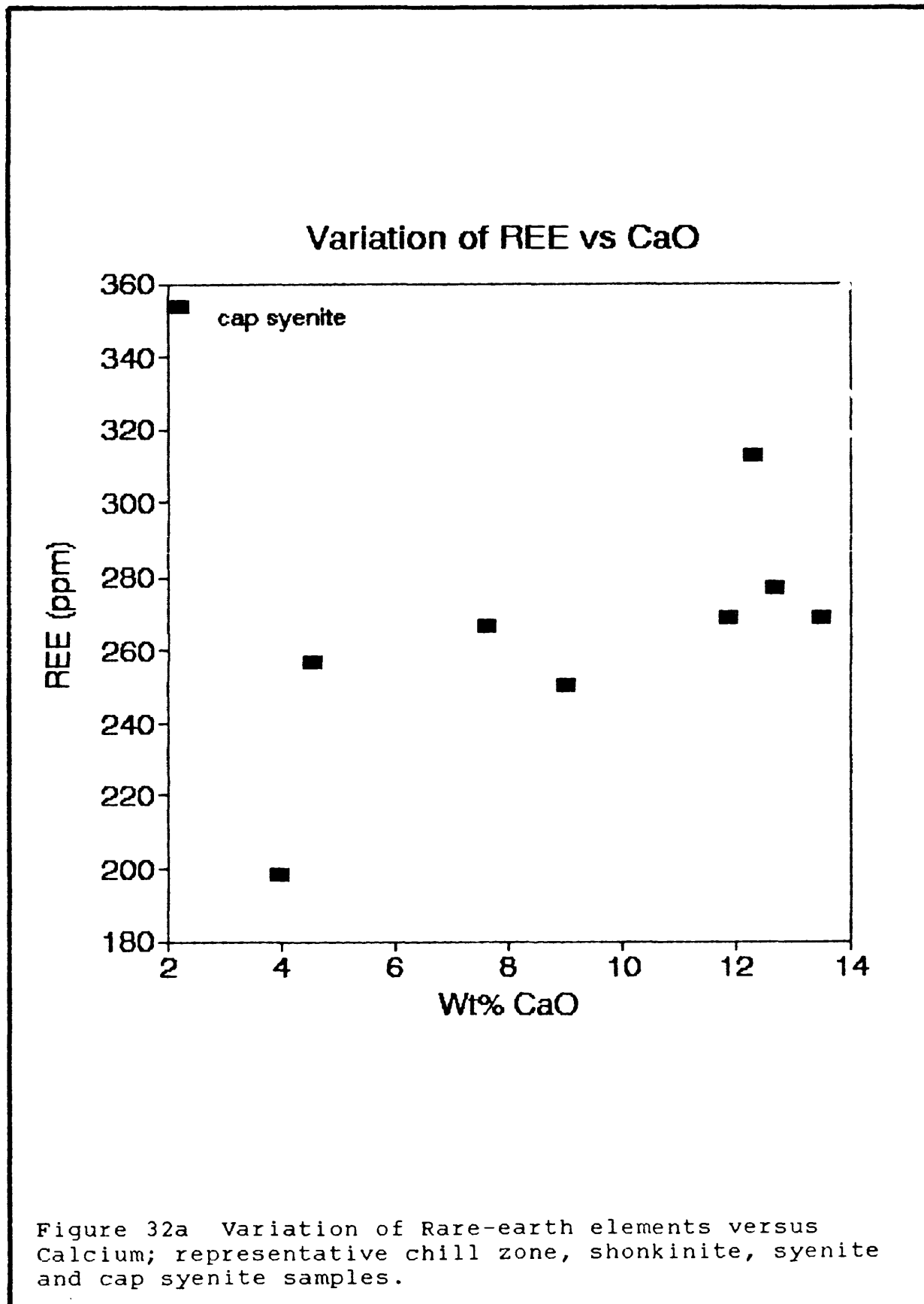


Figure 32a Variation of Rare-earth elements versus Calcium; representative chill zone, shonkinite, syenite and cap syenite samples.

sanidine by a factor of 100 or more (Francalanci et al., 1987). Thus, the samples lower in calcium (cap syenite excluded) show lower concentrations of rare-earth elements.

Barium, is more concentrated in the syenite (Figure 32b). Watson (1976), on the other hand, found that barium concentrates in the immiscible mafic portion of the system $K_2O-Al_2O_3-FeO-SiO_2$. But barium's distribution can also be explained in terms of the partition coefficients calculated by Francalanci et al. (1987). Partition coefficients for barium in biotite and sanidine are quite high, but those in clinopyroxene are not. This explains the relatively flat trend from approximately 8-14% calcium oxide. The syenite samples show some variability in the amount of biotite present and orthoclase begins to appear in the syenite and cap syenite as well. The wide variation in barium could be attributed to the crystallization of these phases and the greater percentage of feldspar in syenite than in shonkinite.

Strontium versus calcium oxide (Figure 32c) produces a plot nearly identical to barium. The partition coefficients for strontium are highest for sanidine, however, and sanidine is ubiquitous. There are no data for strontium in orthoclase, but the numbers are probably similar. If so, the greater percentage of potassium feldspar in the syenite could explain the increase in strontium.

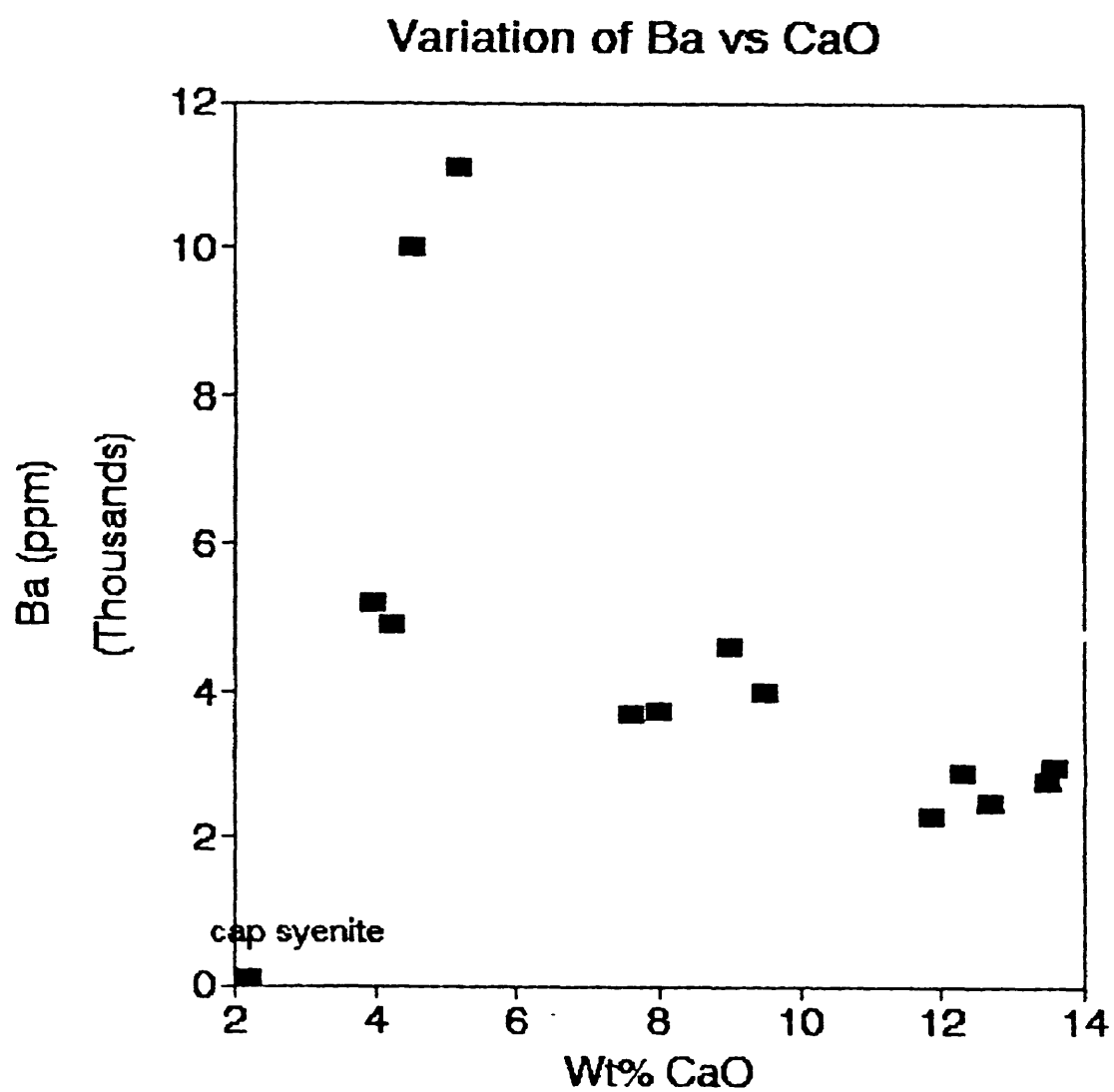


Figure 32b Variation of Barium versus Calcium; representative chill zone, shonkinite, syenite and cap syenite samples.

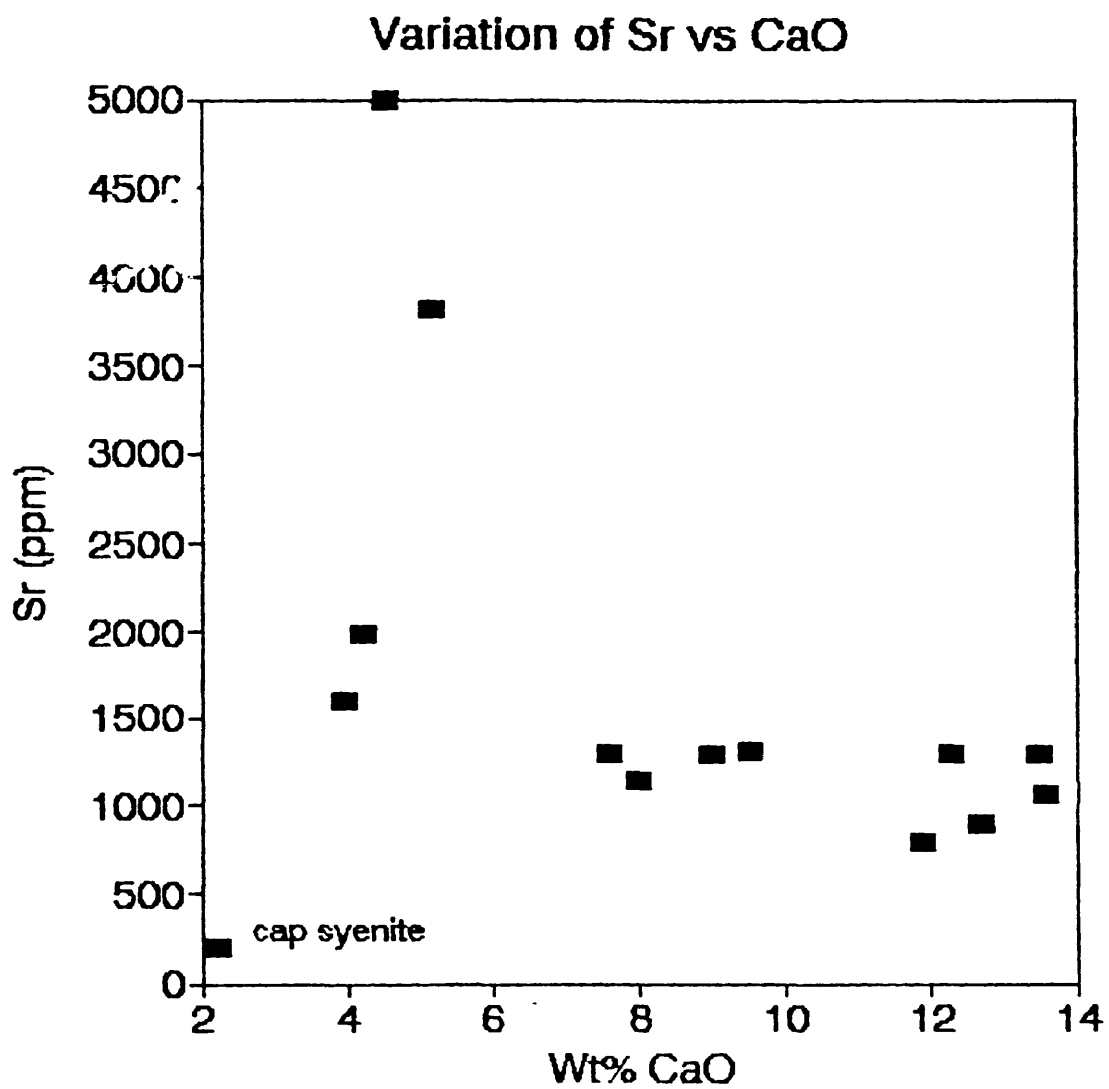


Figure 32c Variation of Strontium versus Calcium; representative chill zone, shonkinite, syenite and cap syenite samples.

A discussion of the abundance (or lack) of rare-earth elements, barium, and strontium in the cap syenite is discussed below under Thermogravitational Diffusion and Pneumatolitic Effects.

3a. THERMOGRAVITATIONAL DIFFUSION

Hildreth (1979) interpreted compositional zoning in a magma chamber as the result of thermogravitational convection and diffusion, not crystal settling or fractionation. This mechanism combines Soret diffusion with convection to produce compositional, thermal, isotopic, and volatile gradients in large magma chambers over long periods of time. Soret diffusion involves the movement of elements along a temperature gradient.

Hildreth suggests that all the zonation seen in the Bishop Tuff was produced by differentiation in an entirely liquid state. Hildreth's model involves a continual build up of water at the roof of the chamber. Convective cells below this roof zone established thermal and volatile gradients which in turn produced compositional zonation throughout the magma chamber.

Although the magma chamber which produced the Bishop Tuff (Long Valley caldera) is not similar to Square Butte, chemically or structurally, the roof zones of both can be compared. The cap syenite at Square Butte represents

a volatile-enriched roof zone, and like the roof zone of the Long Valley caldera, is strongly enriched in sodium, thorium, and uranium (Figure 33a-c) and strongly depleted in magnesium, strontium, and barium (Figure 34a-c). The cap syenite is starkly different from the underlying syenite. It contains miarolitic cavities and presumably formed through the crystallization of late-stage volatile-rich fluids that accumulated in the roof zone from the magma itself, and possibly, from water-rich fluids derived from overlying sediments.

Other features at Square Butte suggest a significant amount of volatiles were moving through the magma. The late-stage syenitic dikes, blobs and streaks in the lower shonkinite were likely produced in the same way. Mineralogically and texturally, they are identical to the cap syenite, containing hydrous phases such as amphibole, biotite and zeolites. These features, however, are not to be confused with the very large syenite blobs that mark the contact zone between the shonkinite and syenite layers.

3b. PNEUMATOLITIC EFFECTS

The following review of volatile streaming, or pneumatolitic action is summarized in more detail in Philpotts, 1990. Volatile streaming occurs when volatile-rich phases separate from the magma due to decreasing

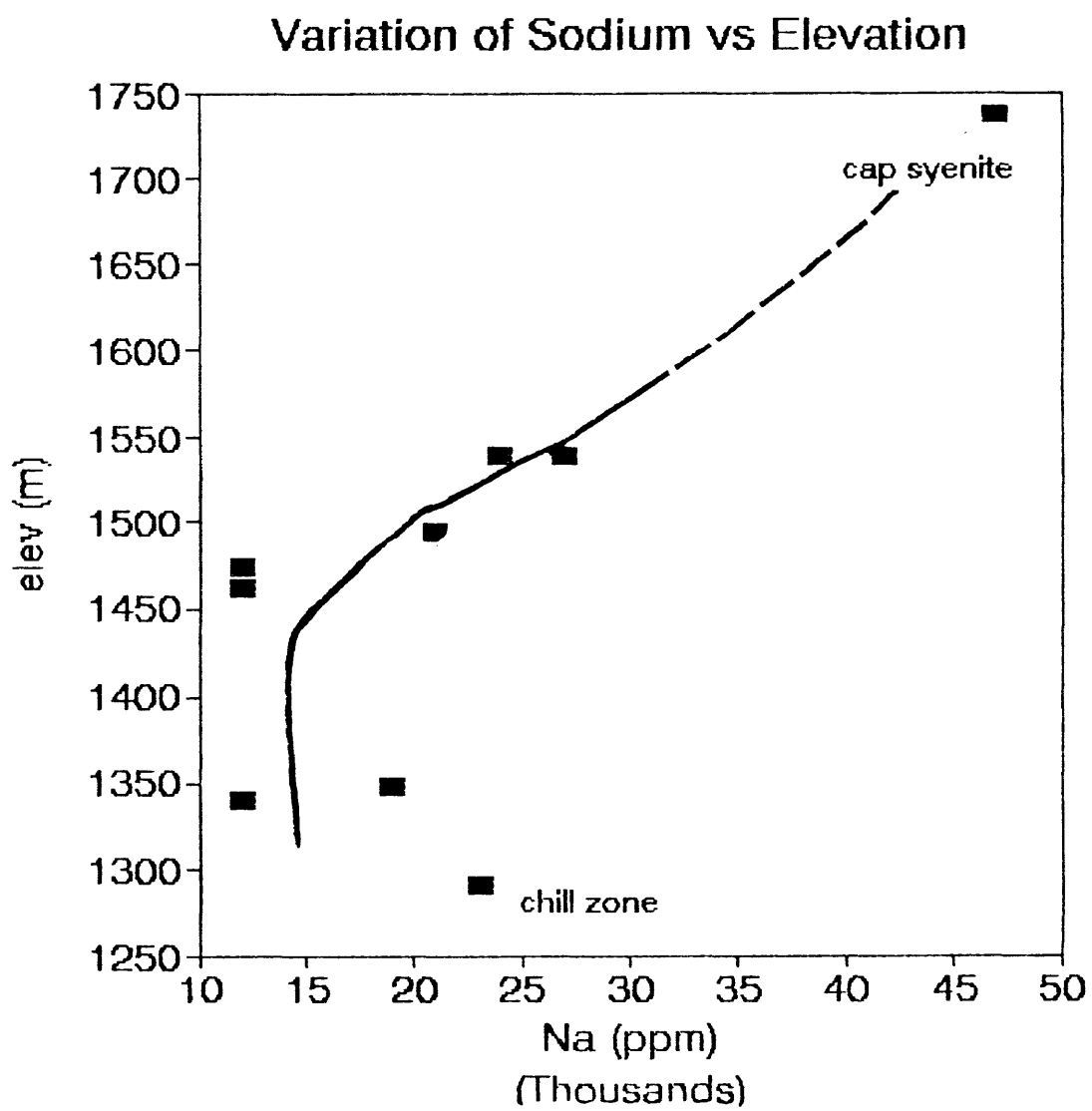


Figure 33a Variation of Sodium with elevation through entire butte.

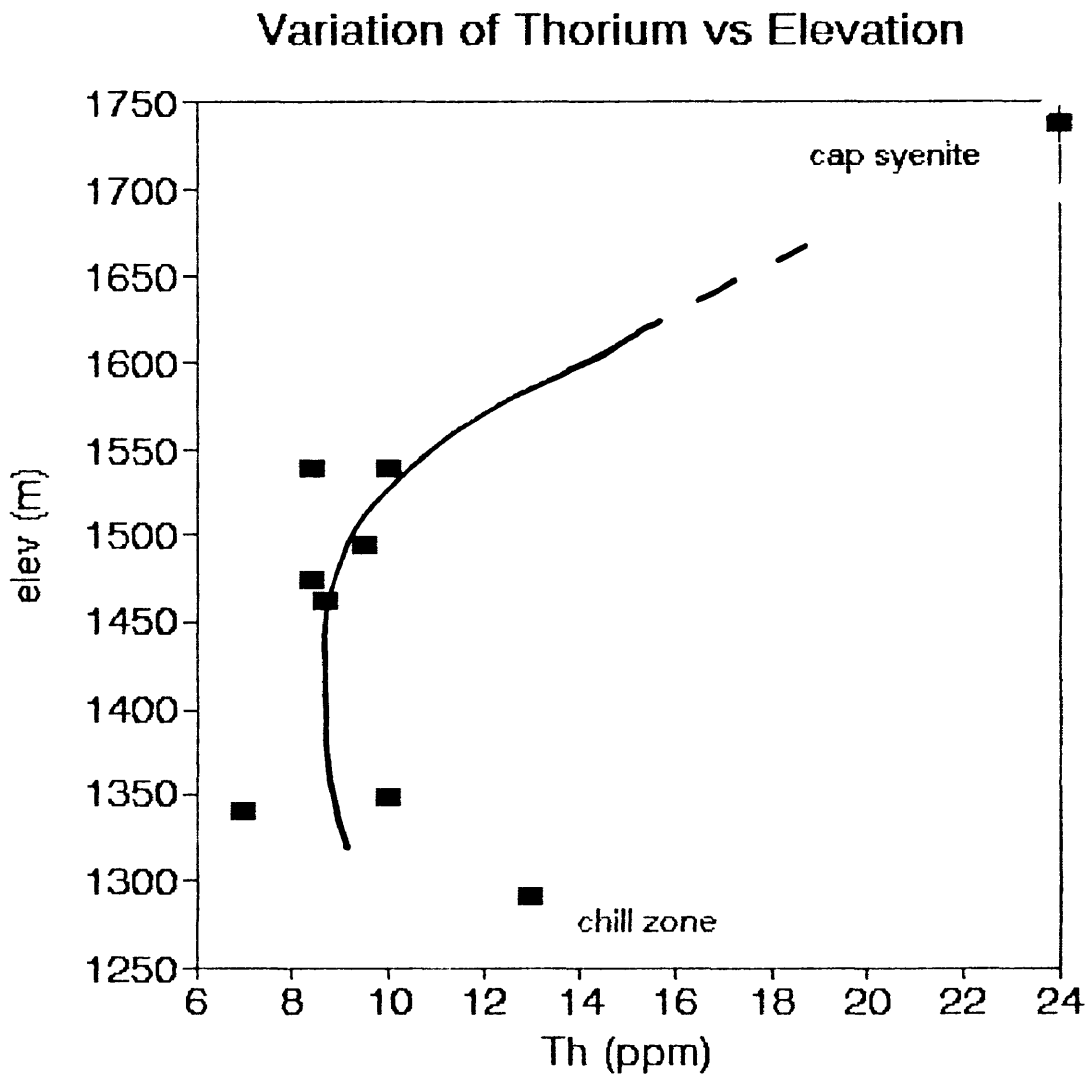


Figure 33b Variation of Thorium with elevation; small, representative suite of samples.

Variation of Uranium vs Elevation

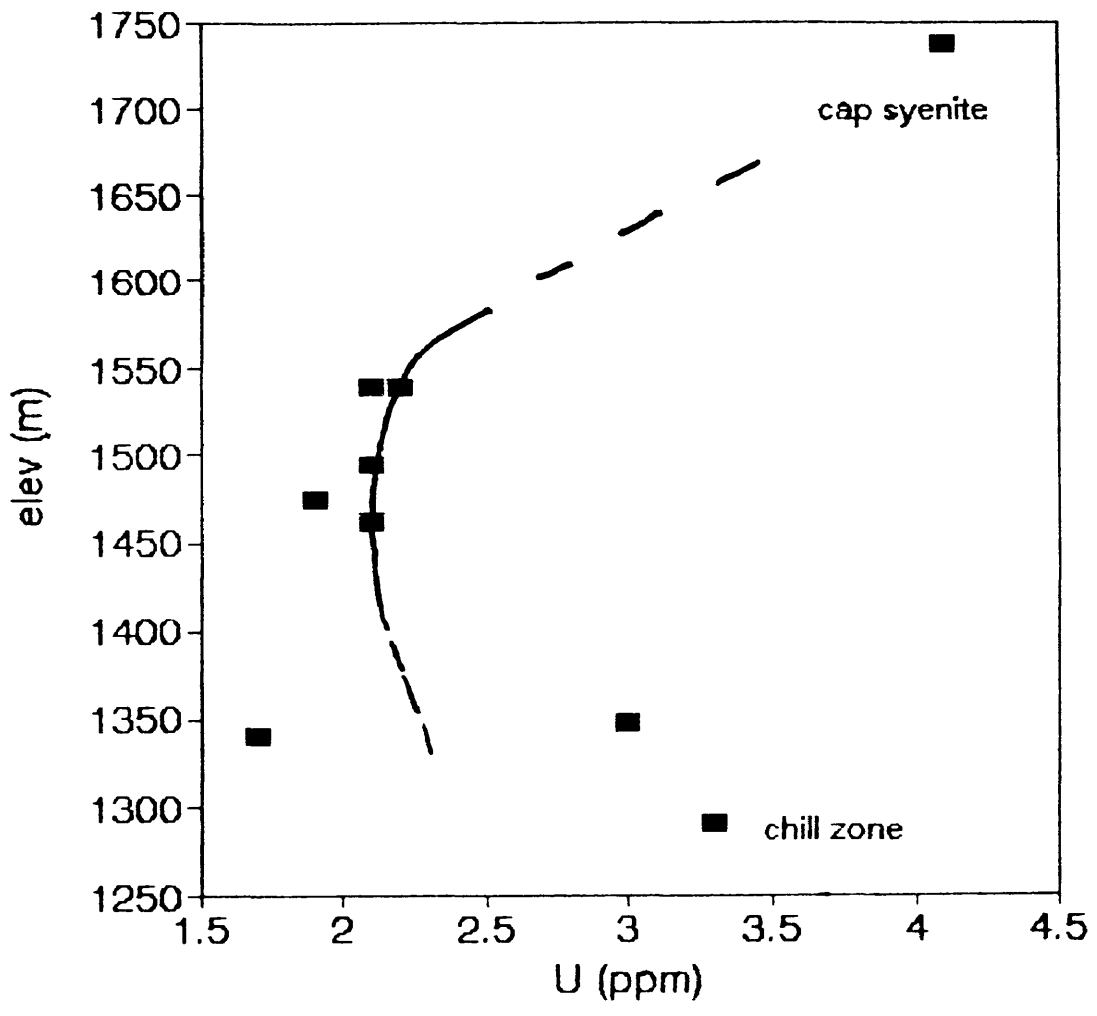


Figure 33c Variation of Uranium with elevation; small, representative suite of samples.

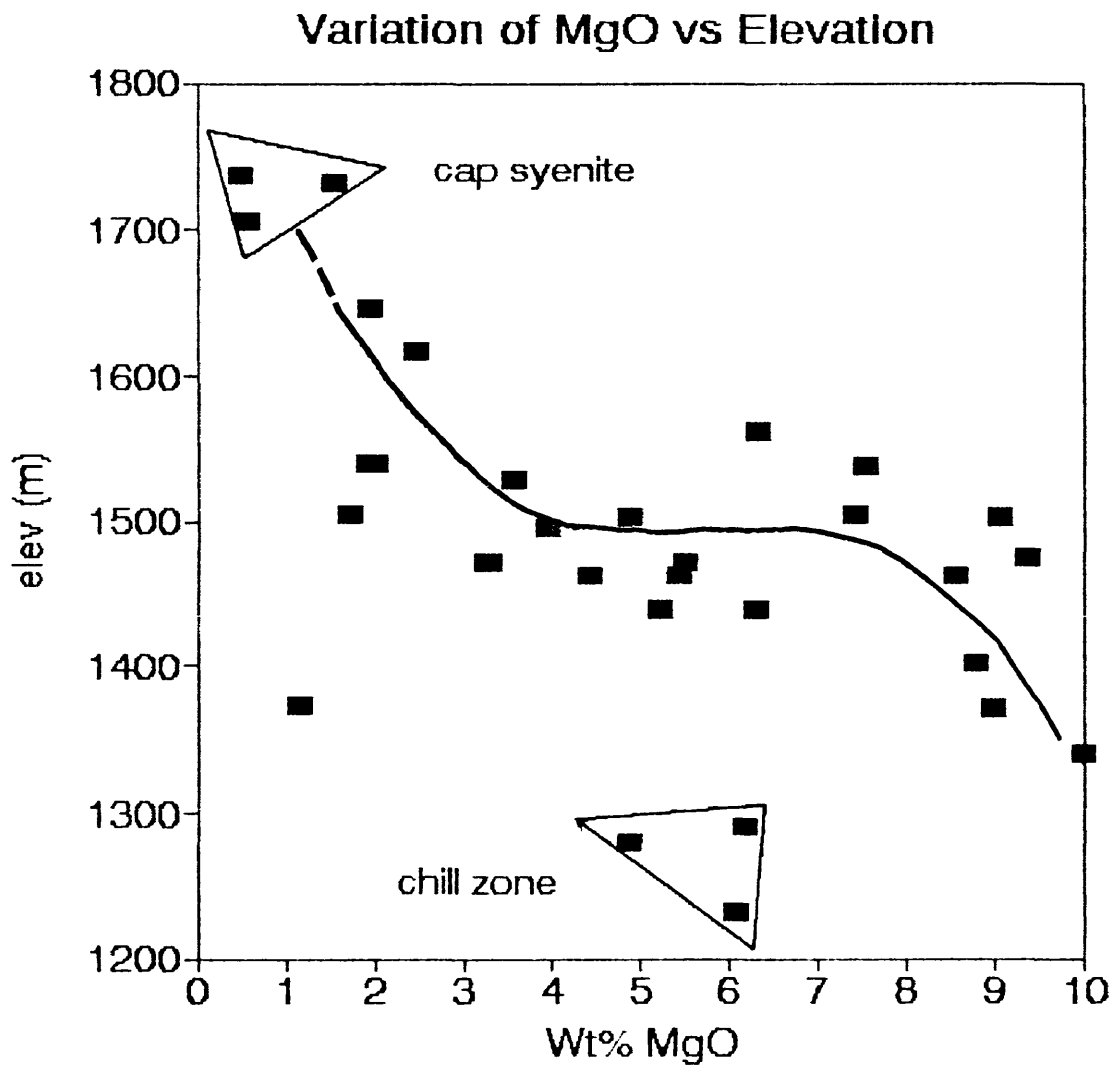


Figure 34a Variation of Magnesium with elevation through butte.

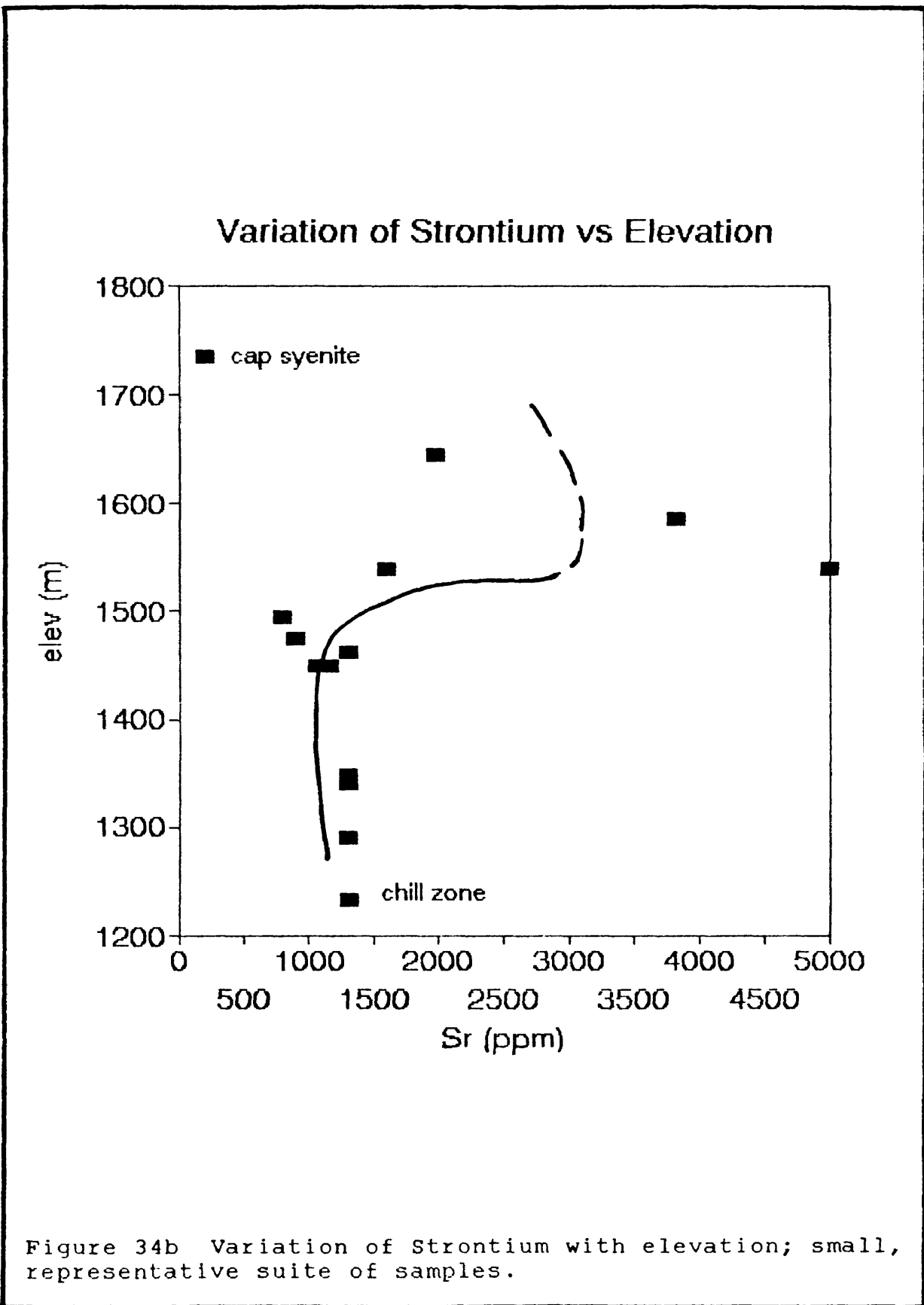


Figure 34b Variation of Strontium with elevation; small, representative suite of samples.

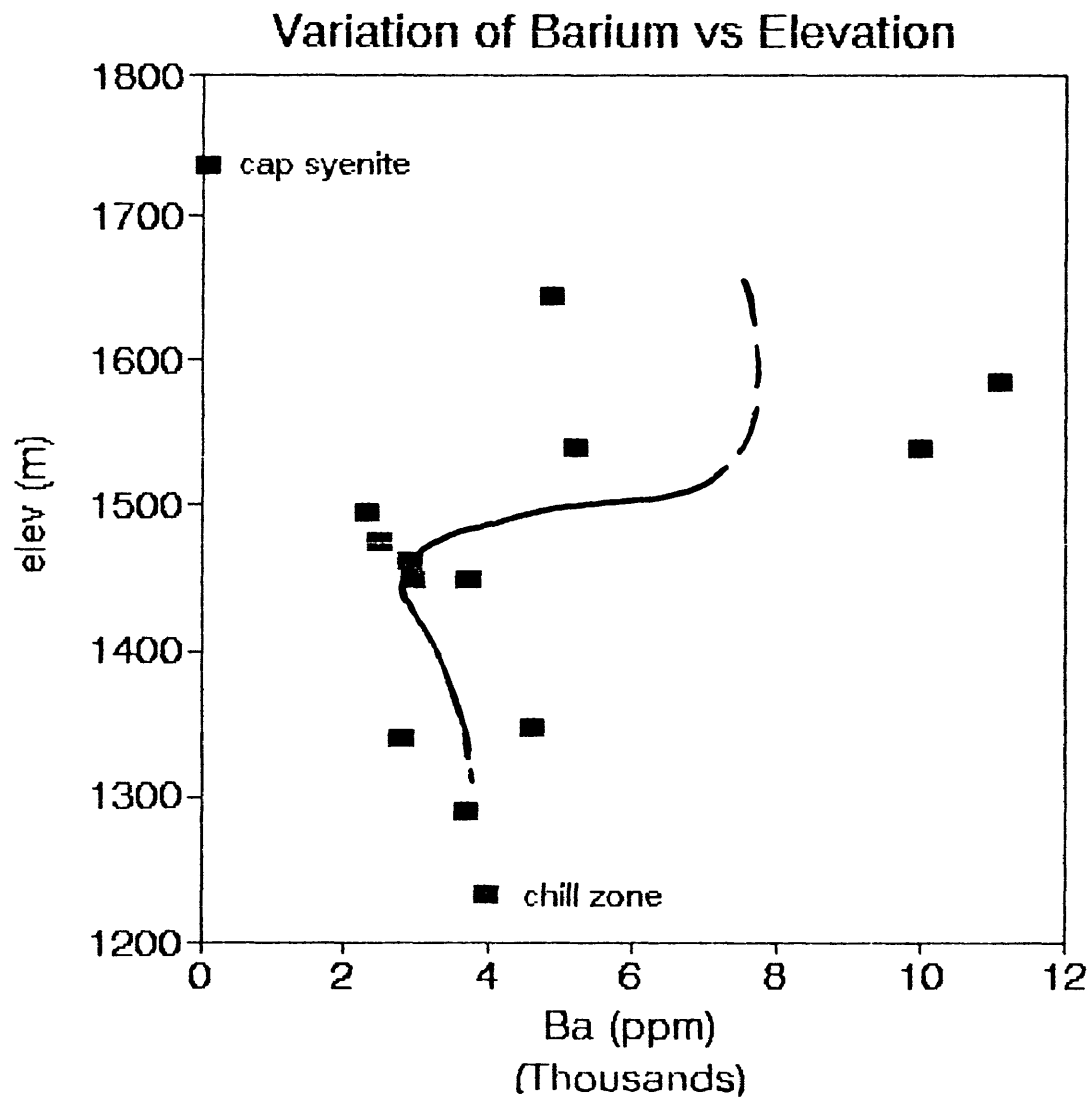


Figure 34c Variation of Barium with elevation; small, representative suite of samples.

pressure or crystallization of anhydrous phases. The upward streaming depletes the lower parts of the magma chamber in elements that can easily enter the fluid phase and may escape through the roof of the chamber and form pegmatites. The resulting differentiate will be enriched in, for example, phosphate, fluorine, chlorine, boron, sulfur, cesium, barium, hafnium, tantalum, thorium, uranium, and rare-earth elements. Referring to the previous figures, the cap syenite is enriched in thorium and uranium, in addition to hafnium and rare-earth elements (Figures 35a, b). But deviating from this enrichment trend are cesium and phosphate which exist in very low concentrations in the cap syenite (figures 35c,d).

This isn't enough information to determine precisely what mechanism is responsible for formation of the cap syenite; however, it is clear that volatile transport and diffusion were active at Square Butte. The geochemical signature of the cap syenite is unique compared with the rest of the syenite and shonkinite, which sets its differentiation apart from the rest of the butte. The geochemistry of the cap syenite and field relationships between syenite and shonkinite, provides just enough information to formulate a model for the differentiation of the entire laccolith.

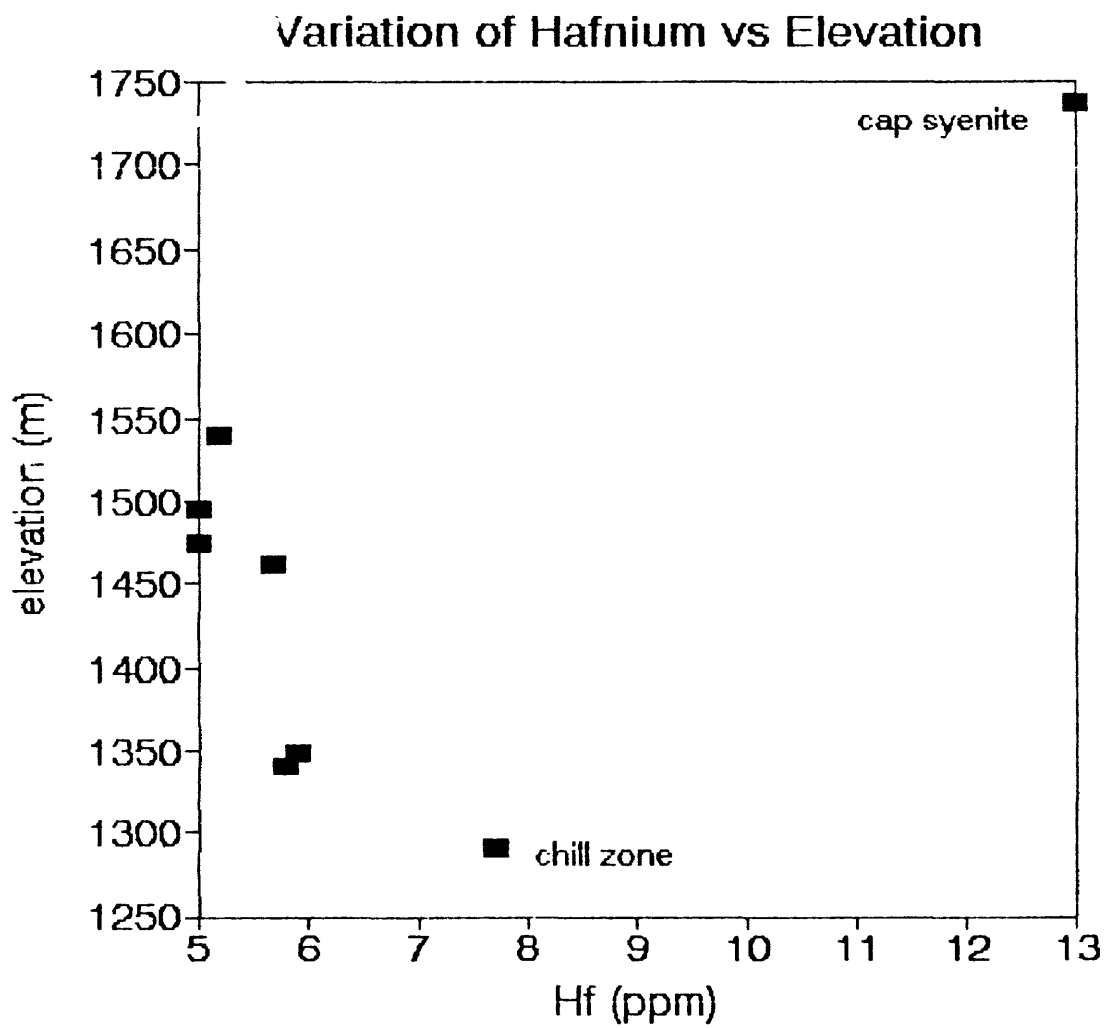


Figure 35a Variation of Hafnium with elevation; small, representative suite of samples.

Variation of Rare-Earth Elements vs Elevation

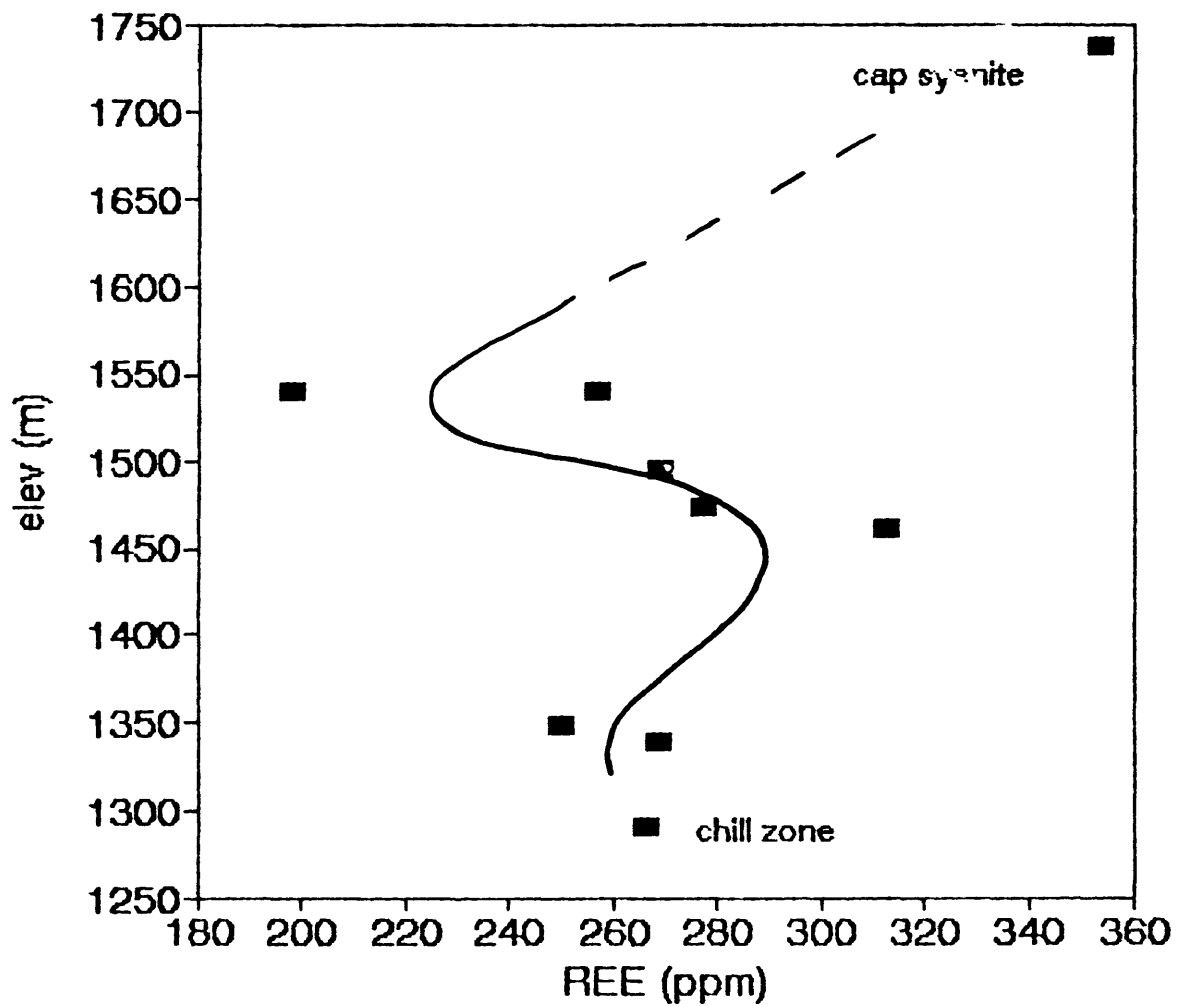


Figure 35b Variation of Rare-earth elements with elevation; small, representative suite of samples.

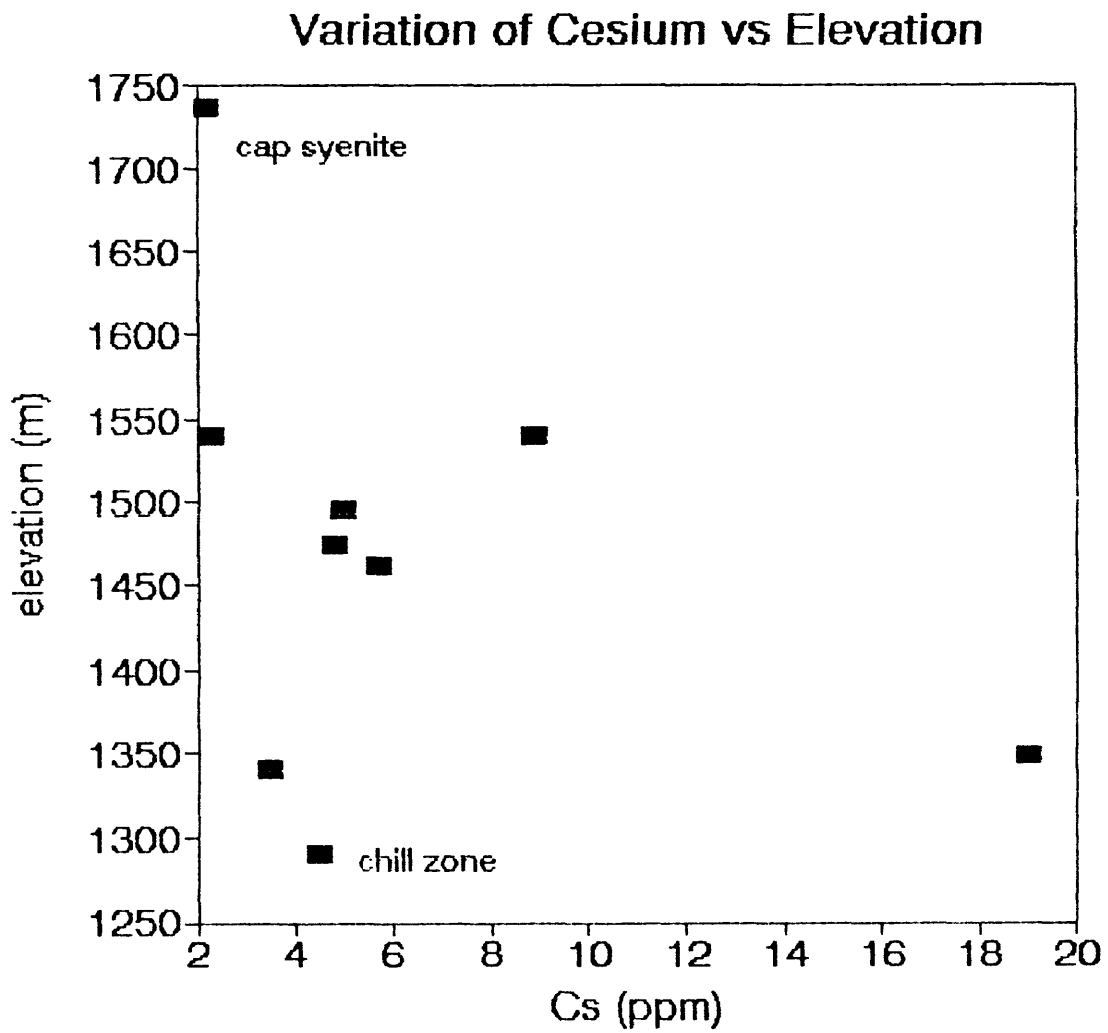


Figure 35c Variation of Cesium with elevation; small, representative suite of samples.

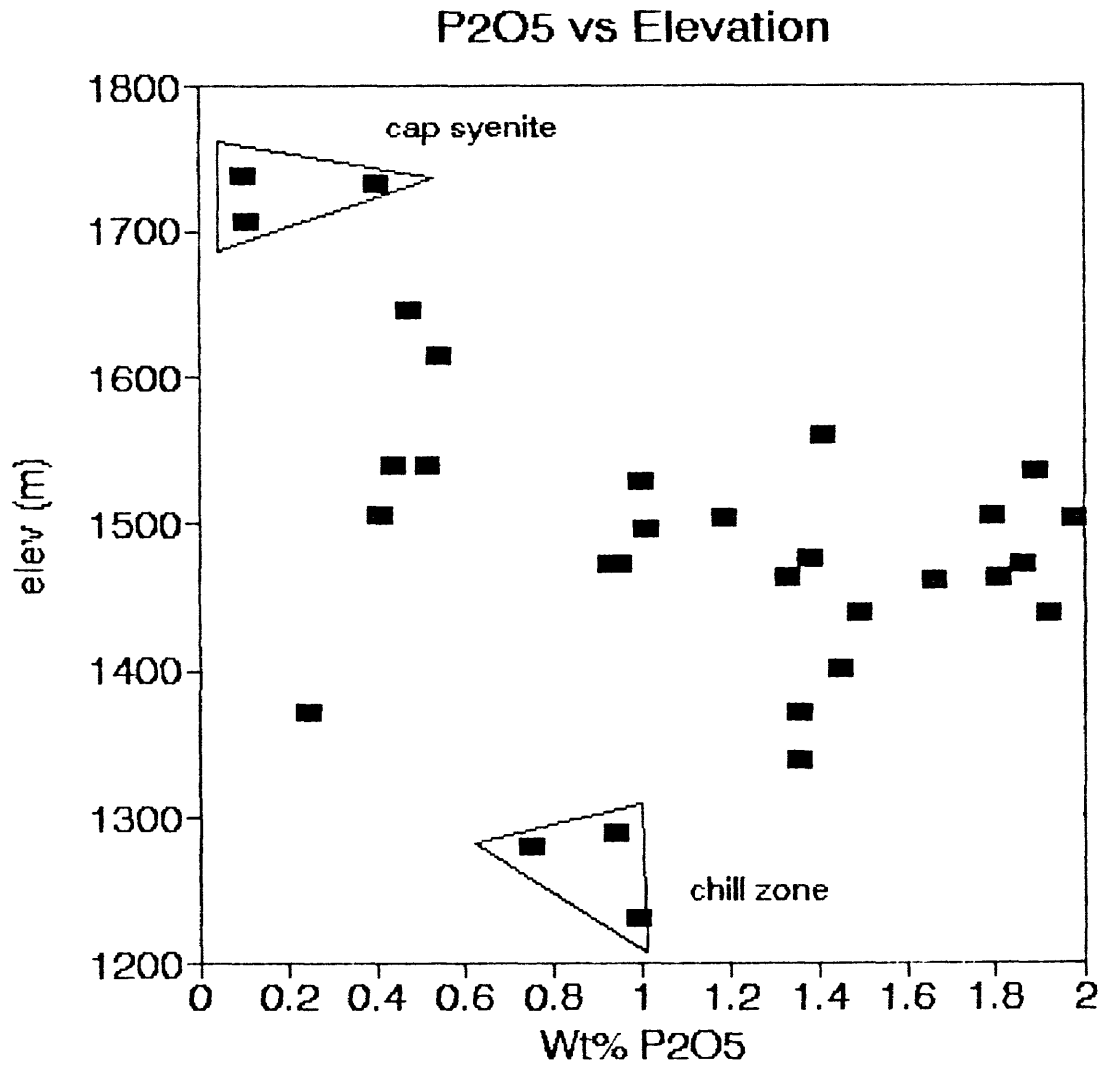


Figure 35d Variation of Phosphorus with elevation through butte -- note wide range of P₂O₅ content in contact zone (1500 m).

CONCLUSIONS/MODEL FOR DIFFERENTIATION

Table 3 summarizes differentiation mechanisms and the evidence supporting each.

The following conclusions can be drawn from evidence presented in this study:

1. The cap syenite formed from a build up of volatiles under the roof zone, and the lower syenite dikes, blobs, and streaks in shonkinite formed through late-stage volatile movement and diffusion (refer to Figures 9 and 12 and Figure 36).
2. Ocelli in shonkinite and syenite represent coalesced crystals of pseudoleucite and not immiscible droplets. This conclusion arises from observing the progressive transition of pseudoleucite crystals from euhedral phenocrysts in the sills to diffuse aggregations of fine-grained sanidine and zeolites. Also observed in the chill zone are multiple pseudoleucite crystals globbed together, often around a pyroxene grain (Figure 37, sketches). Pseudoleucite has been identified in the syenite layer as well. Optical properties, specifically 2V angle, identify sanidine as the fine-grained feldspar in the pseudoleucite, but orthoclase, sometimes quite zoned, is the matrix feldspar.
3. Major-element variation diagrams produce trends which would be expected from crystal fractionation.

TABLE 3 SUMMARY OF DIFFERENTIATION POSSIBILITIES AND EVIDENCE FOR EACH

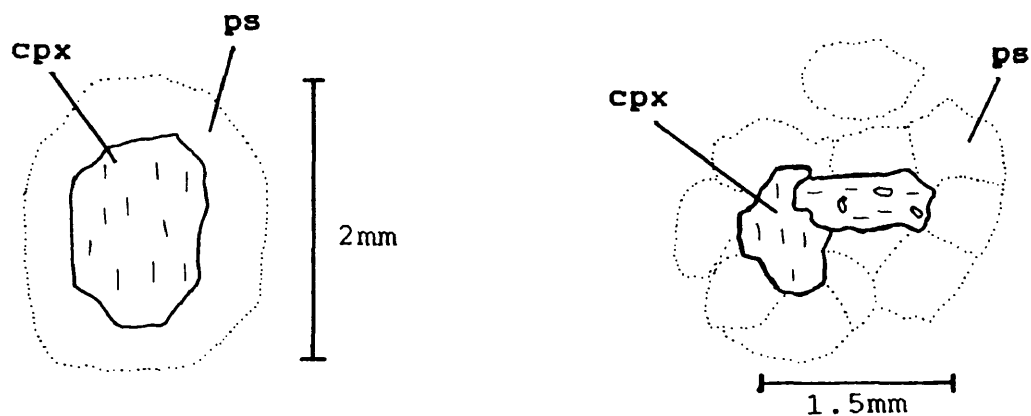
LI=LIQUID IMMISCIBILITY, XF=CRYSTAL FRACTIONATION, VS=VOLATILE STREAMING

CONDITION	MECHANISM
Bi-modal rock sequence	supports LI, contradicts XF. VS?
Field relations (blobs)	supports LI, contradicts XF. VS?
Lack of cumulus textures	supports LI, VS, contradicts XF unless pseudoleucite was fractionating and rising
Specific gravity does not increase upward	supports LI, VS, contradicts XF unless pseudoleucite was fractionating and rising.
Iron & magnesium content of salite in shonkinite remains relatively constant	supports LI, VS, contradicts XF unless pseudoleucite was fractionating and rising.
Ocelli are pseudoleucite, not immiscible blebs	supports XF, contradicts LI
Major-element trends	support XF, but do not exclude LI, VS
Chemical composition of cap syenite	supports VS
Rare-earth elements, and barium slightly enriched in mafic portion	supports LI, does not exclude XF (partition coefficients for high-K rocks)
Phosphate partitioned into mafic portion	supports LI, does not exclude XF (early crystallization of apatite)



lens cap
for scale

Figure 36 Syenite mass in lower shonkinite, formed by the migration of late-stage fluids/volatiles. South side of butte, elev 1381 m (4530 ft).



optically continuous
sanidine enclosing
pseudoleucite and
salite with reaction
rim of biotite

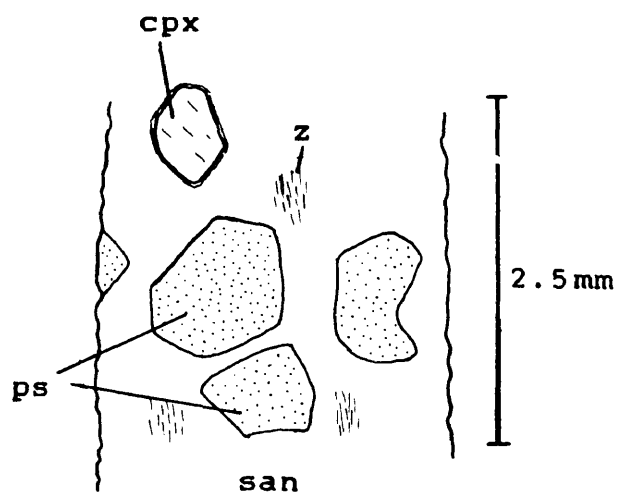


Figure 37 Thin-section sketches of pseudoleucite from chill zone (top) and syenite (bottom). ps=pseudoleucite, cpx=salite, z=zeolite, san=sanidine

Subtraction of an assemblage of pyroxene, biotite, and magnetite + olivine neatly follows the trends as well, further supporting the crystallization of mafic minerals. However, no crystal settling is evident. Aside from a complete lack of field and petrographic evidence revealing crystal settling, specific gravity measurements, iron and magnesium contents of pyroxene, crystal size and modal percentages refute any gravitational settling of mafic minerals. Since crystal fractionation requires a separation of crystallized phases from remaining liquid, other mechanisms must have prevented crystals from settling. These include:

- a) upward streaming of immiscible or miscible felsic material;
- b) floating of pseudoleucite.

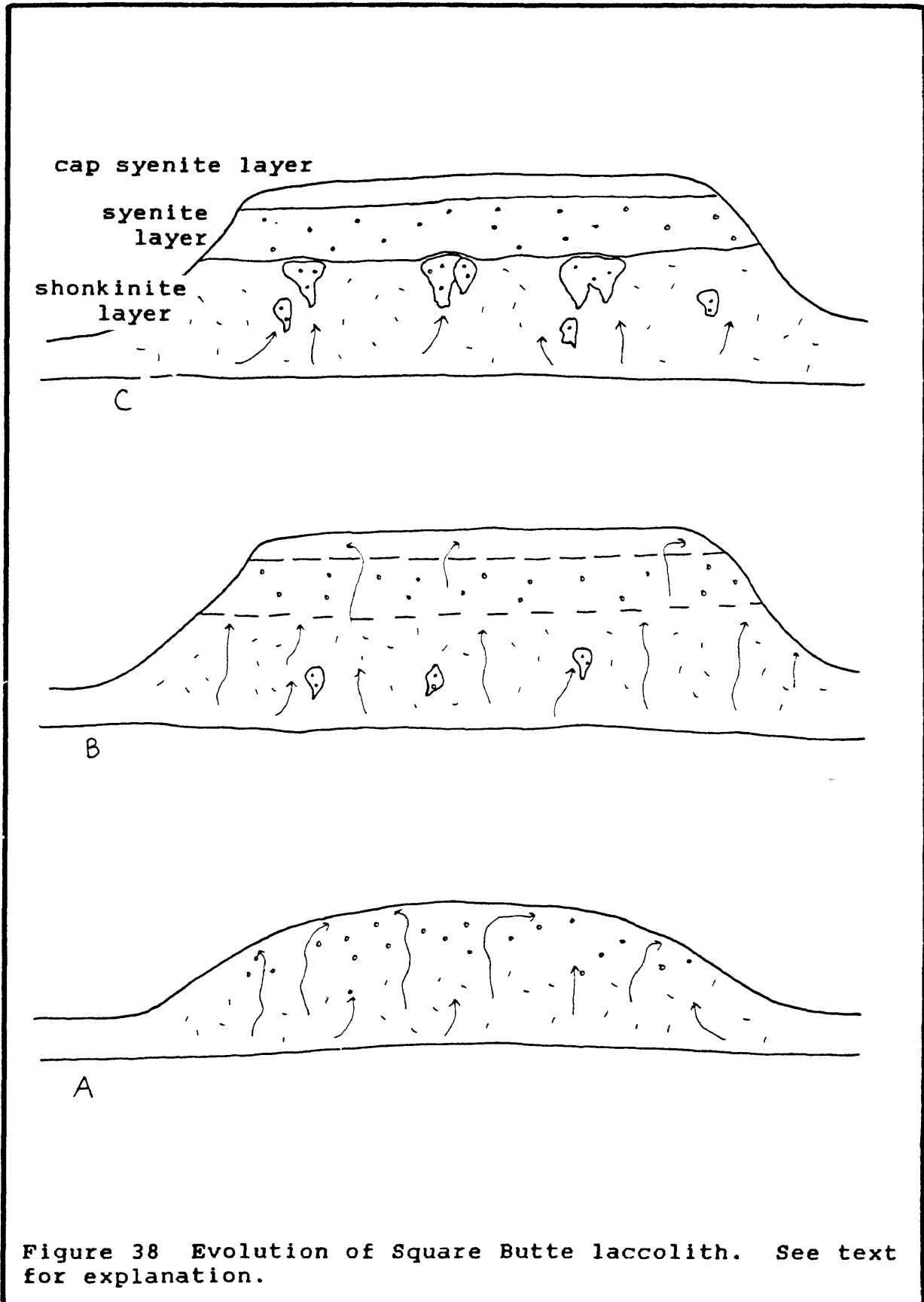
The first option is plausible, although whole-rock compositional data do not support or negate the presence of an immiscible fraction, nor do they support crystal fractionation. If the felsic portion steaming through the magma was immiscible, I would expect to see elemental partitioning trends reflect magma immiscibility, such as extreme enrichment of incompatible elements in the mafic fraction. Strontium, barium, and potassium, however, are not at all enriched in the shonkinite. But the data doesn't

explicitly support the upward movement of felsic material. Thermogravitational diffusion and pneumatolitic effects can explain the formation of the cap syenite, but neither process explains the geochemical patterns seen in syenite and shonkinite. If volatiles such as carbon dioxide and water were moving upward through the shonkinite, forming the cap syenite, they may have been capable of carrying along less dense, felsic material. This upward movement of volatiles and, perhaps, felsic material, may have inhibited crystal settling.

The second option is supported by the fact that pseudoleucite does occur in the syenite and is out of equilibrium with the surrounding material. The sanidine in these syenite pseudoleucites first formed in the shonkinite where the temperature was higher and sanidine was stable. After rising into the syenite layer, the lower temperature promoted crystallization of orthoclase around the pseudoleucite.

Model for Differentiation of Square Butte Laccolith

Figure 38 is a cartoon illustrating the following discussion. Shonkinite magma intruded moist Cretaceous sediments carrying crystals of salite and possibly leucite/pseudoleucite. Leucite/pseudoleucite and salite both crystallized early, as seen in the chill zone, and



leucite/pseudoleucite floated to the top of the magma chamber, coalescing and trapping minor amounts of olivine and clinopyroxene. Concurrently, carbon dioxide and water rose through the chamber, carrying felsic material and pseudoleucite, but inhibiting settling of crystallizing pyroxene (represented by arrows). A volatile-rich differentiate became trapped at the roof of the magma chamber, and the syenite under that. With continued cooling and migration of volatiles, crystal fractionation dominated the differentiation of the magma, as seen from the major-element trends and subtraction of mafic constituents (Figures 31a-c). Rising through a viscous crystal mush, large blobs of felsic material, several meters across, rose through the upper shonkinite layer and into the syenite due to extreme differences in density. These felsic blobs probably inflated to larger and larger sizes upon ascent analogous to bubbles rising through champagne, pulling in more felsic material. The syenite blobs at the contact zone are what remains of the rising syenite, where the felsic material reached a density boundary and failed to rise farther.

Trying to explain the three dimensional blobs at the base of the cap syenite (and protruding up into it) remains difficult. These white syenite blobs which exist well above the shonkinite-syenite contact zone, are the most felsic of

all the rocks at Square Butte. Their occurrence may be similar to that used to explain the syenite blobs at the top of the shonkinite: an even more evolved differentiate forming in the syenite layer was able to rise due to a density differential. Or, since the exact shape of these blobs is not clear, they may just represent protrusions of syenite into the surrounding sediments (see discussion under Field Relations). But that doesn't necessarily work because most of these felsic blobs are surrounded by texturally different syenite (refer to figure 19). Clearly, these features require further study.

This project began with the hopes of providing evidence to support one type of differentiation process over another, and especially to look into the plausibility of liquid immiscibility at the butte. What I found, however, is that the differentiation of Square Butte laccolith is far from simple, and the data collected do not favor one mechanism over another. I tried to find a model that conforms to the puzzling data and field relationships, and have hardly put the problem to rest.

REFERENCES CITED

- Bowen, N.L., 1928, The evolution of the igneous rocks: Princeton University Press, New Jersey, 332 p.
- Deer, W.A., Howie, R.A., and Zussman, J., 1962, Rock-Forming Minerals: Longman, London.
- Eby, G.N., 1980, Minor and trace element partitioning between immiscible ocelli-matrix pairs from lamprophyre dikes and sills, Monteregian Hills Petrographic Province, Quebec: Contributions to Mineralogy and Petrology, v. 75, p. 269-278.
- Edmond, C.L., 1980, Magma immiscibility in the Shonkin Sag laccolith, Highwood Mountains, central Montana: M.S. Thesis, University of Montana, Missoula, 98 p.
- Emmart, L.A., 1985, Volatile transfer differentiation of the Gordon Butte magma, northern Crazy Mountains, Montana: M.S. thesis, University of Montana, Missoula, MT, 83 p.
- Foley, S.F., 1984, Liquid immiscibility and melt segregation in alkaline lamprophyres from Labrador: Lithos, v. 17, p. 127-137.
- Francalanci, L., Peccerillo, A., and Poli, G., 1987, Partition coefficients for minerals in potassium-alkaline rocks: Data from Roman province (Central Italy): Geochemical Journal, v. 21, p. 1-10.
- Freestone, I.C., 1978, Liquid immiscibility in alkali-rich magmas: Chemical Geology, v. 23, p. 115-123.
- Hearn, B.C., Jr., 1989, Montana High-Potassium Igneous Province Field Trip Guidebook T346, B.C. Hearn, Jr. (ed.), 28th International Geological Congress: American Geophysical Union, p. 2.
- Hildreth, W., 1979, The Bishop Tuff: Evidence for the origin of compositional zonation in silicic magma chambers: Geological Society of America Special Paper 180, p. 43-75.
- Hirsch, T.L., and Hyndman, D.W., 1985, Evolution of the Square Butte laccolith, eastern Highwood Mountains, Montana: Northwest Geology, v. 14, p. 17-31.

Hurlbut, C.S., Jr., and Griggs, D.T., 1939, Igneous rocks of the Highwood Mountains, Montana: Geological Society of America Bulletin, v. 50, p. 1043-1112.

Kendrick, G.C., 1980, Magma immiscibility in the Square Butte laccolith of central Montana: M.S. Thesis, University of Montana, Missoula, 89 p.

Larsen, E.S., 1941, Igneous Rocks of the Highwood Mountains, Montana, Part VI. Mineralogy: Geological Society of America Bulletin, v. 52, p. 1841-1856.

Lindgren, W. and Melville, W.H., 1893, A Sodalite-Syenite and other Rocks from Montana: American Journal of Science, v. XIV, p. 286-297.

MacLachlan, M.E., et al., 1981, Geology and mineral resource appraisal of the Square Butte area, Montana: U.S. Geological Survey Map MF-1370.

Marvin, R.F., et. al., 1980, Late Cretaceous-Paleocene-Eocene igneous activity in north-central Montana: Isochron/West, no. 29, p. 5-25.

Nash, W.P., and Wilkinson, J.F.G., 1970, Shonkin Sag laccolith, Montana: I. Mafic minerals and estimates of temperature, pressure, oxygen fugacity and silica activity: Contributions to Mineralogy and Petrology, v. 25, p. 241-269.

O'Brien, H.E., 1988, Petrogenesis of the mafic potassic rocks of the Highwood Mountains, Montana: Ph.D. Dissertation, University of Washington, Seattle, WA, 295 p.

O'Brien, H.E., Irving, A.J., and McCallum, I.S., 1991, Eocene potassic magmatism in the Highwood Mountains, Montana: Petrology, geochemistry, and tectonic implications: Journal of Geophysical Research, v. 96, p. 13,237-13,260.

Phillips, W.J., 1973, Interpretation of crystalline spheroidal structures in igneous rocks: Lithos, v. 6, p. 235-244.

Philpotts, A.R., 1976, Silicate liquid immiscibility: it's probable extent and petrogenetic significance: American Journal of Science, v. 276, p. 1147-1177.

Philpotts, A.R., 1990, Principles of Igneous and Metamorphic Petrology: Prentice Hall, New Jersey, 498 p.

Pirsson, L.V., 1905, Petrography and geology of the igneous rocks of the Highwood Mountains, Montana: U.S. Geological Survey Bulletin 237, 208 p.

Roedder, E., 1951, Low temperature liquid immiscibility in the system $K_2O-SiO_2-FeO-SiO_2$: American Mineralogist, v. 36, p. 282-286.

Roedder, E., 1979, Silicate liquid immiscibility, in Yoder, H.S., Editor, The Evolution of the Igneous Rocks, Fiftieth Anniversary Perspectives: Princeton University Press, Princeton, N.J. p. 15-57.

Ryerson, F.J. and Hess, P.C., 1978, Implications of liquid-liquid distribution coefficients to mineral-liquid partitioning: Geochimica et Cosmochimica Acta, v. 42, p. 921-932

Strong, D.F., and Harris, A., 1974, The petrology of Mesozoic alkaline intrusives of Central Newfoundland: Canadian Journal of Earth Science, v. 11, p. 1208-1219.

Tröger, W.E., 1979, Optical Determination of Rock-Forming Minerals, English edition of the fourth German edition: E. Schweizerbart'sche Verlagsbuchhandlung, Stuttgart, 188 p.

Watson, B.E., 1976, Two-liquid partition coefficients: Experimental data and geochemical Implications: Contributions to Mineralogy and Petrology, v. 56, p. 119-124.

Weed, W.H., and Pirsson, L.V., 1895, Highwood Mountains of Montana: Geological Society of America Bulletin, v. 6, 389-422.

ADDITIONAL REFERENCES

- Eby, G.N., 1979, Mount Johnson, Quebec-- An example of silicate-liquid immiscibility? *Geology*, v. 7, p.491-494.
- Fudali, 1960, Experimental studies bearing on the origin of pseudoleucite and associated problems of alkaline rock systems: Ph.D. Dissertation, Pennsylvania State University, 118p.
- Greenough, J.D., and Papezik, V.S, 1986, Volatile control of differentiation in sills from the Avalon Peninsula, Newfoundland, Canada: *Chemical Geology*, v. 54, p. 217-236.
- Holm, P.M., Lou, S., and Nielsen, A., (1982), The geochemistry and petrogenesis of the lavas of the Vulsinian district, Roman Province, central Italy: *Contributions to Mineralogy and Petrology*, v. 80, p. 367-378.
- Hyndman, D.W., Alt, D., and Tureck-Schwartz, K., 1989, Shonkin Sag and Square Butte laccoliths, Montana in *Field Trip Guidebook T346*, B.C. Hearn, Jr. (ed.), 28th International Geological Congress: American Geophysical Union, p. 37-49.
- Lelek, J.J., 1977, The Skalkaho pyroxenite-syenite complex east of Hamilton, Montana, and the role of magma immiscibility in its formation: M.S. Thesis, University of Montana, Missoula, 130 p.
- Monson, L.M., 1979, The mineralogy and chemistry of natural pseudoleucite: M.S. thesis, University of Utah, Salt Lake City, UT, 110 p.
- Walker, D. and DeLong, S.E., 1982, Soret Separation of Mid-Ocean Ridge Basalt Magma: *Contributions to Mineralogy and Petrology*, v. 79, p. 231-240.

APPENDIX A EXPLANATION OF SAMPLES

The following samples were all collected by the author. Refer to map for exact locations.

SAMPLE	LOCATION	ELEV ft m	EXPLANATION
sb-7	east	4040 1231	fresh sill (chill zone)
sb-10	north	4040 1231	sandstone at contact with sill
sb-15a	northeast	4560 1390	fine-grained shonkinite lens
sb-15b	northeast	4560 1390	gradation from fine-grained to coarser-grained shonkinite
sb-16a	northeast	4520 1378	sedimentary rock at contact with shonkinite, baked
sb-16b	northeast	4520 1378	pseudoleucite shonkinite at contact with sediments
sb-16c	northeast	4520 1378	shonkinite with slickensides at contact with sediments
sb-16	northeast	4520 1378	Cherty sedimentary rock with fossils. Looks tweaked. Using it in pantry as a door stop.
sb-18	southeast	5400 1646	white syenite blob from upper syenite (just below cap syenite)
sb-21	southern- most spine	4920 1500	mafic rind adjacent to syenite blob
sb-21b	southern- from spine	4920 1500	white syenite blob,
sb-23	south	5070 1545	syenite with 1-cm ocelli (pseudoleucite)
sb-24	north	4960 1512	syenite blob with mafic rind

sb-27	northwest valley	4930 1503	capping shonkinite over syenite
sb-29a	south	4530 1381	fine-grained syenite dike cutting through shonkinite
sb-30a	south	4610 1405	shonkinite adjacent to syenite dike
sb-30b	south	4610 1405	syenite dike
sb-31	north	4900 1493	shonkinite
sb-32	north	5040 1536	shonkinite directly above syenite
sb-33	north	5080 1548	less mafic shonkinite
sb-34	north	5230 1594	syenite with ocelli (pseudoleucite) to 1cm
sb-35	north	5580 1701	syenite
sb-36	north	5600 1707	cap syenite
sb-37	top, north	5680 1731	pegmatite from cap syenite
sb-38	southeast	5200 1585	mafic rind of syenite blob
sb-39	southeast	5400 1646	syenite blob
sb-41a	southeast	5500 1676	transition between syenite blob and mafic rind
sb-41b	southeast	5500 1676	shonkinitic rind
sb-43	southeast	4900 1493	shonkinite

sb-44	southeast	4180 1274	sill
sb-45	south	5040 1536	syenite
sb-46	south	5000 1524	syenite
sb-47	south	4930 1503	shonkinite (mottled)
sb-48	south	4880 1487	shonkinite
sb-49	south	4830 1472	shonkinite
sb-50	south	4810 1466	shonkinite
sb-51	south	4760 1451	shonkinite
sb-52	south	4720 1439	shonkinite
sb-53	south	4670 1423	shonkinite
sb-54	south	4640 1414	shonkinite
sb-55	south	4610 1405	shonkinite
sb-56	south	4560 1390	shonkinite
sb-57	south	4520 1378	shonkinite
sb-58	south	4480 1365	shonkinite
sb-59	south	4380 1335	shonkinite

sb-60	south	4350 1326	lowermost well-exposed shonkinite
sb-61	south	4320 1317	sill intruding what looks like severely weathered igneous rock

The following samples were collected by Donald Hyndman and George Kendrick

sbc-3	north- northeast	5700 1737	cap syenite
123ss	northwest corner	5680 1731	cap syenite
122ss	southwest corner	5600 1706	cap syenite
103rp	northeast	5125 1561	shonkinitic rind
sbc-1	southwest	5060 1540	syenite
sbc-2	southwest	5060 1540	more mafic syenite
102p	northeast	5040 1540	syenite
100p	northeast	5040 1540	syenite
101m	northeast	5040 1540	shonkinitic rind
125p	northeast	5000 1529	syenite
126m	northeast	5000 1529	shonkinitic rind
118p	east- northeast	4940 1505	syenite

119m	east- northeast	4940 1505	shonkinitic rind
sbc-4	north- northeast	4900 1495	syenite
sbc-5	north- northeast	4800 1462	shonkinitic
sbc-6	southwest	4850 1475	shonkinitic
138p	south	4840 1472	syenite
139m	south	4840 1472	shonkinitic rind
140p	south	4840 1472	syenite
134p	south	4800 1463	syenite
135m	south	4800 1463	shonkinitic rind
132p	south	4710 1438	syenite
133m	south	4710 1438	shonkinitic rind
130sd	south	4500 1372	syenite dike
131sh	south	4500 1371	shonkinitic
sbc-7	southwest	4400 1340	shonkinitic
sbc-9	southeast	4230 1290	sill
130m	south	4200 1285	shonkinitic

APPENDIX B

WHOLE-ROCK ANALYSES of Square Butte samples.

sample	elev (m)	SiO2	Al2O3	MgO	CaO	Na2O	K2O	TiO2	P2O5	FeO*
sbc-3	1737	55.9	19.6	0.49	2.21	6.08	7.93	0.41	0.1	5.28
123ss	1731	55.49	19.3	1.55	3.86	4.55	6.79	1.23	0.4	6.04
122ss	1706	58.92	20.3	0.56	2.03	5.56	7.56	0.37	0.11	4.02
100p	1536	50.02	15.01	4.91	8.78	2.33	7.06	0.99	1.35	8.46
102p	1536	50.3	16.11	3.8	7.43	2.93	7.25	1.17	1.1	8.96
ctsb-21	1450	49.03	14.86	4.87	8.02	2.51	7.38	0.995	1.187	9.12
ctsb-38	1585	51.78	17.64	2.46	5.18	3.1	7.79	1.166	0.547	7.05
ctsb-39	1640	53.25	18.01	1.95	4.22	3.36	9.22	1.245	0.475	6.02
sbc-1	1540	51.7	18.2	1.93	3.96	3.09	9.58	1.09	0.44	5.57
sbc-4	1495	47.90	15.10	3.97	6.91	2.49	7.67	1.02	1.01	8.88
125p	1529	51.06	18.62	3.57	7.21	2.68	7.82	0.94	1.00	8.07
118p	1505	55.45	19.03	1.72	4.11	4.28	6.75	1.22	0.41	6.22
140p	1472	51.40	16.86	3.26	6.59	3.09	7.67	1.09	0.93	8.09
138p	1472	51.34	17.11	3.30	6.38	3.04	7.75	1.07	0.95	8.04
134p	1463	48.72	15.02	4.45	8.48	2.90	6.75	1.32	1.33	9.07
132p	1438	48.60	13.84	5.23	9.22	2.54	6.37	1.20	1.49	10.25
130sd	1372	58.14	19.28	1.15	2.23	4.33	8.86	0.47	0.25	4.68
sbc-2	1540	50.4	18.6	2.01	4.53	3.39	7.38	1.42	0.52	6.71
ctsb-21	1450	43.95	8.86	9.07	13.59	1.25	3.65	1.451	1.976	14.16
103rp	1561	49.01	12.10	6.34	10.70	2.20	5.72	1.12	1.41	11.89
101m	1536	45.83	10.51	7.54	11.98	2.04	4.36	1.44	1.89	12.79
119m	1505	46.74	10.63	7.42	11.88	2.36	4.72	1.24	1.79	11.72
126m	1529	46.6	11.32	6.75	11.36	1.85	6.52	1.36	1.76	11.97
139m	1472	45.63	12.12	5.52	11.14	2.07	6.08	1.86	1.86	13.10
135m	1463	45.23	11.81	5.45	10.86	1.95	5.68	1.76	1.81	13.74
133m	1438	45.24	11.55	6.32	11.30	2.10	6.33	1.52	1.92	13.09
10sh	1402	49.50	9.65	8.79	12.09	2.28	3.74	0.97	1.45	9.40
131sh	1371	48.90	9.47	8.98	13.54	2.62	3.27	0.97	1.36	9.62
sbc-5	1462	45.30	9.76	8.57	12.30	1.33	4.23	1.18	1.66	12.24
sbc-6	1475	47.50	9.81	9.36	12.70	1.40	4.40	0.93	1.38	10.17
sbc-7	1340	47.10	8.75	10.00	13.50	1.34	3.72	0.85	1.36	9.54
sbc-8	1348	51.10	14.80	4.88	7.61	2.63	6.35	0.72	0.75	7.42
sbc-9	1290	48.40	12.80	6.17	9.01	2.14	5.62	0.83	0.94	8.12
ctsb-7	1231	49.66	13.2	6.07	9.52	1.86	5.79	0.875	0.991	8.34

APPENDIX C

PRECISION DATA for selected elemental and oxide chemical analyses, X-Ray Assay Laboratories, Inc., Ontario, Canada.

	<u>INSTRUMENT STABILITY</u>				<u>SAMPLE PREPARATION REPRODUCIBILITY</u>				
	(10 replicate analyses)				(42 replicate analyses)				
	<u>Mean (%)</u>	<u>SD (%)</u>	<u>Mean (%)</u>	<u>SD (%)</u>	<u>Mean (%)</u>	<u>SD (%)</u>	<u>Mean (%)</u>	<u>SD (%)</u>	
SiO ₂	39.5	0.06	65.1	0.07	80.7	0.25	65.9	0.25	SiO ₂
Al ₂ O ₃	2.92	0.01	18.8	0.03	8.21	0.06	13.0	0.06	Al ₂ O ₃
CaO	1.20	0.005	0.10	0.005	0.05	0.005	0.72	0.005	CaO
MgO	34.8	0.08	0.10	0.005	1.79	0.02	6.08	0.04	MgO
Na ₂ O	0.13	0.01	2.56	0.03	0.13	0.01	0.60	0.02	Na ₂ O
K ₂ O	0.02	0.005	12.9	0.02	1.89	0.01	2.51	0.01	K ₂ O
Fe ₂ O ₃	8.52	0.015	0.12	0.005	4.87	0.03	7.14	0.03	Fe ₂ O ₃
MnO	0.13	0.00	0.00	0.00	0.08	0.005	0.14	0.005	MnO
TiO ₂	0.12	0.005	0.03	0.00	0.19	0.005	0.33	0.005	TiO ₂
P ₂ O ₅	0.04	0.00	0.02	0.00	0.05	0.00	0.10	0.00	P ₂ O ₅
Cr ₂ O ₃	0.33	0.001	0.00	0.00	0.02	0.00	0.02	0.00	Cr ₂ O ₃
					1.59	0.08	2.95	0.09	L.O.I.

NOTE: Mean is the arithmetic mean
SD is standard deviation

	<u>INSTRUMENT STABILITY</u>				<u>SAMPLE PREPARATION REPRODUCIBILITY</u>				
	(10 replicate analyses)				(42 replicate analyses)				
	<u>Mean (ppm)</u>	<u>SD (ppm)</u>	<u>Mean (ppm)</u>	<u>SD (ppm)</u>	<u>Mean (ppm)</u>	<u>SD (ppm)</u>	<u>Mean (ppm)</u>	<u>SD (ppm)</u>	
Rb	210	10	200	10	30	10	220	20	Rb
Sr	260	10	4400	40	<10	10	340	10	Sr
Y	130	10	50	10	20	10	590	20	Y
Zr	280	10	11500	40	60	10	280	10	Zr
Nb	10	10	980	20	20	10	870	20	Nb
Ba	420	20	520	20	660	10	1200	40	Ba

NOTE: Mean is the arithmetic mean
SD is standard deviation

Table 2 Rigaku Automatic XRF Analysis: Instrument Precision
 Repetition of a single bead on the same calibration curve (one run).

Run 0183

		BCRP (10)			GSP-1 (10)			
		Average	S.D. %/ppm	S.D. Rel. %	Average	S.D. %/ppm	S.D. Rel. %	
%	SiO ₂	55.40	0.05	0.08	68.19	0.03	0.05	
	Al ₂ O ₃	13.56	0.02	0.16	15.32	0.02	0.15	
	TiO ₂	2.256	0.0048	0.22	0.672	0.003	0.45	
	FeO	12.73	0.014	0.11	3.87	<0.00	0.08	
	MnO	0.185	0.0007	0.38	0.042	0.00	1.19	
	CaO	6.98	0.008	0.11	2.02	<0.01	0.30	
	MgO	3.44	0.028	0.81	0.95	0.01	1.37	
	K ₂ O	1.73	0.000	0.00	5.63	0.01	0.09	
	Na ₂ O	3.34	0.014	0.42	2.78	0.01	0.40	
	P ₂ O ₅	0.381	0.0018	0.47	0.296	0.001	0.34	
	ppm	Ni	0	0.0	0	18.7	1.06	5.67
		Cr	18.1	1.37	7.6	12.2	2.53	20.74
		Sc	34.8	2.7	7.7	3.7	2.26	61.08
		V	391	6.6	1.7	49.3	7.3	14.81
		Ba	675.5	16.87	2.5	1297.2	17.17	1.32
		Rb	46.6	0.97	2.1	252.4	0.84	0.33
		Sr	325.6	0.8	0.26	233.8	0.9	0.39
Zr		174.3	1.06	0.61	502.6	0.97	0.19	
Y		37.5	0.53	1.4	30.4	1.07	3.52	
Nb		13.8	0.81	5.9	30.3	0.68	2.24	
Ga		-	-	-	-	-	-	
Cu		11.0	1.7	15.5	37.2	1.81	4.87	
Zn		120.7	1.42	1.20	99	1.83	1.85	
Pb		10.8	1.23	11.4	51.6	1.17	2.27	
La	21.1	8.25	39.1	188	4.69	2.49		
Ce	53.8	7.9	14.7	399	13.33	3.34		
Th	6.1	1.37	22.5	103.3	1.42	1.37		

Table 3. Rigaku Automatic XRF Analyses: Estimate of Accuracy, WSU and Recommended Values

	BCR-1 Basalt					AGV-1 Andesite				
	A	F	G	WSU 1	WSU 2	A	F	G	WSU 1	WSU 2
SiO ₂	55.31	55.43	55.33	55.42	55.42	60.64	60.47	60.62	60.61	60.67
Al ₂ O ₃	13.92	13.84	13.88	13.72	13.71	17.49	17.68	17.55	17.55	17.56
TiO ₂	2.29	2.238	2.26	2.245	2.244	1.08	1.07	1.08	1.065	1.068
Fe ₂ O ₃	12.26	12.33	12.33	12.51	12.5	6.24	6.26	6.22	6.34	6.3
MnO	0.18	0.183	0.185	0.188	0.186	0.1	0.099	0.098	0.098	0.098
CaO	7.07	7.04	7.08	7.04	7.02	5.03	5.02	5.05	5	4.99
MgO	3.53	3.52	3.51	3.46	3.48	1.55	1.57	1.57	1.5	1.47
K ₂ O	1.72	1.73	1.72	1.73	1.74	2.97	2.96	2.97	2.99	3
Na ₂ O	3.35	3.33	3.33	3.32	3.33	4.39	4.37	4.35	4.34	4.35
P ₂ O ₅	0.365	0.366	0.377	0.363	0.369	0.519	0.502	0.491	0.499	0.498
Ni	10	15.8	13	4	6	15	18.5	17	17	34
Cr	15	17.6	16	20	17	10	12.2	12	7	26
Sc	33	33	33	36	33	12.5	13.4	12.1	12	13
V	420	399	404	388	404	125	125	123	119	119
Ba	680	675	678	644	657	1200	1208	1220	1224	1190
Hf	47	46.6	47	46	48	67	67	67	68	68
Sr	330	330	330	324	326	660	657	660	662	662
Zr	185	190	191	170	174	230	225	225	218	217
Y	40	37.1	39	37	38	19	21.3	21	20	21
Nb	19	13.5	14	16	14	16	15	15	15	15
Ga	22	20	22	21	20	21	20.5	20	20	18
Cu	16	18.4	18	18	7	59	59.7	60	65	63
Zn	125	120	129	128	123	86	84	88	86	84

A=Abbey, 1983;F=Flanagan, 1976;G=Gladney et al, 1983

Table 3. Rigaku Automatic XRF Analyses: Estimate of Accuracy, WSU and Recommended Values

	PCC-1 Peridotite					BIR-1			DNC-1			W-2		
	A	F	G	WSU 1	WSU 2	F	WSU 1	WSU 2	F	WSU 1	WSU 2	F	WSU 1	WSU 2
SiO ₂	44.56	44.44	44.53	44.04	44.15	48.08	48.21	48.18	47.69	47.84	47.87	53.06	53.05	53.14
Al ₂ O ₃	0.77	0.77	0.79	0.86	0.89	15.57	15.62	15.54	18.55	18.6	18.69	15.53	15.47	15.43
TiO ₂	0.01	0.016	0.015	0.015	0.017	0.96	0.957	0.955	0.49	0.49	0.49	1.07	1.066	1.064
Fe ₂ O ₃	7.9	8.28	7.99	7.92	7.75	10.21	10.19	10.29	9.03	9.01	8.57	9.79	9.78	9.76
MnO	0.127	0.127	0.127	0.126	0.128	0.175	0.174	0.174	0.15	0.15	0.15	0.168	0.169	0.169
CaO	0.58	0.54	0.55	0.58	0.58	13.35	13.31	13.28	11.62	11.4	11.38	10.94	10.94	10.93
MgO	46.04	45.8	45.97	46.43	46.46	9.72	9.72	9.73	10.25	10.24	10.23	6.42	6.43	6.4
K ₂ O	0	0.004	0.005	0	0	0.03	0.02	0.018	0.24	0.22	0.22	0.63	0.63	0.63
Na ₂ O	0.01	0.006	0.029	0.016	0.006	1.82	1.77	1.8	1.9	1.93	1.92	2.22	2.23	2.24
P ₂ O ₅	0.01	0.002	0.002	0.0028	0.003	0.021	0.029	0.025	0.07	0.069	0.071	0.142	0.125	0.126
Ni	2400	2339	2400	2330	2342	166	155	155	247	245	244	70	62	66
Cr	2800	2730	2730	2738	2758	373	371	368	270	265	267	92	86	92
Sc	9	6.9	8.5	5	8	43	40	44	31	31	30	36	37	33
V	29	30	30	43	36	312	318	311	148	142	154	259	253	260
Ba	4	1.2	1.2	48	45	6	4	0	118	106	99	174	158	139
Rb	0.3	0.063	0.066	0	0		1	1	4.7	4	5	21	20	19
Sr	0.4	0.41	0.4	0	0	107	105	106	144	142	143	192	192	190
Zr	7	7	8	12	12	18	29	29	39	47	46	100	94	94
Y				1	2	16	16	17	18.5	19	18	23	23	22
Nb	1		1	0	0	2.3	0	0	3.2	1	1	6.8	7	7
Ga	0.7	0.4	0.7	0	0	15	16	15	14.7	14	12	16.8	17	18
Cu	8	11.3	10	11	11	125	123	123	14.7	94	95	106	105	104
Zn	41	36	42	45	46	70	66	68	100	65	64	80	73	73

A=Abbey, 1983; F=Flanagan, 1976; G=Gladney et al, 1983

Table 3. Rigaku Automatic XRF Analyses: Estimate of Accuracy, WSU and Recommended Values

	GSP-1 Granodiorite					G-2 Granite				
	A	F	G	WSU 1	WSU 2	A	F	G	WSU 1	WSU 2
SiO ₂	68.17	68.18	68.23	68.15	68.29	70	69.88	70.06	69.93	69.87
Al ₂ O ₃	15.47	15.43	15.35	15.37	15.39	15.57	15.58	15.36	15.64	15.68
TiO ₂	0.668	0.668	0.664	0.672	0.672	0.485	0.51	0.499	0.497	0.496
Fe ₂ O ₃	3.9	3.95	3.94	3.97	3.87	2.43	2.44	2.45	2.45	2.46
MnO	0.041	0.043	0.041	0.04	0.043	0.03	0.03	0.035	0.033	0.033
CaO	2.06	2.04	2.07	2.04	2.03	1.98	1.97	2	1.95	1.94
MgO	0.98	0.97	1	1.04	0.98	0.76	0.77	0.77	0.69	0.69
K ₂ O	5.58	5.6	5.58	5.62	5.63	4.51	4.56	4.56	4.56	4.57
Na ₂ O	2.85	2.83	2.84	2.82	2.81	4.11	4.11	4.13	4.18	4.14
P ₂ O ₅	0.284	0.283	0.284	0.281	0.291	0.132	0.14	0.142	0.135	0.134
Ni	9	12.5	10	18	19	3.5	5.1	5	13	13
Cr	12	12.5	3	9	10	8	7	9	5	9
Sc	6.6	7.1	6.1	5	5	3.5	3.7	3.5	2	2
V	54	52.9	53	47	52	36	35.4	36	32	29
Ba	1300	1300	1310	1318	1285	1900	1870	1880	1884	1854
Rb	250	254	254	254	250	170	168	170	168	168
Sr	240	233	234	235	233	480	479	478	476	476
Zr	500	500	530	508	498	300	300	300	299	298
Y	29	30.4	29	30	29	11	12	11.4	12	12
Nb	23	29	26	29	29	13	13.5	13	14	13
Ga	23	22	22	22	24	23	23	22	23	22
Cu	33	33.3	34	36	37	10	11.7	11	14	13
Zn	105	98	103	99	97	84	85	85	83	80

A=Abbey, 1983;F=Flanagan, 1976;G=Gladney et al, 1983

Table 4. Intensity for Trace Elements Using Rh Target
(Counts/Second/Parts Per Million)

	Ni	Cr	Sc	V	Ba	Pb	Sr	Zr
BCRP	5.8	2.2	1	0.1	0.2	4.9	5.0	7.2
GSP-1	10.3	2.2	0.1	0.1	0.2	5.8	6.8	11.5

	Y	Nb	Ga	Cu	Zn	Pb	La	Ce	Th
	4.8	6.3	1.1	4.6	0.98	0.9	0.2	0.2	2.6
	6.3	9.2	1.2	4.3	5.8	2.5	0.2	0.2	2.4

APPENDIX D

CHEMICAL COMPOSITION of clinopyroxene through shonkinite.

CORES

Sample	elev(m)	SiO2	Al2O3	FeO	MgO	CaO	TOTAL
sb61	1317	49.25	3.87	9.70	13.29	22.64	98.75
sb60	1326	48.89	3.29	9.67	13.50	22.66	98.01
sb60	1326	50.41	2.87	8.90	14.09	23.72	99.99
sb60	1326	50.99	2.83	8.49	14.21	23.72	100.24
sb58	1366	51.61	2.37	8.91	14.76	22.89	100.54
sb55	1405	50.66	3.10	8.95	13.84	23.44	100.00
sb55	1405	50.67	2.69	8.83	13.69	24.78	100.65
sb52	1439	50.89	2.55	8.52	14.30	23.04	99.29
sb49	1472	51.33	2.43	8.47	14.22	23.18	99.63
sb49	1472	50.87	2.35	8.54	13.97	24.70	100.44
sb47	1503	50.28	3.64	10.10	12.87	22.42	99.32
sb47	1503	50.79	3.38	8.07	14.01	23.28	99.54

RIMS

Sample	elev(m)	SiO2	Al2O3	FeO	MgO	CaO	TOTAL
sb61	1317	49.69	3.67	9.21	14.14	22.73	99.45
sb60	1326	50.31	2.23	8.95	13.91	21.86	97.25
sb60	1326	50.13	2.63	8.94	13.97	22.29	97.96
sb60	1326	50.62	3.39	9.62	14.12	23.01	100.75
sb58	1366	52.19	2.43	8.99	15.21	22.11	100.94
sb55	1405	49.94	3.11	8.86	13.55	24.42	99.88
sb55	1405	50.23	3.40	8.96	13.66	23.99	100.23
sb52	1439	51.23	2.67	8.72	14.39	23.08	100.09
sb49	1472	50.54	3.57	9.28	13.79	22.95	100.12
sb49	1472	50.78	3.03	9.00	13.95	23.78	100.53
sb47	1503	50.92	3.33	9.75	13.55	23.00	100.55
sb47	1503	51.87	3.00	9.44	12.71	23.10	100.12

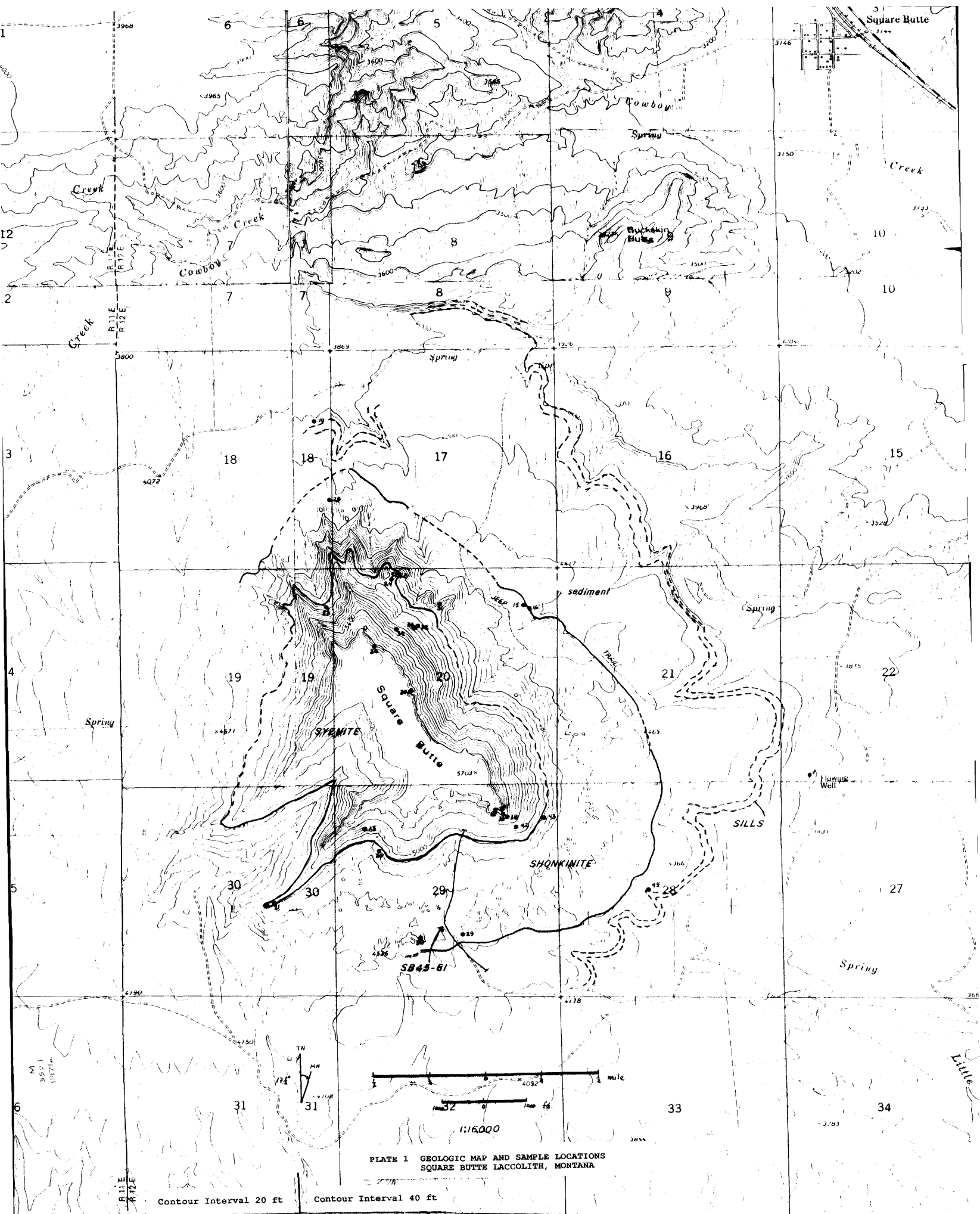


PLATE 1 GEOLOGIC MAP AND SAMPLE LOCATIONS
 SQUARE BUTTE LACCOLITH, MONTANA

Contour Interval 20 ft

Contour Interval 40 ft